2017-08-08

Developing Computational Models for the Biomechanical Assessment of Thoracolumbar Spine Surgeries

Shady Elmasry
University of Miami, shady.elmasry.cu@gmail.com

UNIVERSITY OF MIAMI

DEVELOPING COMPUTATIONAL MODELS FOR THE BIOMECHANICAL
ASSESSMENT OF THORACOLUMBAR SPINE SURGERIES

By

Shady Elmasry

A DISSERTATION

Submitted to the Faculty
of the University of Miami
in partial fulfillment of the requirements for
the degree of Doctor of Philosophy

Coral Gables, Florida

August 2017

UNIVERSITY OF MIAMI

A dissertation submitted in partial fulfillment of
the requirements for the degree of
Doctor of Philosophy

DEVELOPING COMPUTATIONAL MODELS FOR THE BIOMECHANICAL
ASSESSMENT OF THORACOLUMBAR SPINE SURGERIES

Shady Elmasry

Approved:

_____
Francesco Travascio, Ph.D
Assistant Professor of
Industrial Engineering

_____
Loren Latta, Ph.D.
Professor Emeritus of
Orthopaedics

_____
Shihab Asfour, Ph.D.
Professor of
Industrial Engineering

_____
Mohamed Fahmy, Ph.D.
Lecturer of
Industrial Engineering

_____
Moataz Eltoukhy, Ph.D.
Assistant Professor of
Kinesiology and Sport Sciences

_____
Guillermo Prado, Ph.D.
Dean of the Graduate School

ELMASRY, SHADY   (Ph.D., Industrial Engineering)
Developing Computational Models for the   (August 2017)
Biomechanical Assessment of Thoracolumbar Spine Surgeries.

Abstract of a dissertation at the University of Miami.

Dissertation supervised by Dr. Francesco Travascio.
No. of pages in text. (112)

Low back pain and spinal disorders represent a major clinical apprehension as the population ages. With more than 1.4 million annual spine procedures, operative management is exerting a significant healthcare burden in the United States. Despite the new technologies and the advent of minimally invasive surgeries (MIS), the optimal surgical treatment for many spine pathologies is still controversial. Hence, revision surgeries, due to failure in attaining the surgical goals, have been very common. Comprehensive understanding of each patient condition is crucial in determining the best surgical treatment; however, the available tools used in diagnosis and specifying the treatment are still insufficient to provide such knowledge.

Finite element modeling (FEM), an advanced computational method for structural stress analysis, was employed in orthopedic biomechanics applications since 1972 to evaluate the kinematics and kinetics of human tissues. With the advancement of the computational power and the ability to precisely reconstruct 3D models of the spine tissues, FEM is now a well-established tool for basic research in spine biomechanics. However, despite the exceptional capabilities of this method, it is yet not well exploited in patient diagnosis and in optimizing the surgical treatment.

In this dissertation, a new theoretical approach that utilizes FEMs of the thoracolumbar spine to evaluate and compare different spine procedures is developed. In this approach, CT scans of a real human subject were reconstructed to build 3D anatomical models that are used in the FEM. Potential spine procedures were virtually performed on the FEMs and normal physiological loading conditions were applied on each surgical alternative. A novel steady state nonlinear biphasic analysis was employed to solve the model, which couples the fluid problem with a solid mechanics problem. Accordingly, the implications of each spine procedures on the biomechanics of the spine were evaluated and the optimal spine procedure, from a biomechanical perspective, was specified. Moreover, the possibility of the development of adjacent segment diseases due the surgical intervention was investigated.

Spine procedures used in the treatment of lumbar spinal stenosis (LSS); a degenerative disease that accounts for 5% of patients who present with persistent low back pain, and thoracolumbar burst fractures (TBF); the most common site of spinal injury were particularly assessed. Several decompressive and spinal fusion surgeries through open or minimal invasive techniques, that utilized different sets of implantable devices, were examined. The results provided insights on the consequences of applying each surgical alternative and would definitely help practitioners to optimize the operative management for each patient.

ACKNOWLEDGEMENTS

Table of Contents

List of Figures

List of Tables

List of Publications

- **Elmasry, S**., Asfour, S., & Travascio, F. (2017). "*Effectiveness of Pedicle Screw Inclusion at the Fracture Level in Short-Segment Fixation Constructs for the Treatment of Thoracolumbar Burst Fractures: A Computational Biomechanics Analysis*". Submitted to Journal of Computer Methods in Biomechanics and Biomedical Engineering.

- **Elmasry, S**., Asfour, S., Gjolaj, J., Latta, L., Esmont, F., & Travascio, F. (2016). "*Implications of Spine Fixation on the Adjacent Lumbar Levels for Surgical Treatment of Thoracolumbar Burst Fractures: A Finite Element Analysis*". J Spine care.

- Travascio, F., Asfour, S., Gjolaj, J., Latta, L., & **Elmasry, S**. (2015). "*Implications of decompressive surgical procedures for lumbar spine stenosis on the biomechanics of the adjacent segment: A finite element analysis*". J Spine, 4(220), 2.

- **Elmasry, S**., Asfour, S., & Travascio, F. (2017). "*Computational Analysis of the Changes in Intradiscal Pressure at Adjacent Segments After Posterior Fixation for Burst Fracture*". Summer Biomechanics, Bioengineering & Biotransport Conference SB3C.

- **Elmasry, S**., Asfour, S., Gjolaj, J, Latta, L., Eismont, F & Travascio, F. (2017). "*Advantage of Pedicle Fixation at the Injured Level for Treating Unstable Thoracolumbar Fracture: A Finite Element Analysis*". Orthopedics Research Society ORS. (**SPINE SECTION FINALIST**)

- **Elmasry, S**., Asfour, S., Gjolaj, J, Latta, L., Eismont, F & Travascio, F. (2016). "*Implications of Different Fixation Constructs for Treating Thoracolumbar Burst Fractures on Adjacent Lumbar Spine Levels: A Finite Element Analysis*". Orthopedics Research Society ORS. (**SPINE SECTION AWARD**)

- **Elmasry, S**., Asfour, S., Gjolaj, J, Latta, L., Eismont, F & Travascio, F. (2016). "*Treatment Of Thoracolumbar Burst Fracture: A Biomechanical Analysis Of Three Different Fixation Constructs*". Summer Biomechanics, Bioengineering & Biotransport Conference SB3C.

- Gjolaj, J, **Elmasry, S**., Asfour, S., Latta, L., Eismont, F & Travascio, F. (2015). *"Implications of Decompressive Surgical Procedures for Lumbar Spine Stenosis on the Biomechanics of the Adjacent Segment: a Finite Element Analysis"*. North American Spine Society NASS

- Asfour, S., **Elmasry, S**., Latta, L., Gjolaj, J, Eismont, F & Travascio, F. (2015)." *Comparative Analysis on the Implications of Anterior Lumbar Interbody Fusion and Posterior Lumbar Interbody Fusion on Adjacent Segment Biomechanics: a Finite Element Study"*. Orthopedics Research Society ORS.

- **Elmasry, S**., Asfour, S., Gjolaj, J, Latta, L., Eismont, F & Travascio, F. (2015). *"Biomechanical Comparison between Facet Sparing Laminectomy and Laminectomy with Facetectomy in Lumbar Spine"*. Summer Biomechanics, Bioengineering & Biotransport Conference SB3C.

Chapter 1 Specific Aims and Structure of the Dissertation

1.1 Specific Aims

Thoracolumbar spine is the lower segment of the vertebral column that is most vulnerable to degenerative diseases and traumatic fractures. The treatment of these pathologies can be accomplished by either conservative or operative management (2-6). However, in cases of persistent pain due to neurologic deficiency and spine instability, operative management is recommended (2, 3, 7-9). The optimal surgical approach is always a subject of debate between researchers (2, 6, 10, 11). This is attributed to the various clinical factors that need to be considered in the decision-making process of the adopted procedure, such as the neurologic condition of the patient and the level of surgical morbidity. Another important factor in the decision-making process is the post-operative biomechanical performance of the spine. Specifically, it is important to determine to what extent the surgical operation will restore the spine stability and what are the implications of the surgery on the biomechanics of the other spine segments. The ultimate goal of the surgeons is to constantly restore as much spine stability as possible and to minimize the implications of the surgery on the adjacent segments. Failure in attaining these goals may cause adjacent segment diseases (ASD) and necessitate revision surgery. The ASD is the development of degeneration at mobile segments above or below the segment that underwent surgery, and it is associated with low back pain (12, 13). Numerous studies have been conducted to evaluate the post-operative biomechanical performance of the spine; nevertheless, various biomechanical aspects had been overlooked that require further investigation to obtain the best long-term outcomes.

The biomechanical testing on cadavers is deemed the standard method for investigating the post-operative biomechanical behavior of the spine. However, this testing method is limited to some important measures, such as the internal stresses and strains (14). Alternatively, computational modeling has the capability to measure various parameters over the entire domain of interest and provides more insight on the areas that experience the peak levels of the measured quantity (15). One of the well-known computational methods is the finite element (FE) analysis that has shown a distinctive capability to analyze structures with complex geometry. FE can be utilized to measure stresses and strains in such a way that makes it superior to many other computational methods (16). In view of the complexity of spine tissues, FE has become a powerful tool in orthopaedic-related spine research and is used intensively to evaluate and compare the outcomes of various orthopaedic procedures from a biomechanical standpoint.

The **long-term goal** of this research is to develop a patient-specific computational tool to be used in clinics for optimizing surgical treatment of spine pathologies. Towards the achievement of this goal, the **objective** of this project is to develop a computational framework to evaluate different surgical procedures for treatment of spine degenerative diseases (LSS) and traumatic fractures (BF). In order to address this objective, the following specific aims will be pursued:

Specific aim 1: To compare the biomechanical performance of the spine after performing decompressive surgeries for the treatment of lumbar spinal stenosis.

Current knowledge on the implications of surgery for LSS on adjacent segments biomechanics is limited. This is especially true for more recent surgical approaches that aim to reduce invasiveness by limiting the required modifications to spinal anatomy. We hypothesize that decompressive surgeries used for the treatment of LSS may alter the normal biomechanics of adjacent segments, eventually contributing to the development of ASD. Therefore, in this aim, we will characterize the post-operative kinematics, intradiscal pressure, and generated stresses at the adjacent segments due to four decompressive surgeries: unilateral laminotomy, bilateral laminotomy, facet sparing laminectomy, and laminectomy with facetectomy (radical laminectomy). A 3D computational model of the lumbar spine (from L1 to L5) will be developed based on accredited theoretical formulations for tissue mechanics and will be validated via experimental data from the literature. The outcomes will provide additional information on the relation between decompressive surgeries and ASD.

Specific Aim 2: To assess the biomechanical performance of the spine after performing fixation procedures for the treatment of burst fractures.

Approximately 90% of traumatic spinal fractures occur at the thoracolumbar junction (17). Among these fractures, 10% to 20% are considered burst fracture (BF); a spinal traumatic injury that is characterized by the failure of anterior and middle spinal column with partial/complete neurologic deficit (2, 18). Surgical management is commonly indicated for BF trauma aiming to stabilize the fracture, restore spinal stability, and decompress neural elements (3, 11). However, clinical studies reported a number of failures on some implanted devices which necessitate a revision surgery. Moreover,

selecting a fixation procedure that generates an excessive stiffness to the spine may lead to the development of ASD. Such conditions cause extra pain to the patients and add more costs on the healthcare system. To date, there is no unanimous agreement on the optimal fixation procedure that should be adopted for BF to obtain the best long-term results.

Possible fixation procedures for BF can be classified in to two categories: 1- fixation procedures that are performed in BF that is associated with neurologic deficiency and sever comminution of the vertebral body (A3.3 according to AO system (19)), 2- fixation procedures that are performed in BF fractures that is associated with incomplete/low neurologic dysfunction and moderate comminution of the vertebral body (A3.1 according to AO system). To investigate the biomechanics of the spine after performing different fixation procedures for each set of fixation procedures, the following three sub-aims will be addressed:

Sub-aim 2.1: **To compare the post-operative behavior of the spine after fixing the fractured level for the treatment of severe BF (A3.3)**

Surgical correction with corpectomy and subsequent fusion of neighboring levels is a commonly practiced treatment for BF that is associated with neurologic deficiency (11). Surgeries can be performed through anterior, posterior, or combined anterior-posterior approach and may utilize different set of implant devices (20-22). However, it is still unknown how the additional spinal stiffness provided by each approach alters the biomechanics of the adjacent segments. Accordingly, the mechanical stiffness for four

common constructs will be quantified as well as the pot-operative biomechanical alterations at the adjacent segments. 3D computational models of the thoracolumbar junction T12-L2 will be developed and validated to describe all four constructs. Moreover, a 3D model of the lumbosacral spine (L3-S1) will be constructed and integrated to each construct to investigate their implications on the adjacent segments. The results of this study will advance the limited knowledge on the effects of the four fixation constructs on the rest of the spine.

Sub-aim 2.2: **To investigate the advantage of the inclusion of the fracture level in posterior constructs for the treatment of moderate BF (A3.1)**

Moderate BF that requires surgical intervention is usually treated through a posterior approach. Long-segment posterior fixation (LSPF) and short-segment posterior fixation (SSPF) are well-known surgeries for such injuries (23-26). However, LSPF is known to be superior in providing stability to the spinal column (24). The inclusion of pedicle screws at the fracture level has been suggested to improve the outcomes of SSPF (27-29). We hypothesize that pedicle screw inclusion in SSPF will improve the biomechanical performance of the construct and make it comparable to LSPF. A 3D computational model for the thoracolumbar spine (T11-L4) will be developed to describe each construct and compare the post-operative biomechanical performance of the spine. The results of this study will clarify the biomechanical advantage of pedicle screw inclusion at the fracture level on SSPF and compare it to LSPF.

Sub-aim 2.3: **To evaluate the biomechanical behavior of the spine after performing minimally invasive surgeries for moderate BF (A3.1)**

Percutaneous pedicle screws fixation (PPSF) and balloon Kyphoplasty (KP) has become an accredited minimally invasive alternative treatment for BF with incomplete neurologic dysfunction (30-33). However, little is known about the mechanical behavior of KP-augmented PPSF. We hypothesize that reinforcement of PPSF with KP improve spinal stability and decrease instrument failure rates. The mechanical behavior of PPSF and KP approaches will be characterized individually and in combination. A 3D computational model of the thoracolumbar junction (T12-L2) will be developed and used to describe each approach. The results of this study will elucidate the contribution of each procedure to spine stability and demonstrate their implications on the adjacent spinal levels.

1.2 Structure of the Dissertation

In Chapter 2, a background of the spine degenerative diseases and traumatic fractures, and the possible surgical treatments for both pathologies is reviewed. Also, the history of using FE to study spine biomechanics and the significance of the study is presented.

In Chapter 3, the general computational approach employed in all the studies that is covered in this dissertation is explained. Specifically, segmenting the 3D anatomical tissues, performing surgical procedures via CAD tools, meshing the spine components, defining the boundary conditions, and model validation approaches are demonstrated.

In chapter 4, a biomechanical comparison and evaluation of four decompressive surgeries that are used for the treatment of lumbar spinal stenosis is presented. The risk of developing adjacent segment disease is evaluated and the surgeries with the highest risk are identified.

In Chapter 5, the biomechanical implications of four fixation constructs that are used for the treatment of severe burst fractures are investigated. The alteration on the biomechanics of the adjacent segment is quantified and compared between the investigated constructs.

In Chapter 6, the mechanical advantage of adding pedicle screws at the level of fracture in short segment posterior constructs for treatment of moderate burst fracture is investigated, and a biomechanical comparison with the long segment one is conducted.

In Chapter 7, the biomechanical benefits of augmenting posterior constructs with Kyphoplasty in minimally invasive surgery for the treatment of moderate burst fracture is studied, and their implication on spinal stability is evaluated.

In Chapter 8, the major findings of the dissertation are summarized and possible future work is dicussed.

Chapter 2 Background and Significance

This chapter introduces background information of the spine anatomy, spine degenerative diseases, and spine traumatic fractures. A review of the possible surgical treatment for these spine pathologies is also discussed. The chapter concludes by the significance of this dissertation.

2.1 Spine Anatomy

The spine is composed of 33 vertebrae stacked one on top of another to constitute the spinal column. Spine provides the main support for the body and is divided in to four anatomical sections. The topmost section of the spinal column is the cervical spine and is represented at the neck with seven levels of vertebrae. The next section is the thoracic spine that forms joints with the ribs of the rib cage and is composed of twelve levels of vertebrae. Below the thoracic spine is the lumbar spine, which bears the weight of the body and is composed of five levels of vertebrae. Finally, the sacral spine is located at the bottom of the back, between the hips (Figure 1) (34).
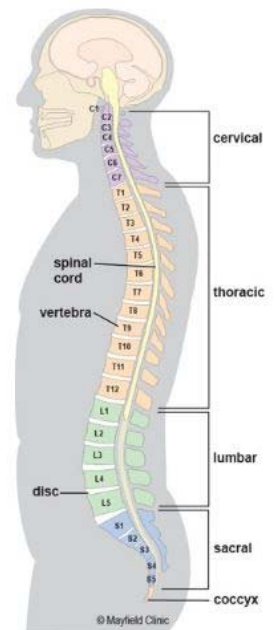
Figure 1: The five regions of spinal column (1)

The human spine consists of different tissues: vertebrae, IVD, spinal cord, muscles, facet joints, and ligaments. The vertebrae are the bones that are bearing the weight of the upper

body and formulate the structure of the spine. Each vertebra is composed of two regions: 1- the vertebral body; a solid cylindrical segment that provides strength and stability to the spine. 2- The vertebral arch; an arch-shaped section consisting of segments of bones, called processes, which articulate with each other and provide attachment points for muscles, ligaments, and tendons. The main processes in the vertebral arch are spinous process, transverse process, and articular process. The vertebral arch is linked to the vertebral body by two channels of bones called the pedicles. Together, the vertebral body, the pedicles, and the vertebral arch form a ring of bone around a channel known as the spinal canal (Figure 2) (34).
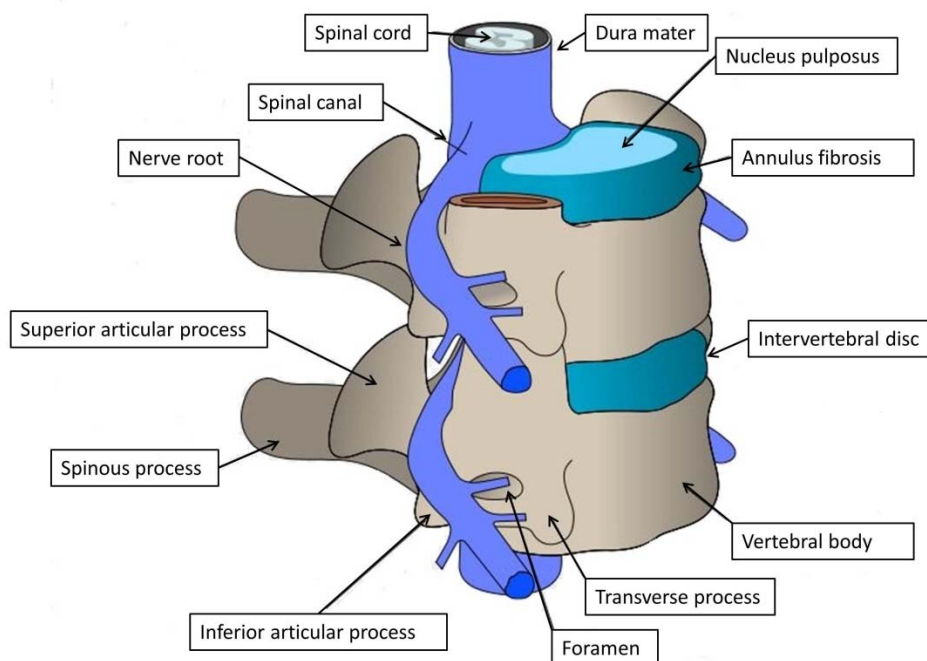
Figure 2: The vertebrae, IVD, and spinal cord (35)

The vertebrae are separated by cushioned IVD which functions as coiled springs to absorb shocks between the vertebral bodies. The IVDs are the main joints of the spinal column and occupy one-third of its height. They are composed of two different zones;

annulus fibrosus (AF) and nucleus pulposus (NP). The AF is a strong radial tire–like structure made up of lamellae; concentric sheets of collagen fibers connected to the vertebral end plates. The NP is a gel-filled nucleus composed mainly by fluid and encircled by AF. The NP is sandwiched inferiorly and superiorly by cartilage end plate; a thin layer of hyaline cartilage positioned between the vertebral endplate and the disc (Figure 2) (36). In addition, facet joints (zygapophysial joints), a low friction moist cartilage, are found at the articular processes of each spinal segment. Their function is to guide and limit the intersegmental motion and to provide stability and flexibility needed for the movement of the spine (37). Beside the IVD and the facet joints, each spinal level is connected to the immediate superior and inferior adjacent level via seven ligaments: Supraspinous ligament (SSL), interspinous ligaments (ISL), flavum ligaments (FL), posterior longitudinal ligament (PLL), Anterior longitudinal ligament (ALL), Intertransverse ligament (ITL), and Facet Capsular Ligament (FCL), see Figure 3.
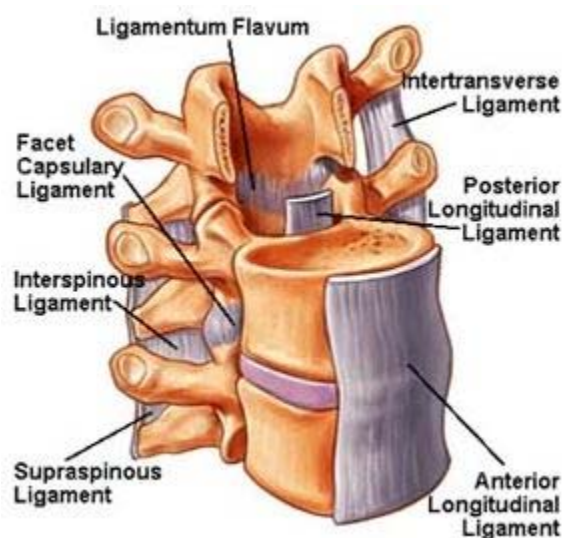
Figure 3: Spine Ligaments (adapted from (38))

Inside the spinal canal are the spinal cord; a subtle bundle of nerves and other tissue that connects the brain to the rest of the body. The spinal canal encompasses the beginning of the spinal nerve roots, which leave the spine through foramina to fork out to the body. Both spinal cord and nerve roots are houses immersed in a liquid called the cerebrospinal fluid CSF. Together, the spinal cord, the nerve roots, and the CSF are wrapped up by membranes called the meninges of which the outermost layer is a tough tissue layer known as the dura mater (Figure 2) (34, 35).

2.2 Lumbar Spine Degenerative Diseases

Degenerative tissue transformation can affect almost every structure of the spine. According to an epidemiological study conducted by the National Institutes of Health (NIH), approximately 60% of people over the age of 40 have some joint degeneration in the lower back, that is not often related to low back pain. Each degenerative disease is associated with characteristic radiographic and pathologic abnormalities (39). A brief review of the leading degenerative diseases that affect the lumbar spine is discussed as follow.

IVD degeneration is a common degenerative disease that can occur at any spinal level and is characterized by biochemical changes in the NP and the inner AF. Such changes induce the formation of clefts and fissures radiating from the central area of the disc towards the periphery (39). IVD degeneration can be caused due to genetic inheritance, impaired metabolite transport, cell senescence and death, or altered level of enzyme activity (40). Any of these degenerative mechanisms may lead to structural failure which

compromise the spine stability and may cause pain (40). Moreover, IVD degeneration can instigate disc herniation in which the fibrous outer portions of the AF crack, allowing some of the jelly-like core to protrude toward the spinal canal and compressing the spinal cord (41).

Facet joint osteoarthritis (FJO) is another degenerative disease of which its prevalence reaches up to 89% in individuals 60- to 69 years-old, with the highest occurrence in L4-L5 spinal level (42). FJO is caused when pressure act at the joints in a way that causes eradication of the cartilage on the joint surfaces (43). Increase in pressure is attributed to fractures, torn ligaments, or disc thinning that reduce the space between the spinal vertebrae, putting more stress on the surfaces of the facet joints (43). Accordingly, the body responses by developing bone spurs around the edge of the facet joints (hypertrophy) that make the articular cartilage arthritic and allow the bones underneath the cartilage to rub against each other causing inflammation, swollen, and severe pain (44).

Spondylolisthesis is a condition where a defect in a part of the spine drive the vertebra to slip to one side of the body (anteriorly or posteriorly) (45). Spondylolisthesis commonly occurs at L5 or L4 spinal levels. The etiology of spondylolisthesis has been classified in to five categories (46): 1- Dysplastic, a congenital abnormality of the upper sacrum or the arch of L5; 2- Isthmic, a lesion in the pars interarticularis; 3- Degenerative, intersegmental instability due to long standing; 3- Traumatic, fractures in the bony hook

other than the pars; 5- Pathological, generalize or localize bone disease. Typical symptoms of spondylolisthesis include back pain and/or leg pain (45).

Lumbar spinal stenosis (LSS) is a clinical syndrome that was the final diagnosis in 22% of patients with chronic back pain and is estimated to present in 5 every 1000 Americans over age 50 (47, 48). The first clinical description of LSS is accredited to Verbiest in 1954 (49). LSS is defined as anatomical reduction of the lumbar spinal canal that causes compression on the spinal cord or nerve roots (6). LSS may involve the central canal, lateral recess or foramina or any combination of these areas (6), and is classified as either caused by congenital abnormalities or acquired stenosis (5). In the latter, LSS can be resulting from degenerative alterations or a consequence of local infection, trauma or surgery (6). The most common symptoms attributed to LSS is neurogenic claudication and pseudoclaudication which eventually resulting in low back and/or leg pain (8).

2.3 Surgical Treatments for Lumbar Spinal Stenosis

Various surgical procedures can be employed for the treatment of each degenerative disease. However, because of focusing on LSS in specific-aim#1, a detailed review of available decompressive surgeries for LSS will be only discussed. In particular, Laminectomy is considered the gold standard operative treatment when there are no indications of pre-operative spinal instability (6, 50). Two procedures are classified under laminectomy; radical laminectomy and facet sparing laminectomy (51). In radical laminectomy, the entire lamina, spinous process, and facets of the vertebra are subtracted, together with the connecting flavum, interspinous, capsular, and supraspinous ligaments.

On the other hand, in the facet sparing laminectomy, all the steps performed in radical laminectomy is performed except removing the facets (52). Despite the effective outcomes of both procedures in treating the compressive symptoms, a number of studies reported postoperative spinal instability (53, 54). The spinal instability is attributed to the disruption caused at the midline structure (the spinous process, interspinous and supraspinous ligaments). More recently, laminotomy has been proposed as a less invasive alternative approach (50, 55-57). In this surgery, only the laminae and the flavum ligament, unilaterally or bilaterally, are subtracted. Accordingly, the midline structure is conserved, maintaining the segmental stability of the spine. However, due to the less resection of the posterior elements, smaller operative window is permissible, which may not allow complete neuro-decompression (51).

On the contrary, if the spinal stability is compromised or the stenosis is associated with spondylolisthesis or degenerative scoliosis, spinal fusion is recommended (58). To increase the fusion rate and provide indirect decompression, interbody fusion is increasingly adopted in open and minimally invasive surgeries. In particular, posterior lumbar interbody fusion (PLIF), anterior lumbar interbody fusion (ALIF), lateral lumbar interbody fusion (XLIF), and transforaminal lumbar interbody fusion (TLIF) are the most common practiced procedures for spinal arthrodesis (59-63). In all of these approaches, the IVD is removed and vertebral endplates are decorticated, followed by implanting different supplemental instrumentation. Each approach has its own pros and cons. For instance, the anterior approach allows better visualization of the IVD and facilitates the creation of a higher degree of distraction and lordosis (61). However, the anterior

approach entails the movement of the great vessels and the peritoneum, which tolerates potential morbidity of vascular injury and ureteral damage (64). In contrast, the posterior approach overcomes the potential morbidity associated with the anterior approach, but provides narrow access to the IVD. In particular, the PLIF procedure requires major retraction of the neural elements and the thecal sac to access the IVD that may increase the risk of neurologic injury (65). Conversely, the TLIF approach can circumvent this injury by accessing the spine from the lateral side. However, it has known drawbacks, such as poor contralateral root decompression and incomplete disc removal (61). Accordingly, the decision of which approach to be utilized must be tailored for each patient considering the analysis of risks and benefits of each possible surgical procedure.

All surgical treatments for LSS, either decompression or decompression with fusion, involve alteration of the bony and soft tissue anatomy in the affected portion of the spine. The particular alterations to the musculoskeletal anatomy generated by each of these procedures may alter the normal physiological biomechanics of the untreated segments of the spine (13, 66). Such alterations might have implications for the development of the ASD. In a recent long follow-up study (~13 years), Mannion and co-workers found that spinal fusion is associated with signs of disc degeneration at the adjacent segments (67). Moreover, both numerical analyses and *in-vitro* studies on cadaveric spine have shown that, as a consequence of fusion or laminectomy, adjacent segments experience larger ranges of motion, increased intradiscal pressure, and increased stress in the IVD (51, 68-70). They also observed that as the number of fused levels increase, intradiscal pressures at adjacent IVDs increase proportionally. Accordingly, it is believed that the surgical

intervention for LSS may trigger another spinal degenerative disease, which may require a revision surgery.

2.4 Thoracolumbar Spine Traumatic Fractures

Traumatic fractures of the thoracolumbar spine, especially the thoracolumbar junction (T10–L2), are the most common fractures of the vertebral column, reaching up to 160,000 annual injury in North America (71). This is because the thoracolumbar junction (T10-L2) represents the transitions from the less mobile thoracic segments to the lumbar spine (72). If the injury is above L1, it damages the lower spinal cord producing a typical upper motor neuron picture of paralysis. If the injury is below L1–L2, however, it may affect only the cauda equine leaving a lower motor neuron flaccid paralysis (72).

Various classification systems of spine fractures have been proposed. In 1983, Denis suggested dividing the spinal column into three columns; anterior, middle and posterior columns (Figure 4) (18). The middle column was considered the biomechanical key to identify whether the fracture is stable or unstable (73). Latter, in 1993, Magerl et al. has introduced a complex hierarchical classification system based on pathomorphologic criteria (19). They subdivided the vertebral fractures into three main types: type A (compression, the most common 66%), type B (Anterior and posterior element injury with distraction), and type C (fracture dislocation with rotation). However, due to its detail and complexity, it was cumbersome for the daily clinical use (74, 75). Recently, Vacarro et al. have proposed a new thoracolumbar injury classification and severity score (TLISS) based on three parameters: the morphology of the fractured vertebrae, the

neurologic status of the patient, and the integrity of the posterior ligamentous complex

(76). This system has not only provided a reliable system to determine injury stability and

prognosis, but also provided a good guidance for surgical treatment. According to these

classification systems, a definition of four fundamental fracture types was introduced:
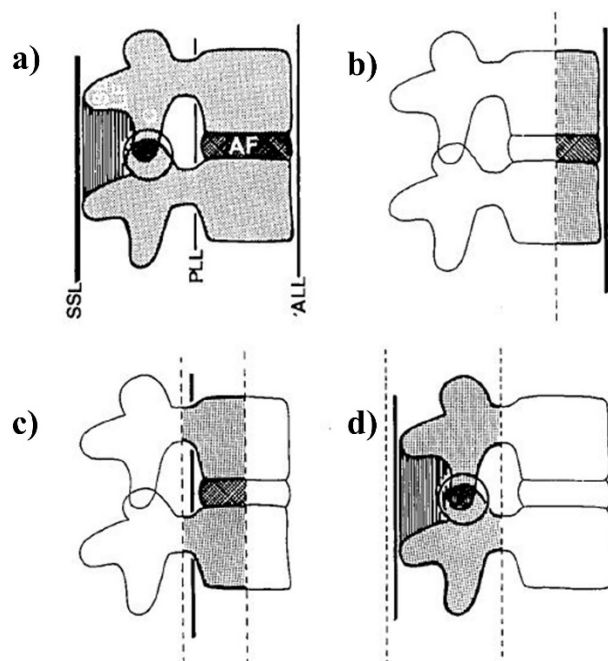
Figure 4: Denis three-column theory: a) all columns; b) anterior column; c) middle

column; d) posterior column (18).

1- **Compression fracture:** This is the most common spine injury and it is typically

occur after moderate trauma and in osteoporotic individuals (Figure 5.a).

Compression fractures are considered stable injury where only the anterior

column is involved while the middle and posterior columns together with the

neural elements remain intact (73).

2- **Burst fracture (BF):** This injury accounts for 28% of all fractures of the thoracolumbar spine (31). BF is characterized by the disruption of both anterior and middle columns of the vertebral segments due to compression loading with or without flexion (18) (Figure 5.b). BF is commonly seen in motor vehicle accidents, falls from heights, or high-speed accelerating sports accidents. According to Magerl et al., a second subdivision is presented for burst fractures: A3.1 corresponds to an incomplete burst fracture, A3.2 to a burst-split fracture, and A3.3 to a complete axial burst fracture. Also, for all subdivisions, complete or partial neurologic deficit could be associated (19).

3- **Flexion-distraction injuries:** It is also known as seat-belt fracture. In this injury, both posterior and middle column fails under tension force generated by flexion with its axis placed in the anterior column (73) (Figure 5.c). Due to the extreme force required to disrupt the entire spinal column, the abdominal viscera can suffer injury as well (77).

4- **Fracture dislocations:** This is the most unstable fracture in which all three columns fail under compression, tension, rotation, and shear (18) (Figure 5.d). It is often associated with other musculoskeletal trauma and neurologic injury.
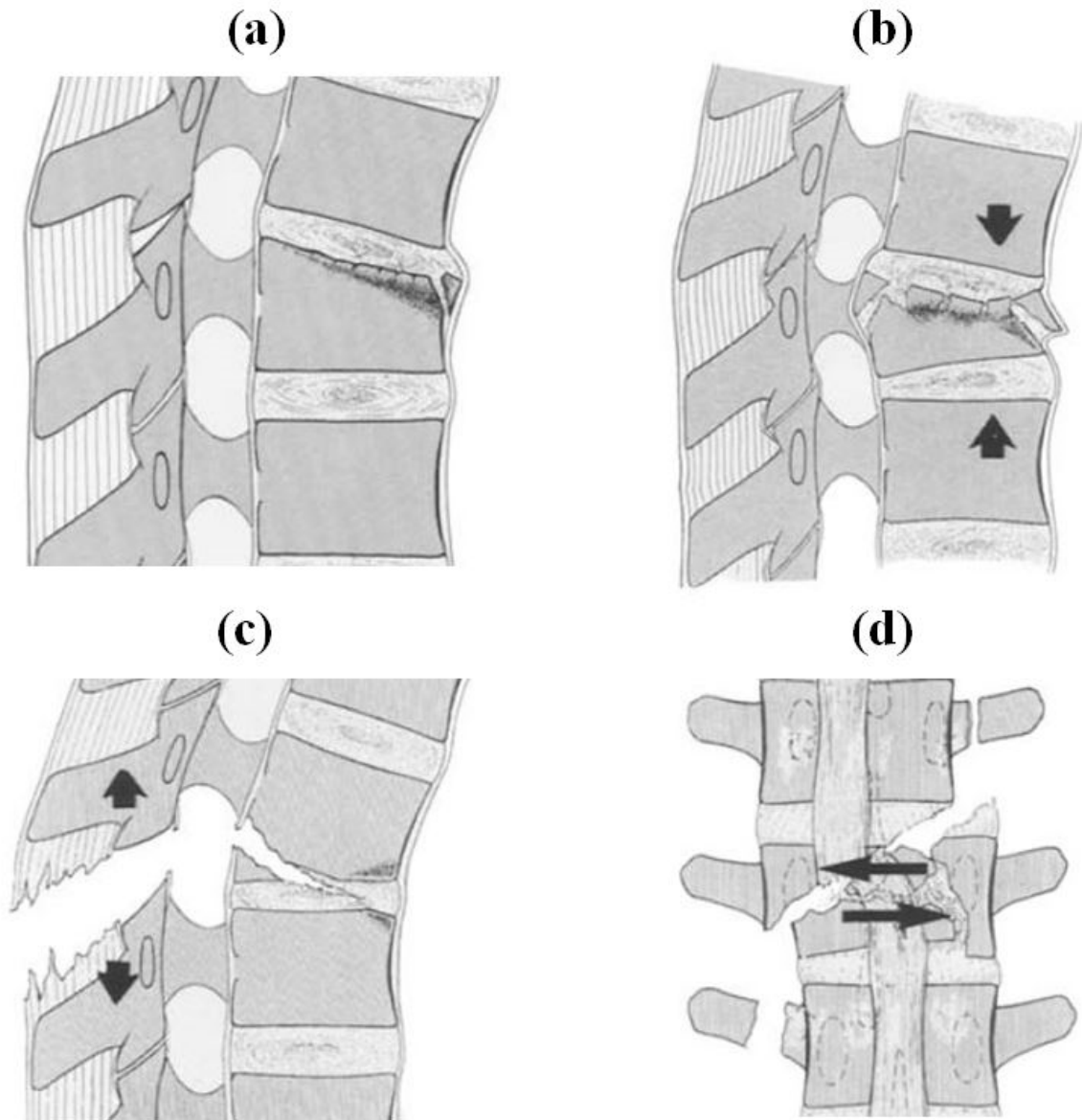
Figure 5: Thoracolumbar spine fractures classification: (a) Compression fracture; (b) Burst fracture; (c) Flexion-distraction fracture; (d) Fracture dislocation (adopted from (19)).

In some cases of compression and burst fractures, the operative management is advocated for better neural decompression and restoration of spinal stability. However, in case of flexion-distraction or fracture dislocation injuries, surgical intervention is vital for the patients (72).

2.5 Surgical Treatments of Thoracolumbar Burst Fracture

Surgical management is typically indicated for most thoracolumbar BFs, especially those associated with neurologic deficiency (78). The goal of the surgery is to stabilize the fracture, restore the sagittal alignment, and decompress the neural elements (2). The optimal operative treatment for thoracolumbar BF is still a matter of debate (11, 74). Multiple approaches have been proposed, such as anterior decompression and fusion, long or short posterior decompression and fusion, posterior fusion without decompression, a circumferential approach by combining anterior and posterior decompression with fusion, posterior stabilization without fusion, and posterior fusion with reconstruction of the spinal column by using interbody implant (79). The neurologic integrity is deemed a key factor in determining the best approach to be utilized. It was found that the incidence rates of neurologic deficit associated with spine fractures ranges from 21% to 41.6% (80). Accordingly, in this study, the surgical approaches for BF are classified to those described for incomplete or complete neurologic dysfunction.

In case of incomplete neurologic dysfunction that is associated to moderate comminution of the vertebral body, decompression of the spinal canal and fracture reduction are essential (81). Various approaches of decompression and fusion are available and have demonstrated no statistically significant differences in terms of restoration of neurological function (82). In particular, the posterior approach, long or short segment fixation, is deemed a straightforward approach that avoids vital viscera often encountered with anterior surgery. Posterior approaches also provides better reduction in cases of distractional and rotational injuries (79). However, in many cases, psoterior approach

may not provide sufficient support to the anterior column, eventually leading to loss of the kyphosis correction and spinal instability (20, 83, 84). On the contrary, the anterior approach provides a combination of decompression, reduction, bone grafting and osteosynthesis (85). This approach requires less spinal motion segments to be fused and is more reliable in maintaining the kyphosis correction by providing more support to the anterior and middle columns (72). However, it is related with higher blood loss and respiratory complications than the posterior approach (86). Moreover, anterior approaches has more contraindications, such as morbid obesity, respiratory insufficiency, purulent pleurisy, and coagulation disorders (86).

On the other hand, in case of neurologic deficit with severe comminution of the vertebral body, solely applying posterior or anterior approach may be insufficient to stabilize the spine and maintain the kyphosis correction (20). In such cases, it is advocated to use a circumferential approach to combine the advantages of anterior and posterior approaches (87). Hence, the surgeon will be able to perform decompression, anterior and middle column reconstruction, as well as posterior tension band restoration. However, the combined approach invokes an extensive surgical procedure that entails longer operative time, higher blood loss, and higher possibility of infection (2).

With the advent of the concept of minimal invasive surgeries (MIS), a new perspective in the treatment of thoracolumbar trauma was offered. The main advantages of the MIS are minimizing conventional approach morbidity, reduced pain, and earlier return to activity (88). Many popular minimally invasive techniques are now available, such as anterior

endoscopic decompression and stabilization, percutaneous pedicle screw fixation (PPSF), Kyphoplasty (KP), and the use of a temporary spinal external fixator and percutaneous end-plate reduction together with augmentation (79). In particular, KP has been suggested to for traumatic fractures after their admirable results in the treatment of osteoporotic compression fractures (89). Another perspective of treatment is to utilize the MIS techniques as an adjunct to conventional posterior stabilization methods (30). For instance, posterior percutaneous stabilization has been used either as a stand-alone procedure, or as an adjunct anterior decompression (90). Moreover, PPSF has also been used in combination with percutaneous balloon KP. Such surgical combination provided excellent immediate reduction of segmental kyphosis with simultaneous reduction of spinal canal encroachment and restoration of vertebral body height at the level of fracture (91). By the advancement in MIS technology, it is believed that these procedures would replace many of the conventional ones.

2.6 Finite Element Analysis in Spine Biomechanics

The finite element (FE) method represents one of many analytical techniques that can be used in combination with experimental testing to investigate the biomechanics of the spine (92). Despite the numerous mathematical tools available for such analyses, none of them can efficiently handle the complex structural geometry of the spine. However, the exceptional capability of the FE method to estimate stresses in the structures with complex geometry, loading, and material behavior makes the technique superior to many other mathematical alternatives (16). According to Maas et al. (15), "In biomechanics, FE modeling has already become a standard methodology, both for interpreting the

biomechanical and biophysical basis of experimental results and as an investigative approach in its own right when experimental investigation is difficult or impossible".

The FE method has been applied to problems in spine biomechanics as early as the 1970s (93). Many articles have reviewed the application of FE method on the literature of spine biomechanics. For instance, in 1986, Yoganandan et al. reviewed static and dynamic FE modeling in the area of spinal mechanics (94). They focused in the continuum and discrete parameter models of the intact spine and aspects of spinal injury. Then, in 1995, Goel and Gilbertson summarized the simple and detailed approach of using the FE method in the thoracolumbar spine (16). They predicted that a comprehensive biomechanical model of the entire trunk will be developed, including the effects of muscles, poroelastic and swelling behavior of the disc, and bone remodeling. Afterward, in 1996, Yoganandan et al. conducted another comprehensive review of cervical spine FE modeling applications in which they focused on the developments in model construction, constitutive law identification, boundary conditions, and validation (95). More recently, Natarajan et al. reviewed the most recent advances in the development of poroelastic analytical models that include physiologic parameters aiming at investigating lumbar disc degeneration due to repetitive loading (96). Nowadays, automated methods for patient-specific FE spine models are the main interest of many research groups to help in customizing the treatment for each patient with spine pathological condition (97, 98).

To use the FE method, the model must be primarily defined as one geometric entity and discretized in to small divisions called elements. These elements are assumed to be joined

at the corners (nodes) to establish the whole structure (92). Different types of 3D elements with different geometric form are available: Tetrahedral Element (4 Nodes, 6 Nodes), Hexahedral elements (8 Nodes, Brick), see Figure 6. Then, by employing these elements shapes, the spine can be modeled with varying degrees of complexity. Importantly, the solution obtained by the FE method is approximate, where it converges to the exact solution for the model when the mesh density approximates infinity (99). Careful formulation of the problem is crucial in order to obtain reasonable results. Simplification of geometry, material properties, and loading conditions is often needed, which may negatively affect the validity of the results. However, the advancements in imaging techniques and the great improvements in computational speed have permitted relaxing of many assumptions and increasing the complexity of the geometry, resulting in more reliable models.

20-Nodes Block Element   8-Nodes Block Element   4-Nodes tetrahedron   6-Nodes prism
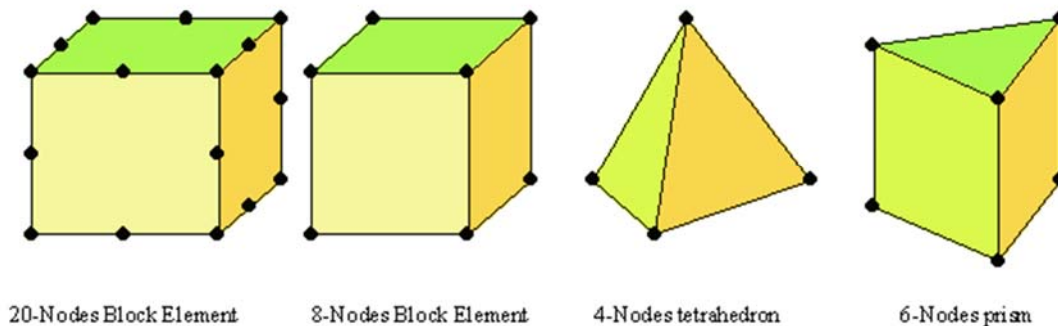
Figure 6: 3D finite element types (100)

2.7 Significance of the Proposed Research

Lumbar spinal stenosis (LSS) is a clinicopathologic disorder that is presented in 5 of every 1000 Americans over age 50 (5). Persistent symptoms of LSS are treated with

decompressive surgeries that entail alterations in the spine anatomy. Longitudinal studies on surgically treated patients reported the occurrence of adjacent segment disease (ASD) without knowing their etiology (101). The first aim proposed in this research attempts to elucidate the biomechanical implications of decompressive surgeries on the health of the adjacent segments. This research work is significant because it will provide more information on the alterations, caused by decompressive surgeries, on the biomechanics of the adjacent segments and contribute to understanding the mechanisms underlying the development of ASD.

The second aim of this research is focusing on evaluating the biomechanical performance of the spine after surgical treatment of traumatic thoracolumbar burst fracture. It was reported that the annual injury rate of this trauma exceeds 25,000 in the United states (72), and it is usually associated with neurologic dysfunction (79). Different fixation procedures, through open or minimally invasive surgeries, are performed for the treatment. However, the mechanical performance of the fixation devices and their implications on the adjacent levels is still unclear. The second aim of this research attempts to evaluate the mechanical behavior of different fixation constructs and to characterize the post-operative changes in the biomechanics of the adjacent segments. This research work is highly significant because it will address, from a biomechanical perspective, the unsolved question of which is the surgical approach for BF that provides the best outcomes in both the short- mid-term (stability of fixation constructs) and long-term (biomechanical alterations on adjacent segments).

Furthermore, the computational tool developed in this research used a more realistic definition for the IVD constituent (i.e. biphasic media) that is highly capable in characterizing the mechanical behavior of the spine. Such tool could be used in clinics for improving the current medical treatments: driven by patient specific image data, the model could be deployed for optimizing the choice of treatment for the patient affected by LSS and traumatic BF, to minimize those alterations of physiological spine biomechanics due to surgical procedures.

Chapter 3 General Computational Approach

This chapter illustrates the general method that is used in the studies presented in the following four chapters to fulfill the specific aims. An explanation of the segmentation process of the spine tissues from CT scan, the CAD tool that is used to virtually perform the surgery, the meshing process, the definition of boundary condition, and the validation of the FE models are explained in detail.

3.1 Spine Segmentation and Computer Aided Design of the Surgeries

Toward building the spine FE models, a unique work flow was developed to translate the 3D anatomy of the spine, replicate the surgical procedures, and simulate postoperative physiological loading conditions in a way that ascertain the validity of the results. A brief illustration of the work flow is shown in Figure 7. The first step in the work flow is to transfer the CT scan of the spine in to a 3D model that describes the anatomy of this particular spine. In this work, a CT scan of a healthy male subject from the Visible Human Project® was utilized (102). A 3D segmentation was performed for the vertebral bodies of the spine from T10 to S1 by using medical imaging processing tool (Mimics Research 17.0x64; Materialise, Louvain, Belgium). Specifically, masks were created for the cortical and cancellous bones of each vertebra by adjusting the threshold of the images within the limits of 262 to 2000. Different mask editing tools were used to delineate the morphology of each anatomical region. A 3D object was calculated for each mask by using the optimal quality option in Mimics which yielded a 3D anatomical

model for all the thoracolumbar spine segments. Finally, all the calculated models were smoothed, wrapped, and polished to make it easily handled in the meshing process.
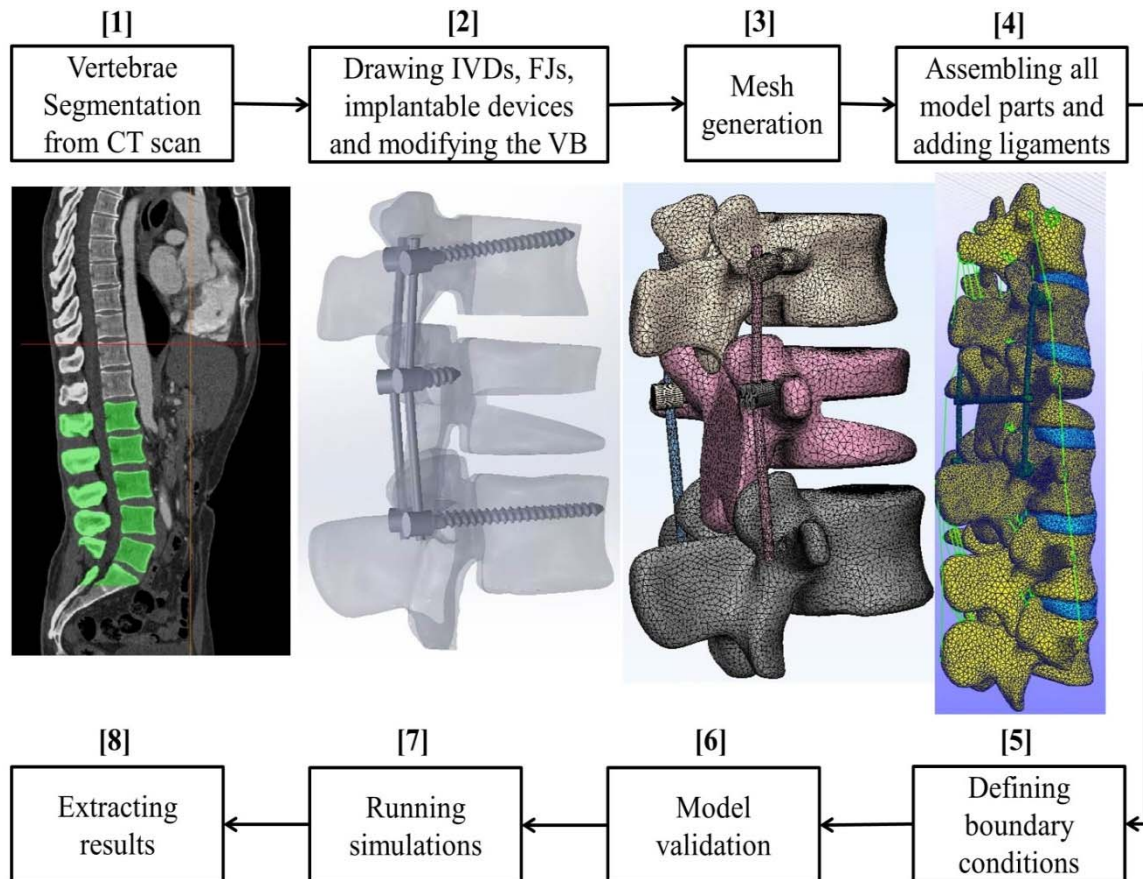
Figure 7: Work flow for creating FE model of the lumbar and thoracolumbar spine

In step [2], all the models were exported as STL files and passed to the CAD tool (SolidWorks 2013x64 edition, Dassault Systèmes SolidWorks Corporation, Waltham, Mass. 02451 USA) to add the rest of the spine tissues, perform surgical procedures, and introduce the implant devices. Specifically, the IVDs and the facet joints between the adjacent vertebrae were imitated by using different surface and 3D tools. In addition, all the surgical procedures were performed in this step. In particular, anatomical subtraction of the bones, facet joints, or IVD was performed by using different cutting tools. For

instance, in the unilateral laminotomy, a portion of the lamina was chopped in only one lateral side. However, in the bilateral laminotomy, laminas were resected from both sides. Moreover, all the implantable devices were constructed and precisely placed in their targeted sites after the surgery in this step. The most important placement was to implant the pedicle screws on the same insertion point and with the same inclination angle as was done on the actual surgery. Once the procedure is resembled on the CAD work, 2D and 3D images of the post-operative spine models were sent to an orthopaedic surgeon for confirming the preciseness of the anatomical subtractions and the placement of the implantable devices.

3.2 Meshing of Finite Element

When the post-operative spine models are approved, all the model components were exported separately from the CAD tool (SolidWorks) to a mesh generating tool (to discretize it in to finite elements) in step [3]. Two different meshing tools were used: ABAQUS/CAE 6.11-1 (Dassault Systèmes SolidWorks Corp., Providence, RI, USA); and 3-matic 10.0 (Materialise, Louvain, Belgium). Also, two element types were utilized in the volumetric meshing process: 4-node tetrahedral element; or 8-node hexahedral element, depending on the complexity of the geometry and the required accuracy (Figure 5). In particular, since the vertebrae and the implantable devices are complex in geometry, they were meshed in 3-matic by using 4-node tetrahedral elements. In this process, different meshing editing tools were utilized such as, Boolean intersection, Boolean subtraction, and Create Non-manifold Assembly to overcome their complexity. It is advised to read 3-Matic tutorial prior starting this process to figure out the optimal

procedure to obtain the best quality mesh. Also, in this step, the cortical and cancellous bones were combined in one part to prevent any contact problem and to unify the nodes at their interfaces. However, the rest of the parts were meshed separately and an interface was defined between them as it will be described latter. On the other hand, since the IVD and the facet joint have more uniform geometry, 8-node hexahedral elements were used for meshing them in ABAQUS (Figure 8). During meshing the IVD, the geometry was partitioned to define for concentric lamella in the annulus fibrosis (AF) area as shown in Figure 5. Generally, the number of elements of a vertebra, IVD, and facet joint were around 50,000, 5000, and 1000 respectively. It is noteworthy to mention that the first 3-steps in the work flow might need to be iterated several times until a satisfactory meshing quality is reached.
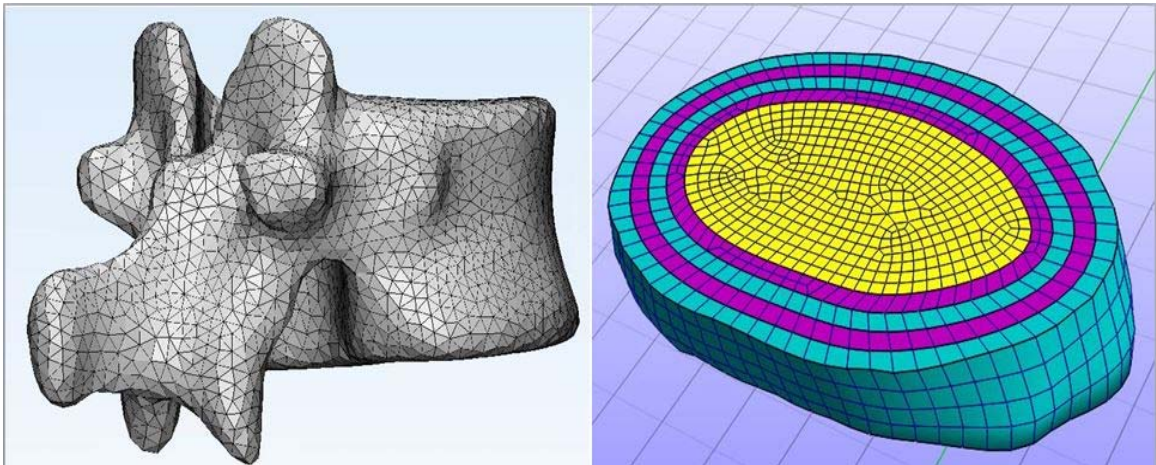
Figure 8: Meshing types used on the FE models

3.3 Defining the Boundary Conditions of the Finite Element Models

Subsequently, in step 4, all the meshed parts were imported in to a nonlinear FE analysis suite (FEBio 1.8.0, Musculoskeletal Research Laboratory, University of Utah, Salt Lake

City, UT). The FEBio software is a nonlinear implicit FE framework designed specifically for analysis in computational solid biomechanics, whose accuracy and the robustness have been documented (15, 103). Model parts were assembled one by one to construct the entire domain of interest. Afterwards, all seven spinal ligaments, including supraspinous ligament, interspinous ligament, transverse ligament, capsular ligament, flavum ligament, posterior longitudinal ligament, and anterior longitudinal ligament were added and defined as linear elastic tension-only spring elements (104).

In step 5, all the boundary conditions (BCs) and material properties of the model components were defined. BCs were divided into two categories: General BC and specific BC. The general BCs were defined for all the models regardless of the application, and it includes defining the contacts between any adjacent tissues, and defining the analysis that is used for solving the FE problem. Specifically, the vertebrae were modeled as composed of an inner trabecular core enclosed by an outer cortical shell. The IVDs were defined as two distinct anatomic regions: the annulus fibrosus (AF) and the nucleus pulposus (NP). Both AF and NP were considered as biphasic media constituted by a solid phase embedded in a fluid phase (105, 106). The solid phase of AF was modeled as a fiber reinforced hyperelastic composite: collagen fibers were modeled as tension-only elements (107) and arranged in a total of four concentric layers enclosing the NP with alternating ±30° orientation, see Figure (5) (108). The ground substance of AF was modeled as a Mooney- Rivlin material (109), while the solid phase of NP was isotropic elastic (110). Water volumetric fractions and hydraulic permeability for both NP and AF were 0.75 and 0.86, respectively (111-113). Each facet joint had a gap of 0.5 mm

and two cartilaginous layers which were modeled as elastic isotropic materials (114). A summary of the values of the material properties is reported in Table 1.

Table 1: Material properties of spine tissues used in the FE model

Material	Property	Value	Reference
Cortical bone	Moduli in MPa	E = 12,000	
	Poisson's ratio	ν = 0.3	(115)
Cancellous bone	Moduli in MPa	E = 100	
	Poisson's ratio	ν = 0.2	
Annulus fibrosis	Ground sub. Mooney-Rivlin coeff.	c1 = 0.18; c2 = 0.045	(109)
	Collagen fibers (tension-only)	Stress–strain curve	(107)
	Hydraulic permeability	0.00021 mm^{4}N^{-1}s^{-1}	(112)
	Volumetric fluid fraction	0.75	(111)
Nucleus pulposus	Ground sub. isotropic elastic moduli	E = 0.2 MPa	(110)
	Ground sub. poisson's ratio	ν = 0.499	
	Hydraulic permeability	0.00067 mm^{4}N^{-1}s^{-1}	(113)
	Volumetric fluid fraction	0.86	(111)
Cartilage	Moduli in MPa	E = 35	(114)
	Poisson's ratio	ν = 0.4	
Ligaments	Stiffness (tension-only)	Linear elastic	(104)

The second element that was defined in the general BCs was the contacts between all adjacent tissues and between the implantable devices as illustrated in Figure 9. In particular, a tied-biphasic interface was defined between the interfaces of the IVD and the cortical bones of the superior and inferior vertebral bodies, and between the interfaces of the cartilage of the facet joints and the articular process of the vertebrae. The tied biphasic interface connects two non-confirming meshes (master and slave surfaces) and

does not allow interference of both sides. It can tie any combination of solid, biphasic, and rigid materials, while enforcing continuity of the fluid pressure across the interface when both materials are biphasic (116). In addition, a sliding interface was defined between the two cartilage surfaces of the facet joint. For the models that comprised implantable devices, either sliding or tied interface was defined according to the actual reaction between the surfaces as demonstrated in Figure 6. It is important to mention that the augmented Lagrangian algorithm was always used to solve the contact problem. Also, penalty factors were tuned in each contact site to allow the convergence of the problem while minimizing the interference between both sides of the interface. Moreover, of all investigated models, a follower load of 400 N was applied at the most superior level. A follower load is a compressive load applied along a follower load path that approximates the tangent to the curve of the lumbar spine, thus subjecting the whole lumbar spine to nearly pure compression (117). It represents the muscle forces that act to stabilize the spine. Finally, a steady state nonlinear biphasic analysis was utilized to solve the model. This analysis couples the fluid problem with a solid mechanics problem which is the most appropriate solver technique for this application. On the other hand, the specific BCs are described in the methods section of each study. Specific BCs encompass the loading condition, the testing protocol (flexible or hybrid), and what levels were fixed. The flexible and hybrid testing were used because they are the most common in the biomechanical testing field (118).
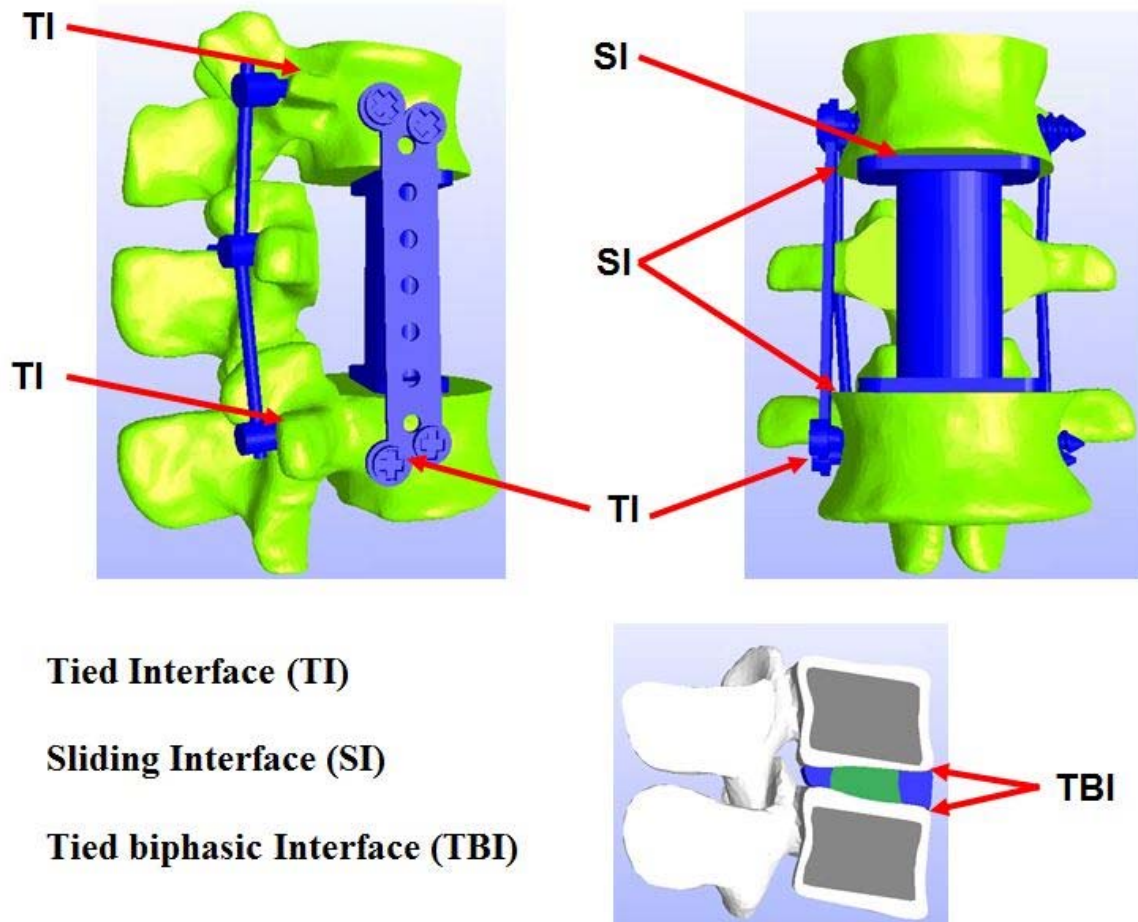
Figure 9: Types of contacts used between model components

3.4 Model Validation

Next, in step [6], the models were validated by comparing their predictions of two parameters to either experimental data conducted by our collaborators on the Max Biedermann institute for Biomechanics or documented data in the literature. Specifically, the intersegmental range of motion (ROM) and the intradiscal pressure (IDP) were utilized in the validation process. The results of the validation with the intersegmental ROM are reported in the results section of each study and all of them showed a good agreement. However, since there are few experimental studies that reported the values of

the IDP, the validation with the IDP was carried out only for two cases: 1- the predicted values of the IDP for all lumbar spinal levels of the intact spine model were compared with an *in-vitro* study (117). 2- The predicted values of the IDP at one adjacent level (i.e. L3-L4) for the procedures investigated on aim 1 (i.e. intact, bilateral laminotomy, and facet-sparing laminectomy) were compared to a pilot *in-vitro* experiment that was conducted in the Max Biedermann institute for biomechanics. The results of these comparisons are reported here because the loading condition used in these experiments was different than the one that was used in those studies. Accordingly, different simulations were carried out, using the same material properties, for the sake of validating the IDP. A detailed explanation of the IDP validation for the two cases is as follow.

Case 1: In a previous *in-vitro* experiment (117), Rohlmann and coworkers conducted tests on lumbar spine specimens to measure the IDP under different loading conditions. Flexible pressure transducers with a diameter of 1.2 mm were placed in the pulpy nucleus of each of the four discs (from L1-L2 to L4-L5). However, the exact location of the transducer's tips was not described. The reported IDP values obtained from applying 3.75 Nm pure flexion moments were compared to the predicted IDP values from the intact spine model after applying the same loading condition (Figure 10). Since the placement of the pressure transducers was not precisely described, the range of IDP generated at all the finite elements on the NP was reported in Figure 7 (the range on the red bars). Hence, for all spinal levels, the IDP values of the experiments were always within the range of the values generated in the FE model. It is important to mention that the initially chosen elastic moduli of some ligaments as well as the discs were slightly modified in the finite

element model within the physiological range to improve the agreement with the experimental results. Such parameters tuning is accepted and was previously reported in the literature (108). The final material properties that achieved the best agreement with the experimental results are reported in Table 1.
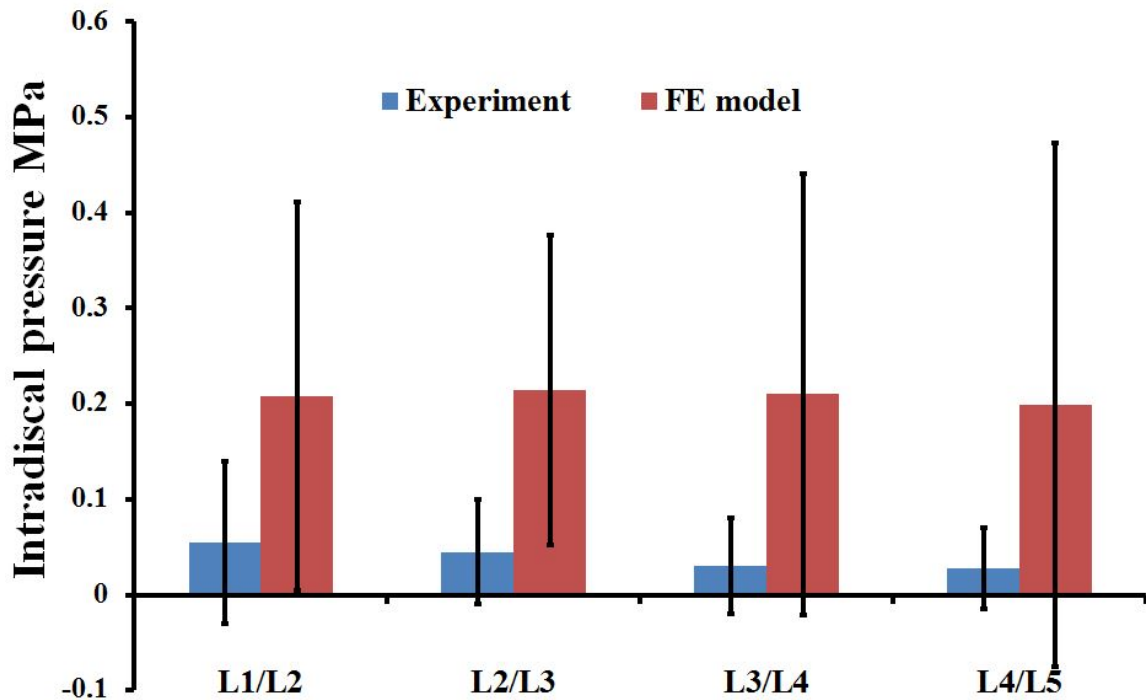
Figure 10: The IDP obtained from the intact spine model compared to experimental data (117). The bar on the blue data represents the maximum and minimum values among all tested specimens. The bar on the red data represents the maximum and minimum values among the finite elements of NP

Case 2: the IDP values obtained from the FE models in specific aim 1 were compared to the IDP obtained from a pilot *in-vitro* experiment that used one cadaveric spine. Specifically, in this experiment, the spine was tested with flexion/extension pure moments of 5 Nm for the intact case and after performing bilateral laminotomy and facet-sparing laminectomy. Pressure transducers were inserted via a needle into L3-L4 disc

along the anteroposterior direction, and their location within the tissue was verified by fluoroscopic images (Figure 11). The IDP was measured in a total of 3 points along the anteroposterior axis, progressively sliding the needle through the posterior annulus fibrosus (P-AF), the nucleus pulposus (NP), and the anterior annulus fibrosus (A-AF). Again, since the placement of the pressure transducers at L3-L4 level was not precisely described, the range of IDP generated at all the finite elements on the three regions (i.e. P-AF, NP, and A-AF) was reported. A good agreement was found between both set of data (Figure 9).
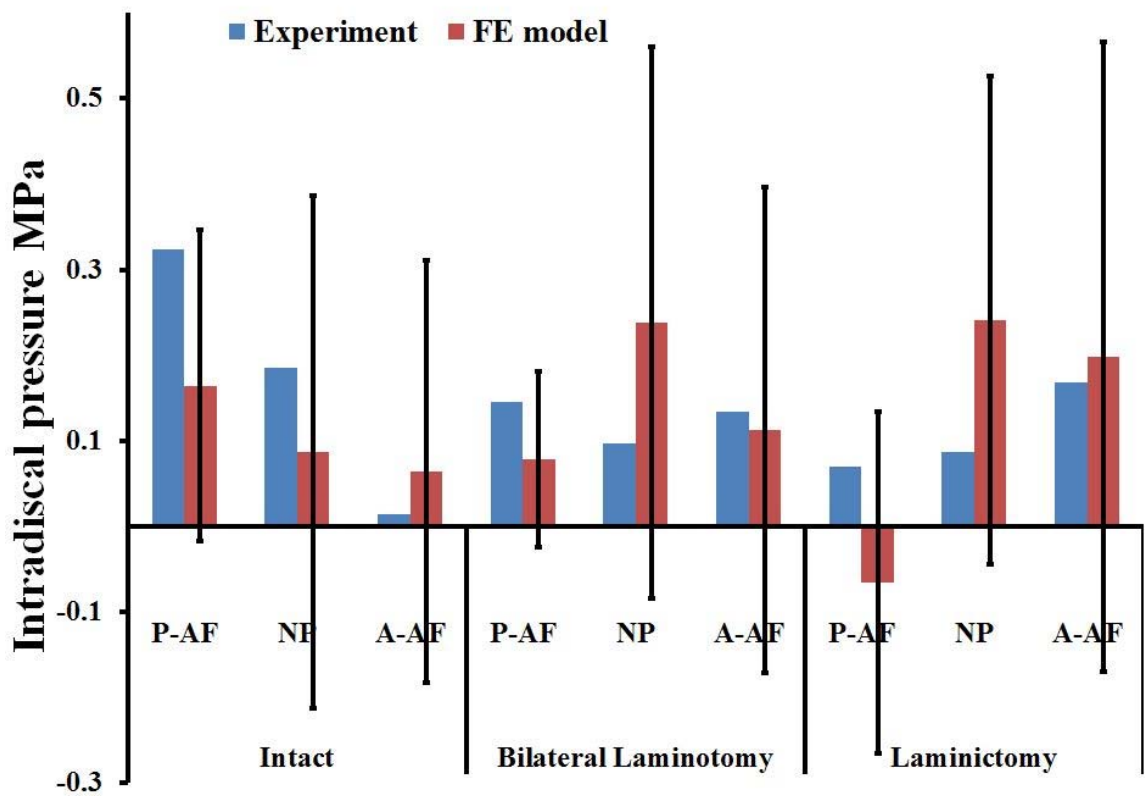
Figure 11: The average IDP values obtained from the FE models compared to those obtained from the pilot experiment at level L3-L4. The bar on the red data represents the maximum and minimum values among the elements of each region

Once the model was validated, in step [7], all the settings were fixed and only the applied moments were changed to perform the planned simulation that is specific for each study (more details are explained on the method section of each study). Finally, in step [8], all the results of the simulations were extracted and analyzed.

Chapter 4 The Biomechanical Implications of Decompressive Surgeries on The Spine

4.1 Introductory Remark

With a prevalence of approximately 20% in individuals older than 60 years, and up to 80% in those older than 70 years, LSS is exerting a greater clinical impact as the population ages (8, 119). LSS is characterized by the constriction of the spinal nerve at one or more spinal levels due to the development of spine degenerative disease, such as disc degeneration, disc herniation or spondylolisthesis (5). The clinical symptoms of LSS, defined as radiculopathy or myelopathy, is identified by lower extremity pain, paresthesia, and low back pain [3-5]. In many LSS patients, surgical treatment is preferred (5). The goal of surgery is to decompress the spinal nerves without compromising spinal stability (4). In the past 60 years, a myriad of surgical techniques have been developed for achieving this goal (5, 6); however, longitudinal studies on surgically treated patients reported a significant number of revision surgeries due to the development of ASD (e.g., disc herniation, spondylolisthesis, newly developed stenosis, etc. at the adjacent segments) (6, 120, 121). The etiology of ASD is still unclear, but many studies suggested that the disease could be developed due to the procedures performed for LSS treatment (122, 123).

All surgical treatments for LSS involve alteration of the bony and soft tissue anatomy in the affected portion of the spine. The particular alterations to the musculoskeletal anatomy generated by each of these procedures may mutate the normal physiological biomechanics of the adjacent spinal segments (13, 66), eventually leading to the

development of ASD. Typically, laminectomy or laminotomy are the common surgical approaches performed when there are no indications of pre-operative spinal instability (55, 56, 124). The implications of such surgical approaches on the biomechanical behavior of the spine have been investigated via clinical (55-57, 124), *in vitro* (51, 66, 70, 125), and numerical studies (126-129). However, information on the specific alterations on the biomechanics of the adjacent spinal segments was overlooked and requires more investigation to minimize the risk of the development of ASD. Accordingly, the objective of this study is to investigate the implication of four different laminectomies and laminotomies procedures on the biomechanics of the adjacent segments. Specifically, the post-operative kinematics, intradiscal pressure, and generated stresses at the adjacent segments due to unilateral laminotomy; bilateral laminotomy; facet sparing laminectomy; and laminectomy with facetectomy (radical laminectomy) were evaluated.

4.2 Methods

A lumbar spine model from L1 to L5 was developed according to the general computational approach in Chapter 3. The only exception was assuming the vertebrae as a solid rigid body. The IVDs and the cartilaginous layers at facet joints were meshed by 8-node hexahedral elements (~3200 elements for each IVD, and ~1000 element for each cartilage layer).

Surgical procedures of unilateral laminotomy, bilateral laminotomy, facet-sparing laminectomy, and laminectomy with complete facetectomy were simulated at L4-L5 level (Figure 12). In the FE model, the ligamentum flavum at each spinal segment was

modeled as composed of two spring elements (one element for each operative side). Accordingly, for unilateral laminotomy, only the spring element corresponding to the operative side was removed, together with part of the vertebral lamina (Figure 12.a). In contrast, in bilateral laminotomy, the entire ligamentum flavum (i.e., both spring elements) was removed (Figure 12.b). When simulating facet-sparing laminectomy, the entire lamina of the vertebra was removed, together with the connecting flavum, interspinous, and supraspinous ligaments (Figure 12.c). Finally, for laminectomy with complete facetectomy, in addition to all the steps performed in the case of facet-sparing laminectomy, the facet joints (including cartilaginous layers and capsular ligaments) were also removed (Figure 12.d).

(a)
(b)
(c)
(d)
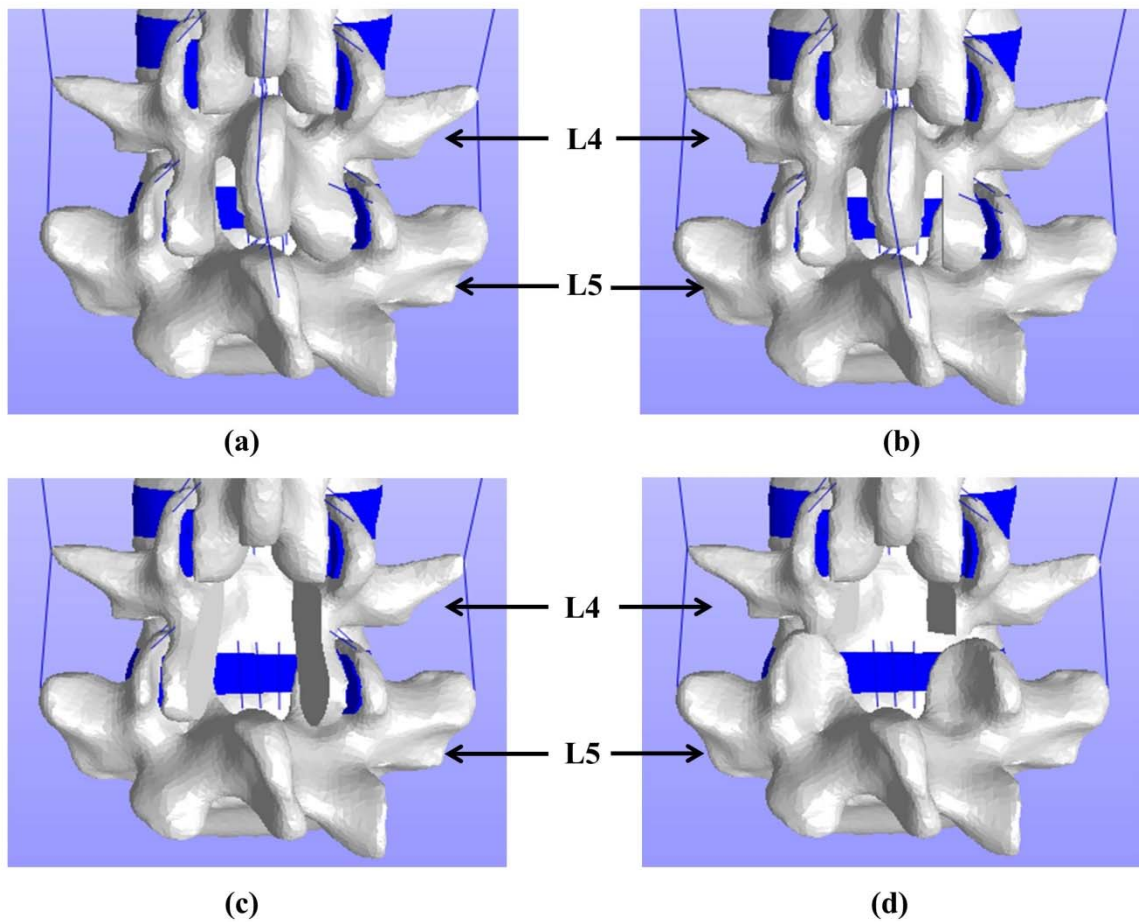
Figure 12: Anatomical reduction for simulated surgeries: (a) Unilateral Laminotomy; (b) Bilateral Laminotomy; (c) Facet sparing Laminectomy; (d) Laminectomy with Facetectomy

A preliminary validation was performed by comparing model predictions to experimental data reporting the effects of laminotomy and laminectomy on lumbar spine kinematics. The *in vitro* analysis conducted by Lee et al. (51) was used as it reported information on spine biomechanics after bilateral laminotomy and laminectomy in human spine. Accordingly, the experimental conditions used by Lee and co-workers were replicated in the simulations. More specifically, in the investigated cases, the inferior endplate of L5 was fixed (equivalent to potting the lumbar spine at L5), and a pure flexion/extension moment was applied at the superior endplate of L1 (8 Nm in flexion and 6 Nm in extension, respectively) with a frequency of 1 Hz. In addition, a follower load of 400 N was applied to the spine as previously described (130). Both laminotomy and laminectomy procedures were performed on L2-L5 segments (Figure 13). The ranges of motion (rotations in the sagittal plane) of L2-L3, L3-L4, and L4-L5 segments were estimated and compared. In order to improve the agreement with the experimental results, the initially chosen elastic moduli of some discs were slightly modified in the computational model within their physiological range. For all the cases investigated, it was found that the predicted range of motion of the model followed the same trend of *in vitro* data, and their differences were always less than one standard deviation (Figure 14).
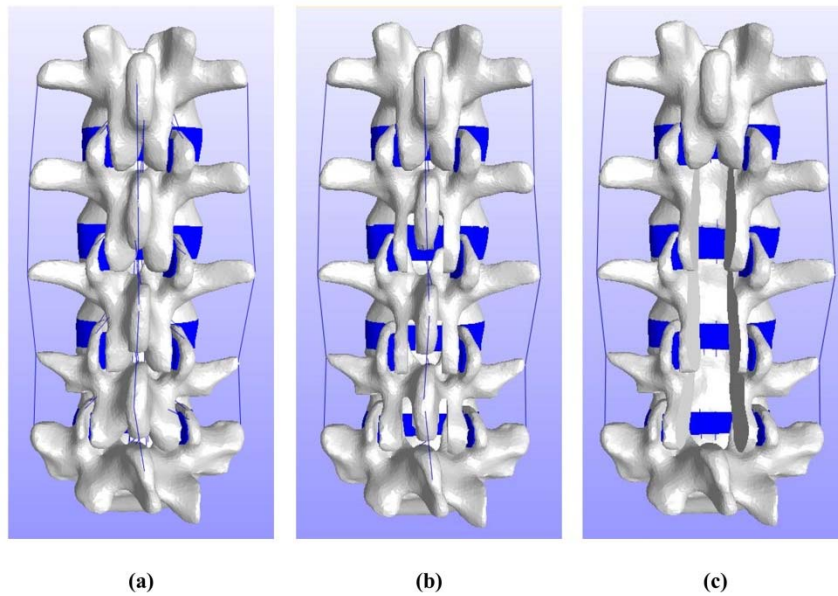
Figure 13: Lumbar Spine models used in validation: (a) Intact spine; (b) bilateral laminotomy at L2-L5; (c) Facet sparing laminectomy at L2-L5
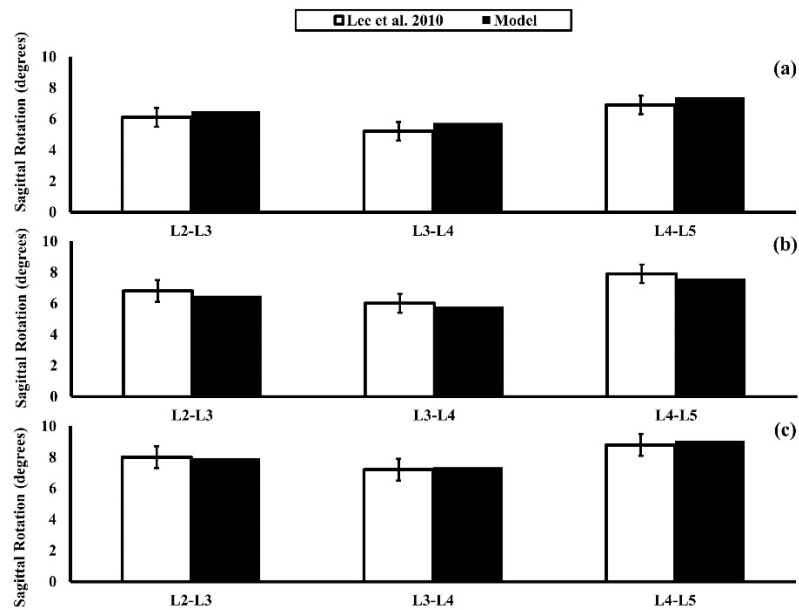
Figure 14: Validation of the FE models by comparing the rotations in the sagittal plane predicted by the model to experimental data: (a) intact spine; (b) bilateral laminotomy at L2-L5; Facet sparing laminectomy L2-L5.

4.3 Results

In this analysis, the post-operative changes in range of motion (i.e., rotation in the sagittal plane), intradiscal pressure, and normal and shear stress in both AF and NP were evaluated at all spine levels. A hybrid test method (118) was adopted as a protocol for spine loading conditions. In particular, the 'intact' spine was tested with the same loading conditions used for validation, and its total range of motion was computed. When testing the spine for each surgical procedure, the pure flexion/extension moment applied at L1 was varied in order to make the total range of motion equal to that attained in the 'intact' case.

The total range of motion of the spine (L1-L5) in the sagittal plane resulting from loading the intact model was 11.46° for flexion and 14.3° for extension. The moments required to produce the same range of motion after performing the surgical procedures are shown in Table 2. Moments changed during flexion, decreasing up to 42% for the case of laminectomy with facetectomy. Conversely, minimal changes were found during extension for all procedures investigated.

Table 2: Flexion/Extension moments of the simulated surgeries required to achieve the same total ROM of the intact spine

	Flexion (Nm)	Extension (Nm)
Intact	8	6
Unilateral Laminotomy	7.84	5.87
Bilateral Laminotomy	7.6	5.89
Facet sparing Laminectomy	4.96	6.04
Laminectomy with Facetectomy	4.64	5.94

Post-operative alterations of spinal segments biomechanics during extension were minimal (<5%). The post-operative motion redistribution during flexion for the individual spine segments is shown in Figure 15, and compared to the 'intact' case. For all procedures, sagittal rotations increased at L4-L5 and L3- L4, and decreased at L2-L3 and L1-L2. Major changes were found after laminectomies, with increments up to 18% and 23% (at L3-L4 and L4-L5, respectively), and reductions up to 15% and 39% (at L2-L3 and L1-L2, respectively). In contrast, post-operative changes after either unilateral or bilateral laminotomy were minimal (<5%).
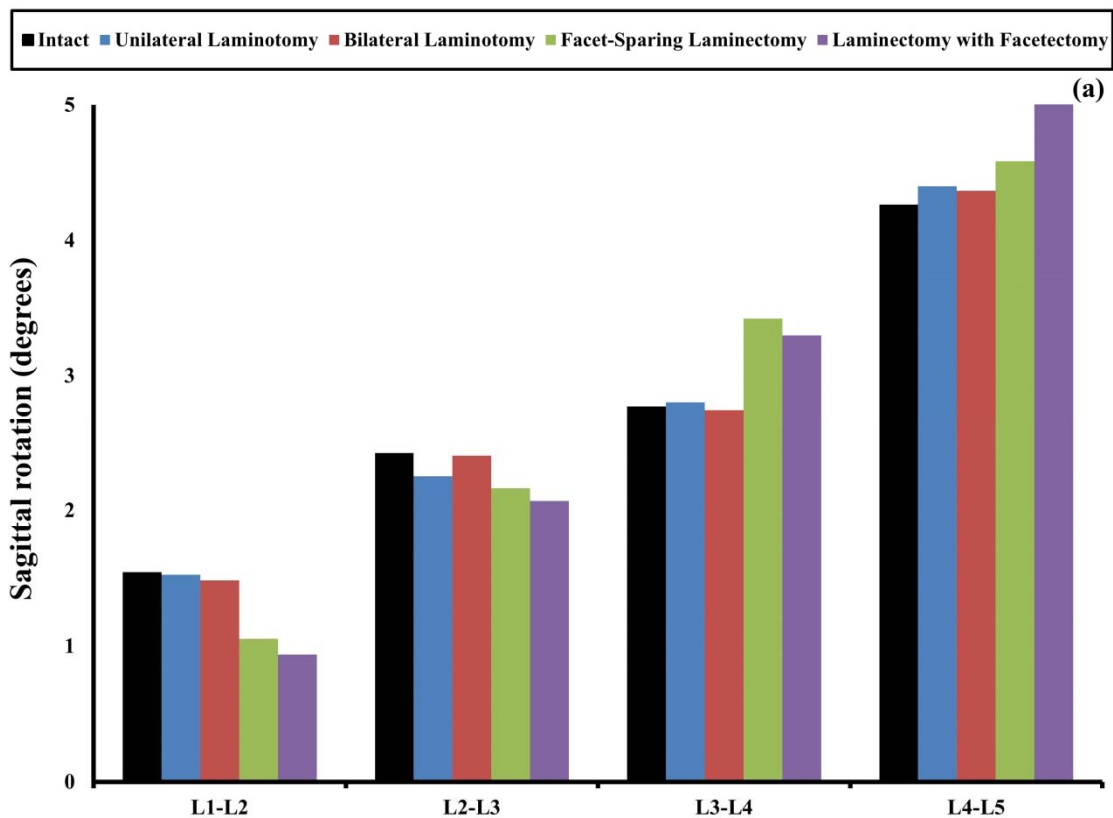
Figure 15: Post-operative changes due to rotation in the sagittal plane for spine segments

Post-operative alterations of spinal segments kinematics were reflected in changes of intradiscal pressure and stresses in the IVDs. After laminectomy procedures, intradiscal

pressure increased in both NP and AF at L3-L4 (up to 20%) and L4-L5 (up to 10%). Conversely, at L2-L3 and L1-L2, pressure reduced up to 35% and 31%, respectively (Figure 16). After either unilateral or bilateral laminotomy, pressure changes were minor at all spine levels, with the exception of L3-L4, whose fluid pressure in AF dropped up to 30% (Figure 16b). Changes in the normal stresses were similar to those found in intradiscal pressure: after laminectomy procedures, stress in both NP and AF increased one-fold in L4-L5 and L3-L4, and decreased up to 30% to 35% in L2- L3 and L1-L2, respectively, (Figure 17.a and 17.b). Again, after unilateral and bilateral laminotomy, no major changes from the 'intact' case were observed for all the spine levels. Major changes in shear stress were only observed in the NP of L3-L4 after laminectomy procedures, increasing up to 120% the value attained in the 'intact' case (Figure 17.c and 17.d).
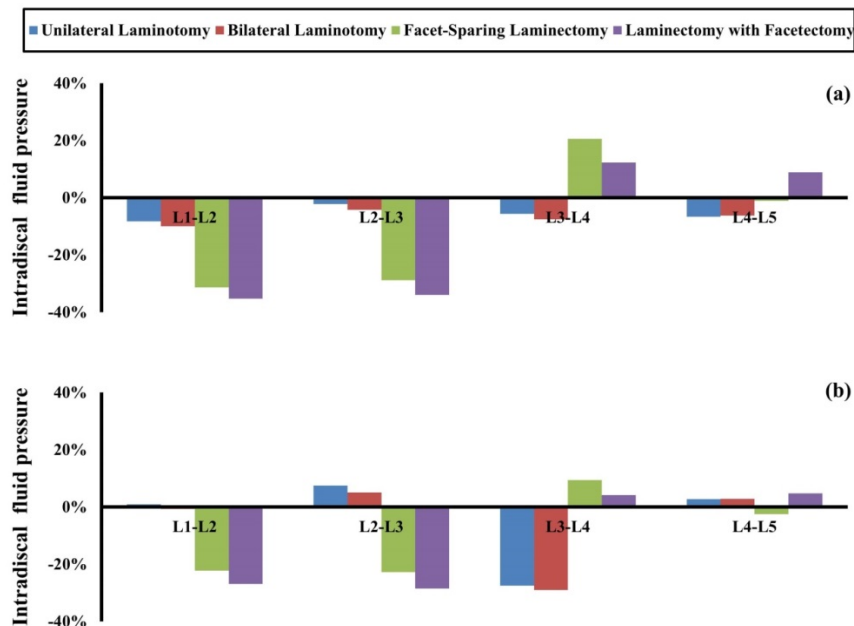
Figure 16: Post-operative changes in intradiscal pressure in spine segments: (a) NP; (b) AF. Data are reported in terms of percent change with respect to the 'intact spine'
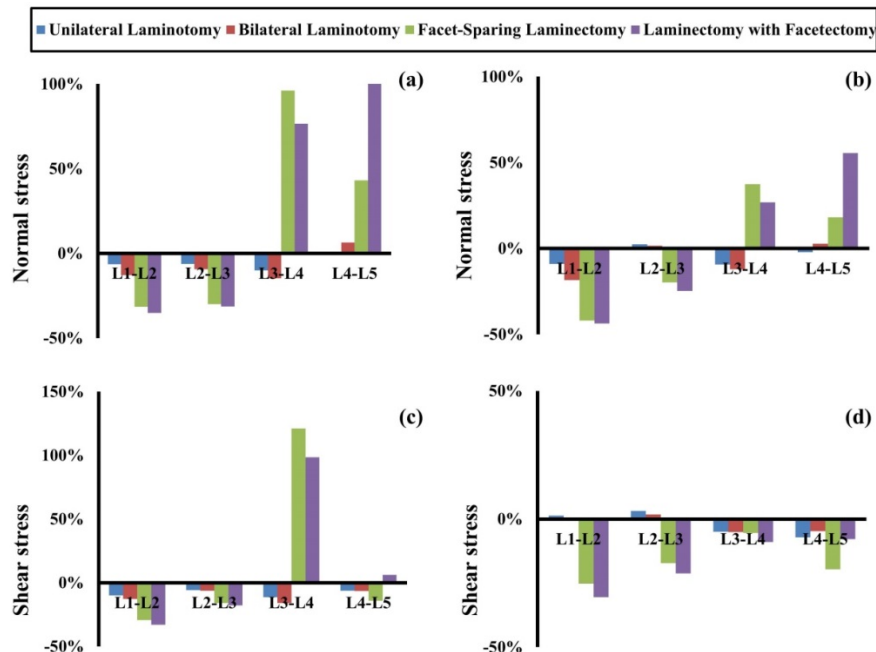
Figure 17: Post-operative changes in peak stress: normal stress in NP; (b) normal stress in AF; (c) shear stress in NP; (d) shear stress in AF. Data are reported in terms of percent change with respect to the 'intact' case.

4.4 Discussion

In this study, we adopted a realistic three-dimensional finite element model of human lumbar spine to investigate the implications of surgical procedures for lumbar stenosis on the biomechanics of the adjacent segments. Specifically, the model was implemented to simulate biomechanical tests on a L1-L5 spinal column undergoing unilateral laminotomy, bilateral laminotomy, facet-sparing laminectomy, and laminectomy with facetectomy at L4-L5 to yield changes in kinematics, intradiscal pressure, and disc stress at all spine levels. Such metrics are especially relevant when investigating the etiology of ASD since altered range of motion of spine segments is believed to increase the risk of spinal instability, eventually leading to spondylolisthesis and LSS (131). Besides, abnormal levels of fluid pressure or stress

may suggest ongoing IVD degeneration, which also contributes to the development of stenosis.(131-134)

The post-operative changes of spinal segments biomechanics were tested during flexion/extension. In agreement with both in-vitro (135-137) and numerical studies, (138-140) no changes were observed during extension. The kinematic analysis carried out in this study shows that the largest increase in post-operative spine motion is attained at the operated level (L4-L5) and the immediate adjacent one (L3-L4) after laminectomies are performed (Figure 15). This is in agreement with previously reported in-vitro (135, 136, 141) and numerical biomechanical analyses.(138, 140, 142) Moreover, these results are also consistent with clinical studies observing that laminotomy generates a lower level of instability when compared to laminectomy (50, 143).   Post-laminotomy alterations of the kinematics at the levels L3-L4 and above are caused by the reduction of stiffness at L4-L5. In contrast, laminectomy of L4 also entails the removal of flavum, interspinous, and supraspinous ligaments, which connect this vertebra to both L3 and L5. These anatomic changes directly affect the stiffness of the adjacent segment L3-L4. It has been reported that over 60% of the flexion movement of the spine is taken up by the posterior ligaments. Among them, interspinous and supraspinous ligaments withstand the highest tensile force(144). This would explain the fact that: (1) after laminotomy, alterations of L4-L5 kinematics were minor; (2) after laminectomy, the model predicted increase in motion during flexion, and almost negligible changes during extension.

Changes in intradiscal pressure and stress can lead to altered metabolism within the disc, with potential long-term disc degeneration (133, 134, 145, 146). Minor changes are found after either unilateral or bilateral laminotomy (<10%). In contrast, after laminectomy, variations of fluid pressure (up to 20%) and stress (up to 120%) occur in NP and anterior AF (Figures 16 and 17). However, these changes occurred at the operated level (L4-L5) and its immediate adjacent level L3-L4, while the other spine levels experienced reduction of both intradiscal pressure, and normal and shear stresses. These results are in agreement with an *in-vitro* study on calf spine reporting that, after laminotomy, intradiscal pressure changes at the operated level did not statistically differ from those found in intact spine. In contrast, after laminectomy, significant pressure increase was found in the anterior portion of IVD (141). Similar findings were also reported in a recent computational study showing intradiscal pressure increase up to 50% after laminectomy, and minor changes after laminotomy (138).

It has been historically reported that laminectomy with complete facetectomy induces excessive spinal instability, so that the more conservative facet-sparing laminectomy is typically performed to treat LSS (53, 137, 147-149). This study confirms that, compared to facet-sparing laminectomy, the complete facetectomy model yielded a larger increase in spine kinematics and, consequently, larger intradiscal pressure and stress at the operated level L4-L5. However, at the immediate adjacent level L3-L4, facet-sparing laminectomy caused the largest biomechanical alterations (Figures 16 and 17). Hence, according to model's predictions, the two laminectomy procedures are similarly detrimental for spine health, with laminectomy with facetectomy mostly altering the biomechanics of the operated level L4-L5, while facet-sparing laminectomy mainly affecting the adjacent segment L3-L4.

Some limitations of this study must be noted. The model schematizes vertebrae as rigid bodies, so that the only deformable structures in the spine are the soft tissues (i.e., intervertebral discs, cartilage at facet joints, and ligaments). Such simplification may have affected the results of both kinematic and stress analyses hereby reported. However, the stiffness of the soft tissues in the spine is about two and four orders of magnitude lower than those of cancellous and cortical bone in vertebrae, respectively (150). Accordingly, one would expect that, for the surgical procedures and loading conditions investigated in this study, spine strains mostly occur in the soft tissues. Also, spine ligaments were modeled as linear elastic elements, whose stiffness corresponded to the slope of the most linear portion of the force-deformation curve experimentally determined by Pintar and co-workers (104). Ligaments linear behavior is considered the normal (physiologic) response of the tissue to routine external stimuli (151, 152). Accordingly, a linear behavior may be used as an initial approximation of ligament characteristics in computational models (104). Finally, the computational model used in this study was validated through kinematic data from an *in-vitro* study only reporting spine kinematics during flexion/extension (135). Accordingly, the results reported in this study are only relevant for the case of flexion/extension spine motion, since other physiologically relevant movements (e.g., axial torsion, lateral bending, etc.) were not studied, and will be addressed in the future upon further model validation.

For the loading conditions investigated in this analysis, our results suggest that laminotomy, whether unilateral or bilateral, represents a superior technique in terms of potential risk reduction for developing either spine instability or mechanically-accelerated disc degeneration

in the adjacent segment. However, additional tests, under different and more complex physiologically relevant loading conditions, should be performed in order to confirm our findings. Moreover, it is recognized that surgical decision-making must take into account many other factors, among which the severity of the stenosis. While laminotomy has been recommended for cases of moderate or unilateral stenosis, and it might not allow for adequate decompression of severe central or bilateral stenosis (143), in which case laminectomy may represent a better surgical solution despite the increase in instability shown in our study.

Chapter 5 The Post-operative Behavior of the Spine After Implanting Fixation Constructs for The Treatment of Severe Burst Fractures

5.1 Introductory Remark

The majority of traumatic spinal fractures are found at the thoracolumbar region and nearly 10% to 20% of these injuries are burst fracture (BF) (2, 17). Surgical correction with corpectomy and subsequent fusion of neighboring levels is a commonly practiced treatment for BF injury (11). The goal of the surgery is to correct sagittal deformity, stabilize the spine column, decompress neural elements, and restore vertebral body height (3, 20, 78, 153). The optimal surgical approach for treatment of BF is controversial (72, 79). It can be performed through anterior, posterior, or combined anterior-posterior approach (20-22). Short-segment posterior fixation, by solely fusing the immediate superior and inferior levels of the injured level, is preferred by many surgeons to preserve natural spine mobility and to reduce surgical insult (154, 155). Such procedure can be attained through various types of constructs which may employ pedicle screws, posterior rods, expandable cages, and transverse plate (156-159). In particular, pedicle screws together with the posterior rods had become the gold standard in fixing spine levels due to its capability of retaining bony purchase until the fusion mass stabilizes (160). Also, expandable cage is considered among the superlative implants that maintain anterior column reconstruction (159). Moreover, lateral fixation by transverse plate has been proposed in anterolateral approach to avoid second posterior surgery (158). Each of these implants has different mechanical properties and provides dissimilar stiffness to the fixed junction. Accordingly, it is hypothesized that the postoperative mechanical behavior of the spine will vary based on the adopted construct.

Many studies reported that the excessive stiffness, produced from fixing spinal levels, causes greater motion on the adjacent intervertebral disc (IVD) to compensate the range of motion lost by fusion (13, 161, 162). Such alterations may potentially lead to adjacent segment disease (ASD) (12). To date, no study investigated the implications of short-segment fixation procedures used in treatment of BF on the health of the adjacent segments. Accordingly, the objective of this study was to quantify the biomechanical alterations at the adjacent lumbar spine segments after implanting different short-segment fixation constructs aimed at treatment of thoracolumbar BF. Since the higher is the stress on the adjacent discs the higher is the risk of disc degeneration [23], this study specifically quantified the changes of stress at adjacent segment after adding pedicle screws and transverse plate to the fixation construct. This was attained by developing finite element (FE) models of the thoracolumbar spine that described four different fixation constructs.

5.2 Methods

Short-segment fixation constructs for treatment of BF that is associated with neurologic deficiency and requires corpectomy were considered. Such constructs only involve one level above and below the level of fracture, and comprise of combination of expandable cages, pedicle screws, transverse plate, and posterior rods. Four 3D nonlinear FE models from T12 to L2, representing four fixation constructs, were developed and validated. Next, each construct was integrated with a lumbar spine to constitute a thoracolumbar spine model (from T12 to S1). Then, these models were examined by simulating flexion-

extension moment. Finally, the generated stresses at the adjacent IVDs were computed and compared among the four constructs.

Four FE models for different fixation constructs were developed following the same general work flow in Chapter 3. Before adding the constructs to the thoracolumbar junction, a complete corpectomy at L1 level was performed by subtracting both the L1 vertebral body and the adjacent IVDs (T12-L1 and L1-L2). In all the investigated constructs, an expandable cage was placed between T12 and L2 to restore the height of the anterior column. The combination of devices that constitute the investigated constructs were as follows: (1) 2RPC which includes two titanium posterior rods of 5.5 mm diameter , six pedicle screws of 6 mm diameter and 45 mm long, an expandable cage, and a transverse plate laterally fixed (Figure 18.a); (2) 1RPC which includes the same instrumentation of 2RPC with the exclusion of the posterior rod contralateral to the transverse plate (Figure 18.b); (3) 2RC which includes posterior rods, pedicle screws, and expandable cage (Figure 18.c); (4) PC which includes the expandable cage and the transverse plate (Figure18.d). All the devices were developed by using SolidWorks 2013x64 edition and were assumed to have material property of titanium with an elastic modulus of 110 GPa and Poisson's ratio of 0.3 (163). Sliding interfaces were defined between the expandable cage and the surfaces of the vertebral bodies of T12 and L2, with friction coefficient of 0.8 to prevent the cage from slipping (164). The pedicle screws were placed posteriorly and connected with posterior rods by a tied contact. The transverse plate was connected via four lateral screws to T12 and L2 vertebral bodies,

and a sliding contact with 0.1 friction coefficient was assumed between the plate and the vertebral body (165).
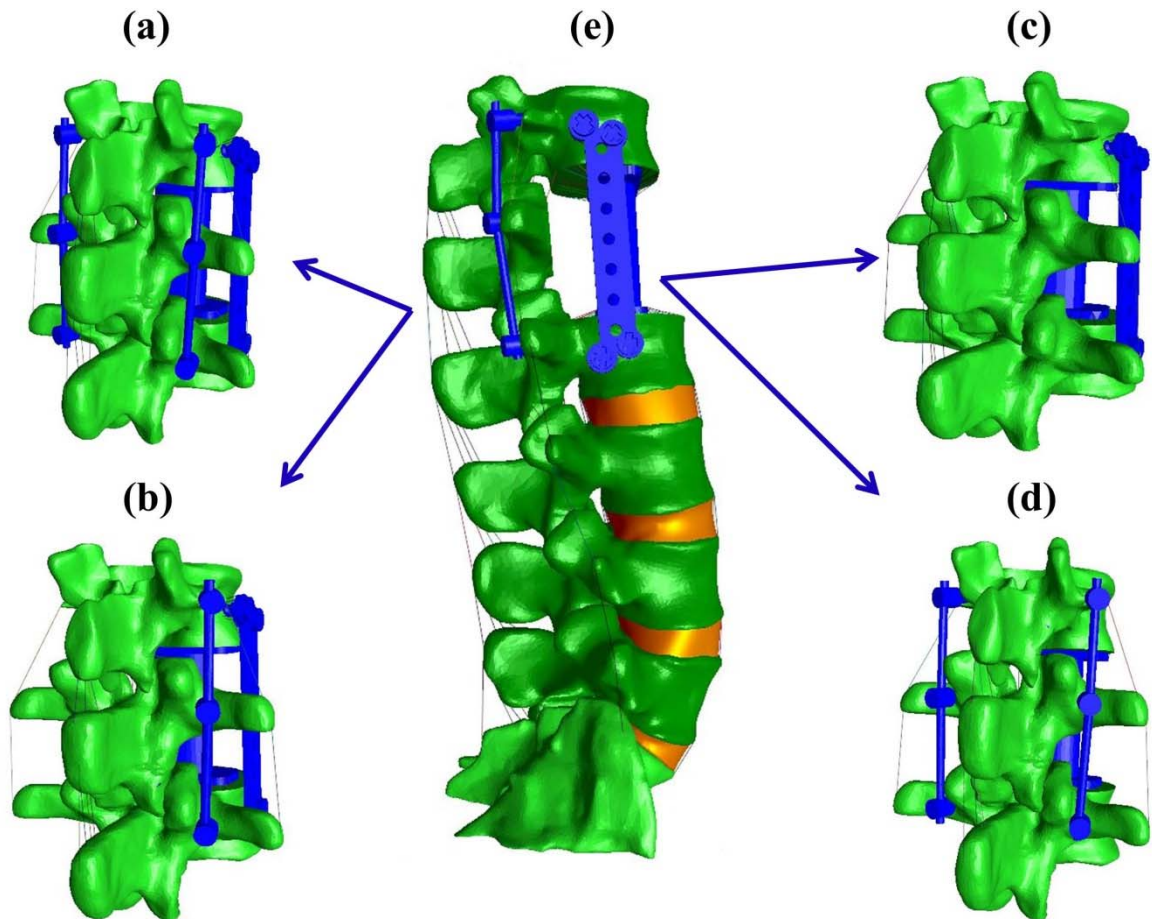
Figure 18: Thoracolumbar spine FE model with different fixation constructs. (a) 2RPC construct; (b) 1RPC construct; (c) PC construct; (d) 2RC construct; (e) constructs integrated with the intact lumbar spine. Each construct will replace the intact spine levels (T12-L2) to generate the studied FE models.

An experimental setup for the same investigated constructs was carried out by our collaborators in the Max-Biedermann Institute for Biomechanics (Figure 19) (166). The loading conditions used in the experiment were replicated in our models. Specifically, a

flexion-extension moment was applied at T12 while fixing the inferior endplate of L2 with a frequency of 0.25 Hz. In addition, a follower load of 200 N was applied normal to the superior end plate of T12. The flexibility testing method was adopted as a protocol for loading the spine. Such approach guarantees that the pure moment is equally applied to all the segments as the spine deforms (167).

(a)   (b)
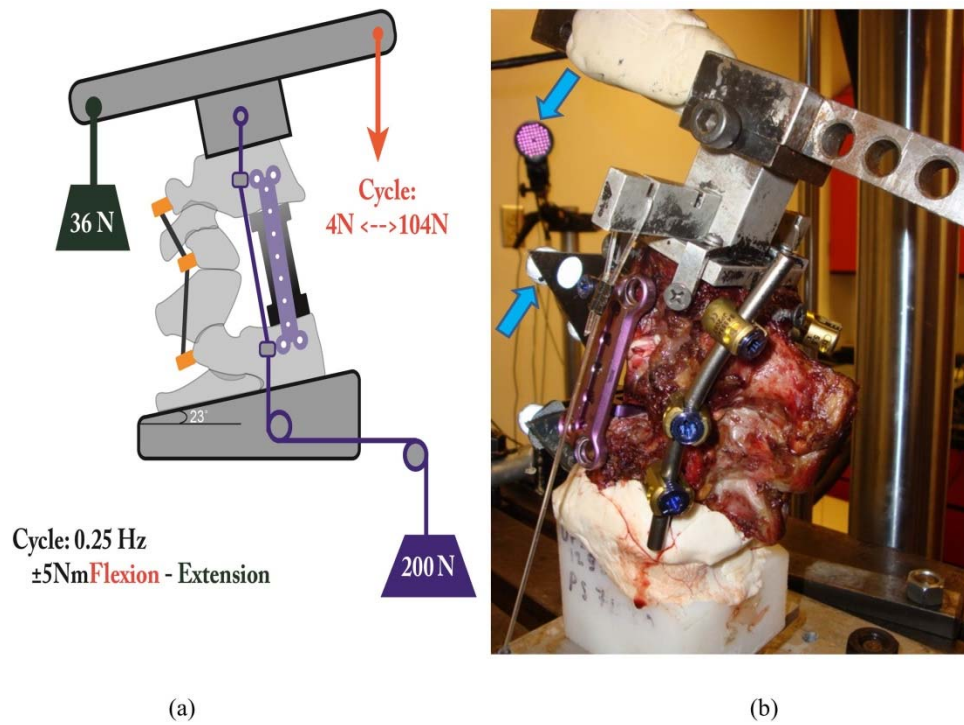
Figure 19: Photograph of biomechanical testing: (a) schematic showing testing conditions, (b) T12-L2 specimen instrumented with 1RPC construct in the testing apparatus (166)

After validating the models of the four constructs, four vertebrae (from L3 to S1) with its associated intervertebral discs (IVDs), facet joints, and major ligaments were added to each model (Figure 12.e). Four-node solid elements were used for discretizing the cortical and cancellous bones, the IVDs, and the facet joints. On average, each vertebra,

IVD, and facet joint consisted of 65,000, 3500, and 1000 elements, respectively. Testing conditions were similar to that of the previous step. However, here the models were constrained by fixing the S1 in all directions instead of L2. The post-operative alterations of von-misses stress at all adjacent segments (i.e., L2-L3, L3-L4, L4-L5, and L5-S1) were calculated and compared.

5.3 Results

For all investigated constructs, the predicted ROM during flexion-extension was in agreement with the *in vitro* experimental data, see Figure 20. The smallest range of motion corresponded to the 2RPC construct, while the largest ones were found in the PC constructs.
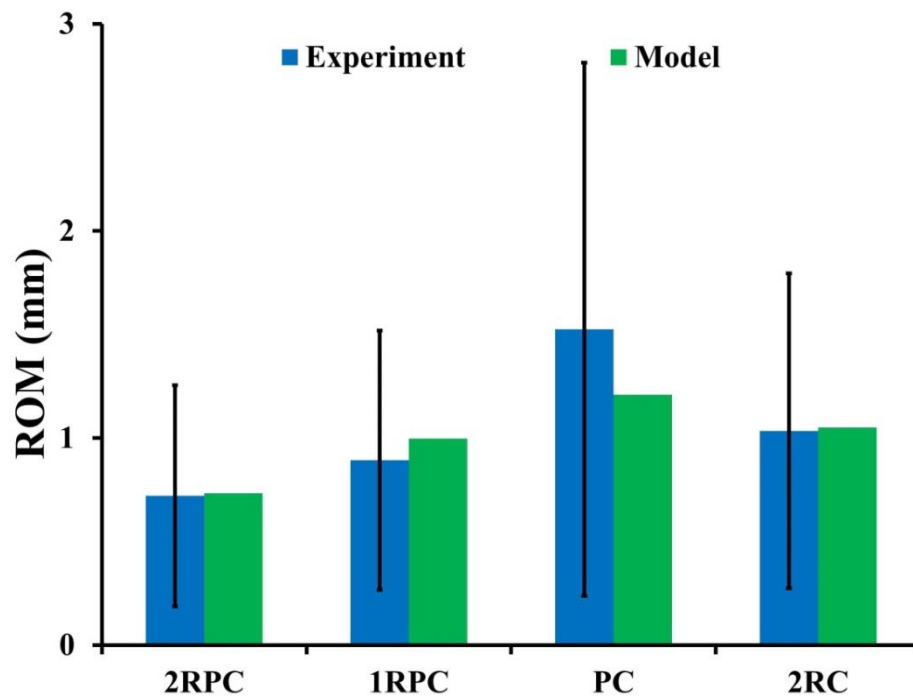
Figure 20: FE constructs models' prediction of ROM compared to experimental data during flexion-extension (bars represent +/- σ).

On the adjacent spine levels, all the constructs that comprised pedicle screws (i.e. 2RPC, 1RPC, 2RC) generated comparable magnitude of stresses which was always higher than that produced form the PC construct. In particular, in flexion, the highest stresses in AF and NP were found at L5-S1 level reaching up to 5 MPa and 0.37 MPa, respectively (Figure 21). Similarly, during extension, the maximum stresses in AF and NP were found at L5-S1 level reaching up to 4 MPa and 0.56 MPa, respectively (Figure 22). The only exception was at L2-L3 level during flexion, where the stresses produced by 2RC in AF was 30% less than that attained with 1RPC or 2RPC. Stress levels produced by the PC construct in all the investigated cases were approximately 50% smaller than those corresponding to the other constructs.
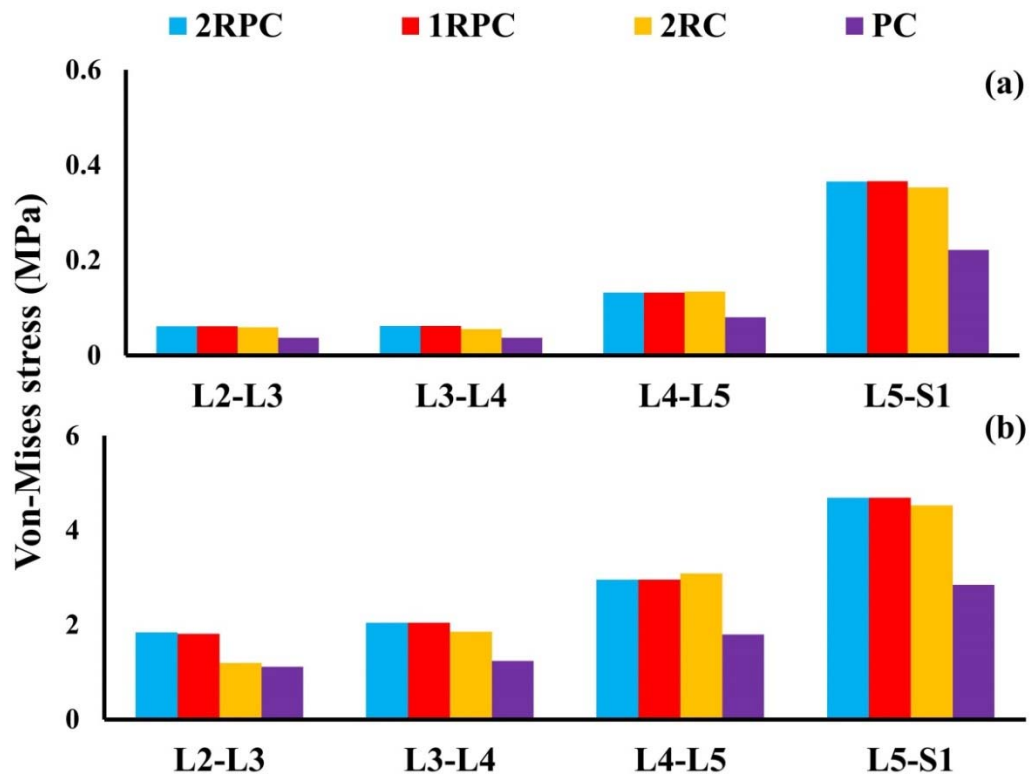
Figure 21: Von-Misses stress at the adjacent IVDs during flexion for all investigated constructs: (a) NP; (b) AF.
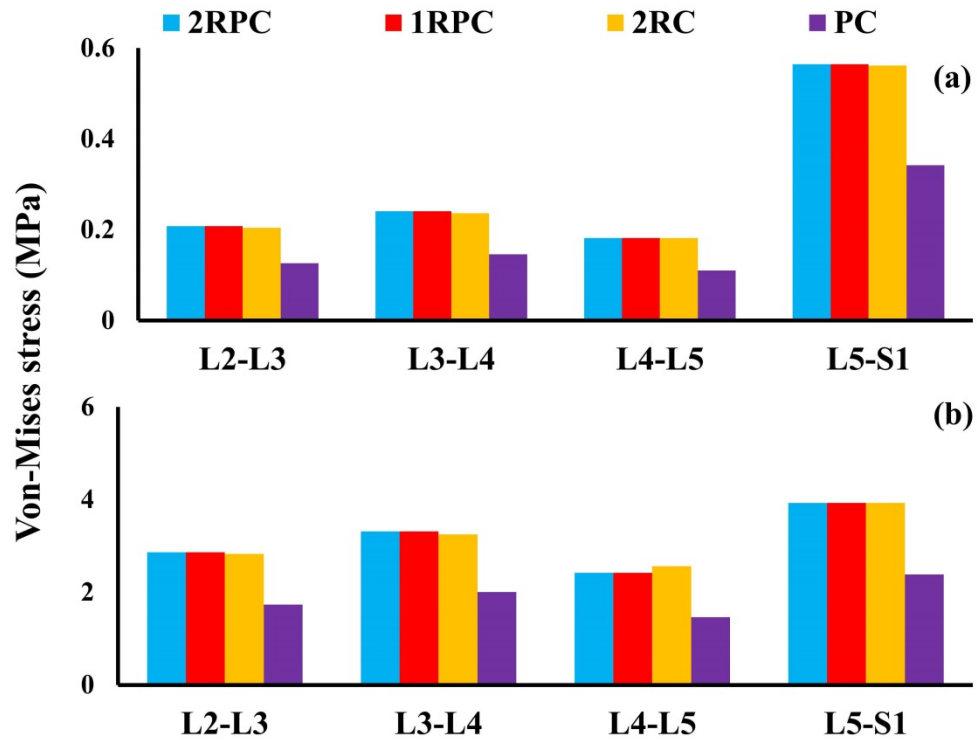
Figure 22: Von-Misses stress at the adjacent IVDs during extension for all investigated constructs: (a) NP; (b) AF.

5.4 Discussion

Spinal fixation is believed to be a possible cause for degeneration of the adjacent segments (122, 168). In a recent long follow-up study (~13 years), Mannion and co-workers found that spinal fusion is associated with signs of disc degeneration at the adjacent segments (67). Moreover, biomechanical experiments showed that the mobility and stresses experienced by a spinal segment increased when the neighboring segments were fused (13, 162). Hence, monitoring the stresses generated at the adjacent segment due to implanted construct provides an indication on the potential risks of degeneration of the adjacent IVD.

In this study, four different constructs that are commonly used in short-segment fixation constructs for treatment of BF were compared to investigate their implication on the biomechanics of the adjacent lumbar segments. This was done by developing four thoracolumbar FE models, each of them comprising an expandable cage and different combination of pedicle screws and transvers plate. A flexion-extension moment was simulated and the generated stresses at all adjacent segments were computed. The results showed that the three constructs that comprised posterior pedicle screws (2RPC, 1RPC, and 2RC) yielded similar rigidity and were the stiffest. Specifically, the 2RPC construct produced the lowest ROM (0.73 mm), while the PC construct produced the highest (1.2 mm), see Figure 20. Moreover, the stress levels on the adjacent lumbar segments varied according to the adopted construct. In particular, for 2RPC, 1RPC, and 2RC constructs, stresses at all adjacent levels were approximately 50% higher than that produced by the PC construct (Figures 21 and 22). It has been suggested that mechanical loads and stresses alter the structure, material, and failure properties of the disc, eventually leading to IVD degeneration (169). Also, the higher stiffness induced by constructs that comprised pedicle screws might be attributed to the major role that pedicle screws are playing in constraining the fused junction during flexion-extension loading conditions (160).

Some limitations in this study must be noted. The thoracolumbar spine was reconstructed from a CT scan of only one subject. The geometry of the vertebral body may influence the mechanical behavior of the spine (170). Hence, in the future, it will be important to extend the analysis by including CT scans of several subjects to broaden the validity of

the results of this study. Also, muscle forces were not included in the models. Spinal muscles contribute to the stability of the spine (171). However, all the constructs investigated underwent the same testing protocol. Thus, minor relative changes would be expected in the biomechanical performance of the four constructs. Moreover, only flexion and extension loading conditions were simulated. This was due to the lack of experimental data for the other loading conditions that is required for model validation. In the future, other loading conditions will be considered to broaden the conclusion of this study. Finally, the flexibility test method was used instead of the hybrid test method, which is considered the most appropriate protocol for investigating the adjacent segments due to fusion (118). However, in this analysis, the objective was to compare the implications produced from each construct not to quantify how much it will change from the intact spine. Also, no data are available in the literature for the total ROM for the thoracolumbar spine (T12-S1) when pure moment is applied, as is required for conducting the hybrid protocol.

In conclusion, this study provides new insights on the implications of choice of fixation construct for treatment of thoracolumbar BF on the biomechanics of the adjacent lumbar segments. The results suggest that the PC construct, although less stable in fixing the injured segment, yields the least amount of stress on the lumbar adjacent segments. Since high mechanical stresses are believed to be a potential cause of disc degeneration, the PC construct represents the most conservative approach for preventing the development of ASD.

Chapter 6 The Mechanical Advantage of Pedicle Screw Inclusion at The Level of Burst Fracture

6.1 Introductory Remark

Motor vehicle accidents, and falls are likely causing 40% to 80% of thoracolumbar burst fractures (172). Surgical management is typically indicated for those BFs involving the anterior and middle spinal columns, and associated with neurologic deficiency (78). The goal of the surgery is to stabilize the fracture, restore the sagittal alignment, and decompress neural elements (78, 173).

Long-segment posterior fixation (LSPF) has been traditionally adopted in treatment of high-energy BF at thoracolumbar junction to provide spinal stability and maintain sagittal correction (174, 175). A less invasive option for the treatment of BF is the short-segment posterior fixation (SSPF). In this procedure, only levels immediately adjacent to the fractured segment are fixed (174, 175). However, clinical studies reported high failure rates of the hardware and progressive loss of sagittal alignment for almost 50% of patients treated with SSPF (176).

Several strategies have been proposed to improve the post-operative outcomes of SSPF (30, 177-179). In particular, the inclusion of pedicle screws at the fracture level has been suggested to decrease the failure rate of the hardware and preserve sagittal correction (28, 180, 181). Clinical studies reported that the success rate in maintaining sagittal correction and stabilizing the spine of a SSPF construct with pedicle screws at fracture level (SSPFI)

is comparable to that of a LSPF construct (182). However, the equivalence of SSPFI to LSPF has never been proved from a biomechanical perspective. The objective of this study is to determine whether SSPFI can achieve a biomechanical performance similar to that of LSPF. Specifically, we used three-dimensional FE models of a thoracolumbar junction (T12-L2) to simulate and compare the biomechanics of short- and long-segment constructs with and without the inclusion of pedicle screws at the fracture level.

6.2 Methods

The posterior constructs used for the treatment of BF associated with incomplete neurologic deficiency and moderate vertebral body commination was biomechanically compared. In particular, four fixation constructs representing SSPF and LSPF with/without inclusion of fracture level were considered (Figure 23). In addition, an intact spine model form T11 to L4 was established and used as a baseline for comparing the fixation constructs. The mechanical performance of each construct was evaluated by estimating three metrics: (1) stiffness of the thoracolumbar junction (T12-L2), (2) magnitude and distribution of the stress in the implants, and (3) magnitude and distribution of intradiscal pressure at adjacent IVDs (i.e. T12-L1 and L1-L2). These metrics were chosen to evaluate the rigidity of the constructs and assess the stability of the anterior column.
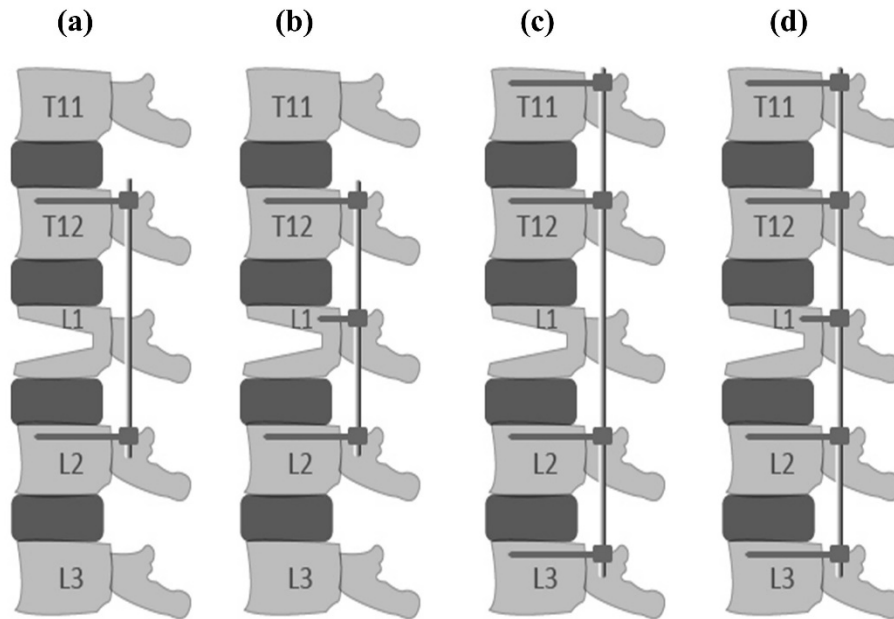
Figure 23: a schematic representation of the four investigated constructs: (a) SSPF; (b) SSPFI; (C) LSPF; (d) LSPFI

3D FE models from T11 to L4 were constructed following the same general computational approach described in chapter 3. On average, each vertebra, IVD, and facet joint consisted of 25,000, 5000, and 1000 elements, respectively. BF was simulated at L1 by subtracting a portion from the vertebral body at the anterior and middle spinal columns area, together with the anterior longitudinal ligaments at T12-L1 and L1-L2. In addition, laminectomy was performed at the same level by removing the spinous process with the associated supraspinous, interspinous and flavum ligaments (Figure 24.a). Four fixation constructs were modeled: (1) SSPF, which includes pedicle screws at T12 and L2; (2) SSPFI, with pedicle screws at T12, L1 and L2; (3) LSPF, requiring pedicle screws at T11, T12, L2, and L3; (4) LSPFI, including pedicle screws at T11, T12, L1, L2, and L3 (Figure 24b-e).
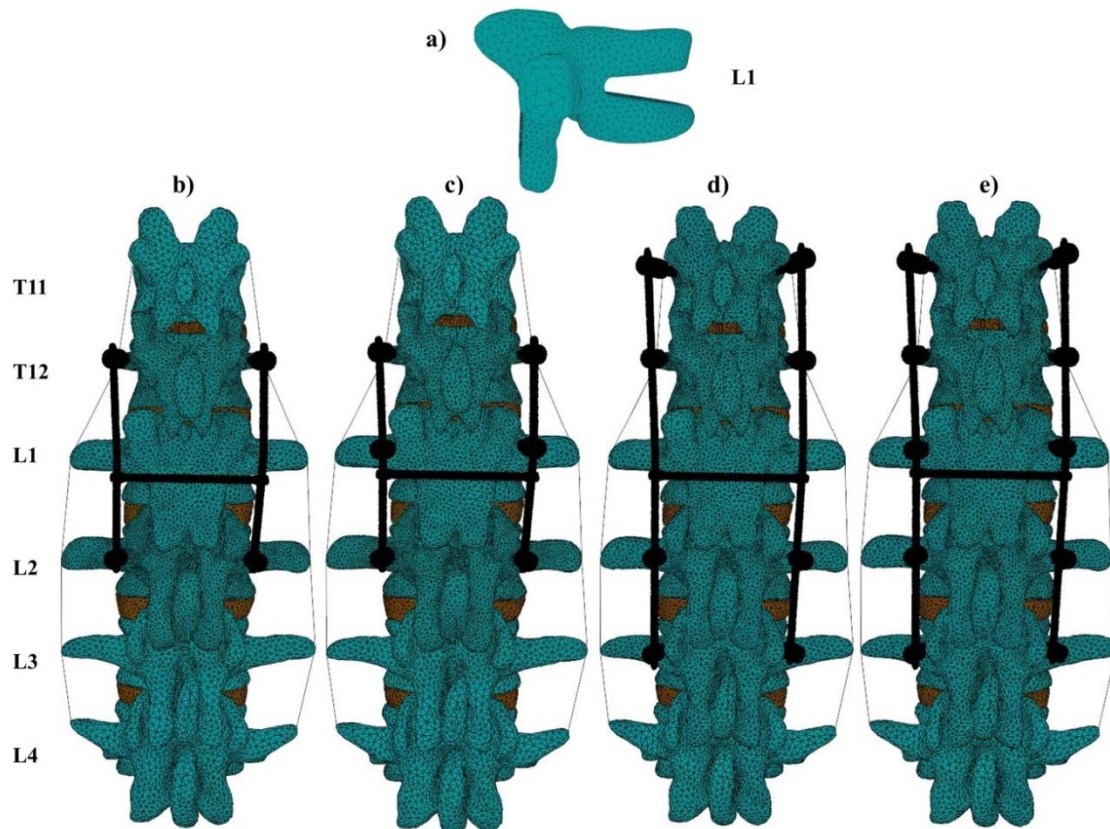
Figure 24: Finite element models of the fixation constructs: (a) L1 disruption due to burst fracture and laminectomy; (b) SSPF; (c) SSPFI; (d) LSPF; (e) LSPFI.

To replicate the experimental conditions of Baaj et al. (183), the models were constrained by fixing the inferior endplate of L4 in all directions and loading T11 with a pure moments of 7.5 Nm about the three anatomical axes to induce flexion, extension, axial torsion, and lateral bending with a frequency of 0.25 Hz. Validation of all the models (including the intact spine) was carried out by comparing the models' predicted segmental range of motion (ROM) to the experimental data. Models' predicted angular ROM of T12-L2 junctions were in agreement with the experimental data with the only exception of LSPF and LSPFI in lateral bending (Figure 25).
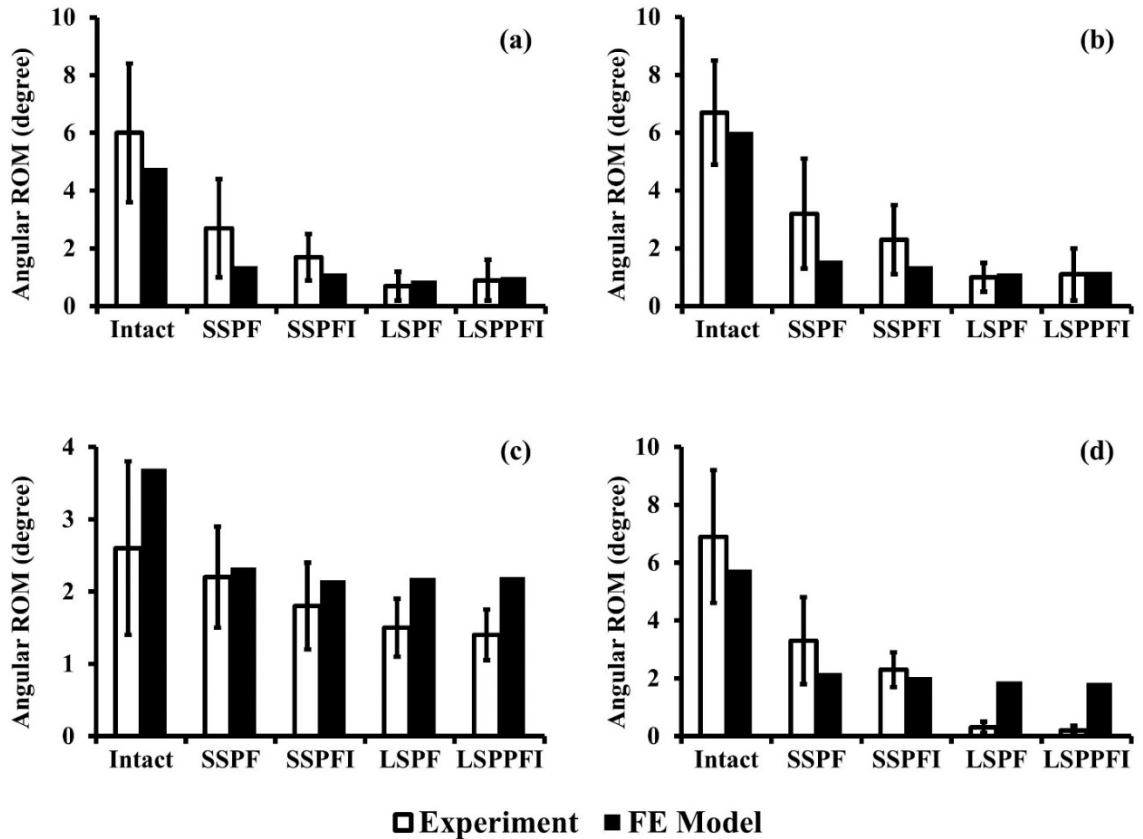
Figure 25: Angular ROM of thoracolumbar junction (T12- L2). Models' predictions are compared to in vitro results reported in [18] for four loading conditions: a) Flexion; b) Extension; c) Axial torsion; and d) Lateral bending. The range represents ± one standard deviation.

6.3 Results

For all the loading conditions simulated, the stiffness at the T12-L2 junction of all four constructs was higher than that found in the intact spine, see Table 3. For most loading conditions, long-segment models were stiffer than short-segment ones. When comparing the two short-segment fixation models, SSPFI showed higher stiffness than SSPF, with the largest difference (23%) attained during flexion. The LSPF and LSPFI constructs

produced nearly the same stiffness in axial and lateral bending. However, LSPF was stiffer than LSPFI in flexion (14%) and extension (5%).

Table 3: Stiffness at T12-L2 junction. Values are reported in Nm/deg.

	Flexion	Extension	Axial torsion	Lateral bending
Intact	1.56	1.24	2.03	1.30
SSPF	5.35	4.75	3.22	3.44
SSPFI	6.58	5.37	3.47	3.68
LSPF	8.44	6.52	3.42	3.97
LSPFI	7.41	6.34	3.41	4.08

For all the cases investigated, the largest stresses were concentrated at the posterior rods. The stress magnitude of long-segment models was higher than that of short-segment ones, see Table 4. In the short-segment models, the inclusion of pedicle screws at the fracture level increased the magnitude of the Von-Mises stress. In particular, during lateral bending, the maximum stress in SSPFI construct was 50% larger than that in SSPF. The largest stress values were observed in axial torsion. In long-segment constructs, LSPFI produced slightly higher stresses than LSPF during all loading conditions with the exception of axial torsion.

In both long- and short-segment constructs, the inclusion of pedicle screws at the fracture level lent more uniform distribution of the stress along the T12-L1 and L1-L2 segments of the posterior rods. As an illustrative case, during flexion, the maximum stress values for SSPF were 105 MPa at T12-L1 segment and 80 MPa at L1-L2 segment.

Table 4: Maximum Von-Mises stress at posterior rods. Values are reported in MPa.

	Flexion	Extension	Axial torsion	Lateral bending
SSPF	105	72	176	75
SSPFI	125	100	188	112
LSPF	162	199	338	146
LSPFI	186	205	318	152

In contrast, in SSPFI, the maximum stresses at T12-L1 and L1-L2 segments were 125 MPa and 118 MPa, respectively (Figure 26a-b). Similarly, in LSPF model, the maximum stress at T12-L1 segment was 162 MPa and that at L1-L2 segment was 92 MPa; in LSPFI, the stresses at T12-L1 and at L1-L2 segments were 187 MPa and 171 MPa (Figure 27a-b). Similar trends were observed in all the other loading conditions.

The magnitudes and the distribution of the intradiscal pressure were similar across the constructs, with the only exception at L1-L2 during axial torsion and extension: SSPFI generated 15% higher pressure than SSPF (Figure 29). When compared to the values attained in the intact spine, the intradiscal pressure at T12-L1 reached up to 500% during flexion, and decreased to 50% in lateral bending; no major changes were observed in extension or axial torsion (Figure 28). Also, at L1-L2, the intradiscal pressure increased in flexion (~300%), axial torsion (~200%) and extension (~150%), and decreased in lateral bending (75%) when compared to the intact case (Figure 29).
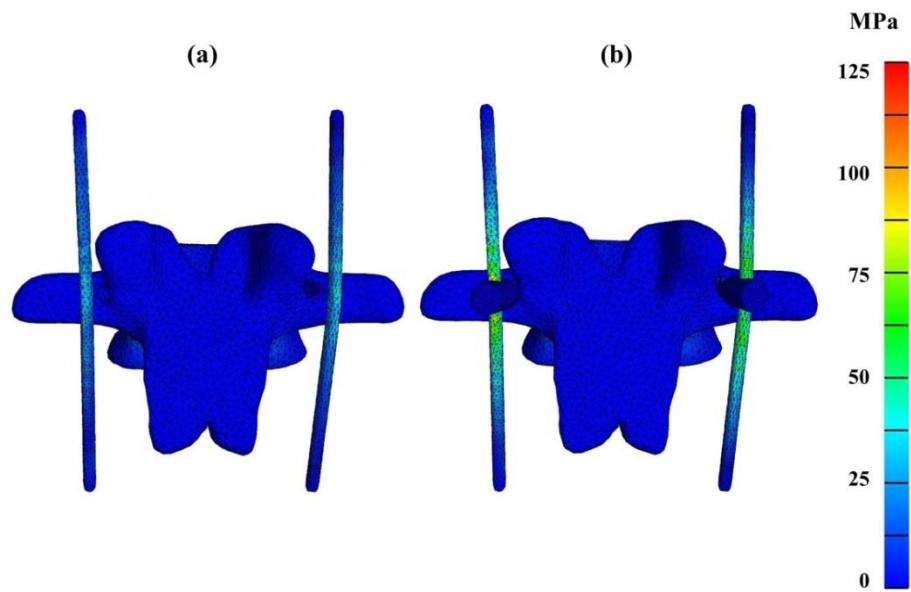
Figure 26: Von-Mises stress distribution at the posterior rods during flexion: a) SSPF; b) SSPFI.
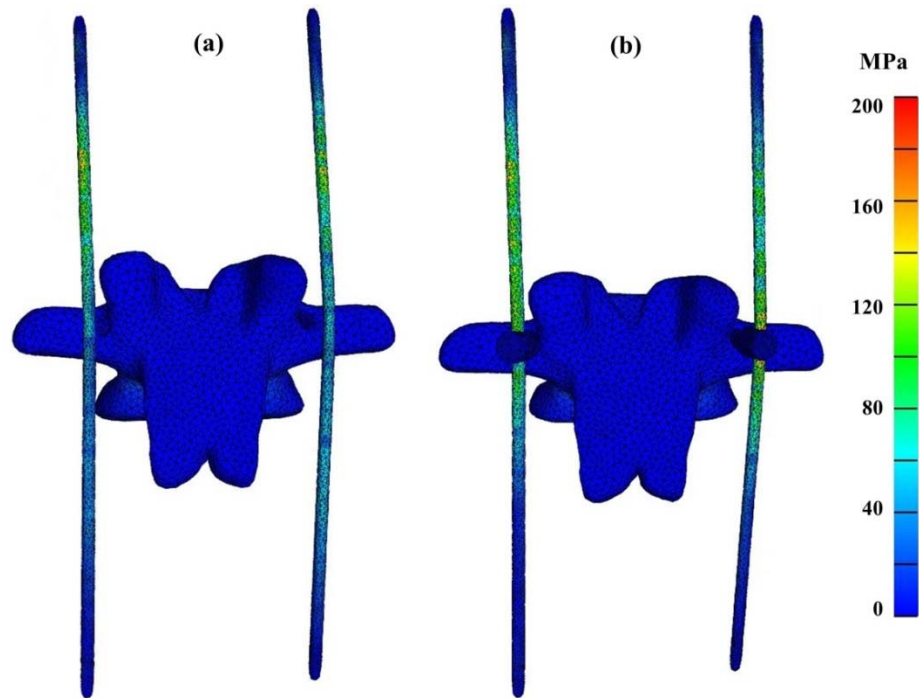
Figure 27: Von-Mises stress distribution at the posterior rods during flexion: a) LSPF; b) LSPFI.

	Flexion	Extension	Axial bending	Lateral Bending	MPa
Intact	1.15	4.41	3.10	5.18	
SSPF	6.8	5.21	4.28	3.01	
SSPFI	6.91	4.72	3.98	2.83	
LSPF	6.71	4.79	4.95	2.61	
LSPFI	6.43	4.11	3.97	2.5	
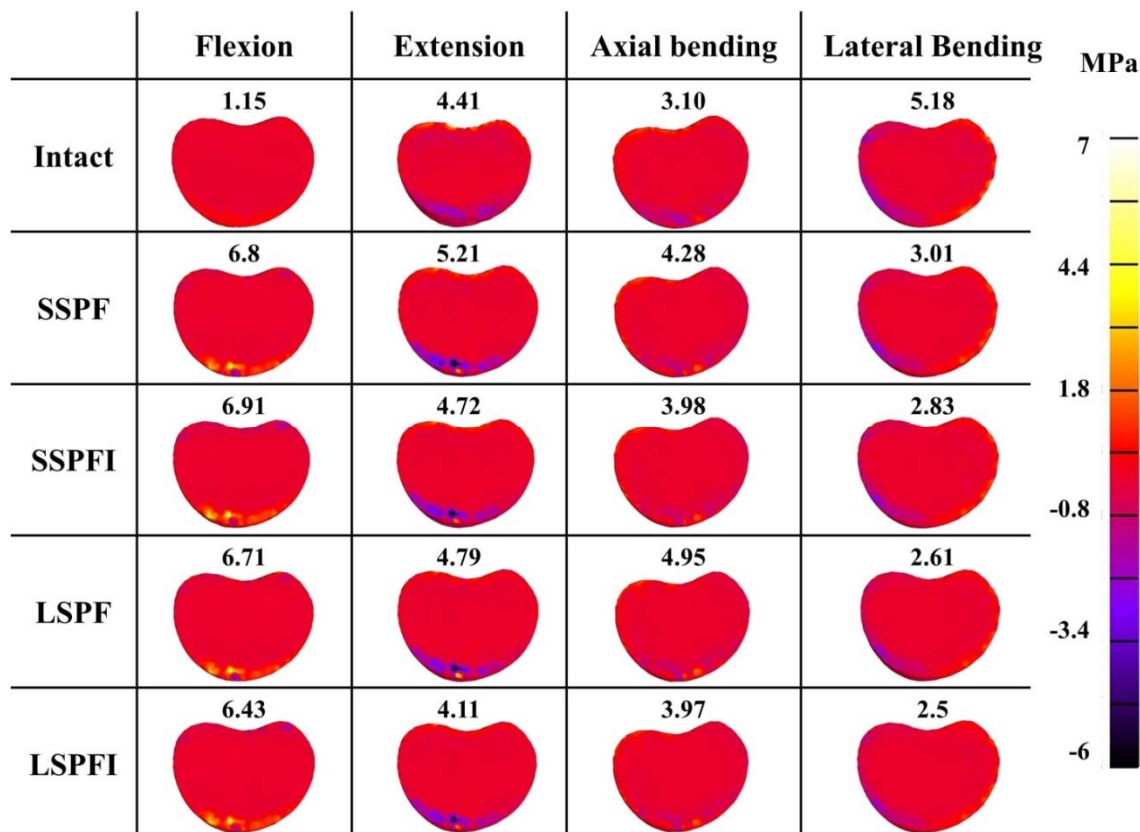
Figure 28: Intradiscal pressure distribution at T12-L1 IVD. The maximum pressure is reported in MPa.

6.4 Discussion

The SSPF is a surgical procedure alternative to the traditional LSPF approach when treating thoracolumbar BF (174). Compared to the LSPF, the SSPF is less invasive but, at the same time, less reliable in case of severe BF: high failure rates of the hardware and progressive loss of sagittal alignment have been reported (176). The inclusion of additional pedicle screws at the fracture level has been proposed as a strategy to improve the stiffness and the reliability of the SSPF (180, 184). The objective of this study was to investigate whether the inclusion of pedicle screws at the fracture level in SSPF construct enhances its biomechanical performance making it comparable to that of LSPF construct.
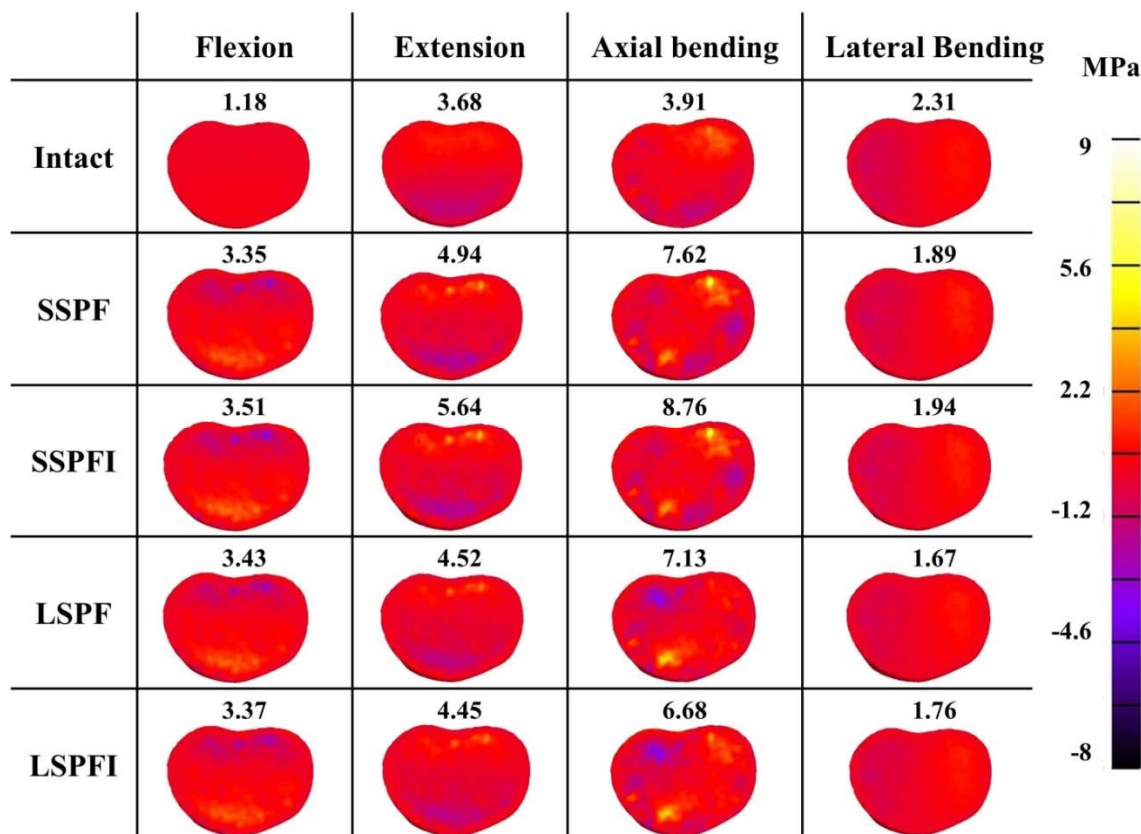
Figure 29: Intradiscal pressure distribution at L1-L2 IVD. The maximum pressure is reported in MPa.

This was done by conducting a computational biomechanical analysis using a three-dimensional finite element model of a human thoracolumbar spine (T11-L4) instrumented so as to simulate four different fixation constructs: SSPF, SSPFI, LSPF, and LSPFI. Simulations were carried out to evaluate the biomechanical performance of the four constructs undergoing flexion, extension, axial torsion and lateral bending. To validate the computational models, it was shown that their predicted angular ROMs were in good agreement with the experimental data reported in an *in vitro* study (183), see Figure 19. Subsequently, three metrics were evaluated and compared among constructs: the stiffness of T12-L2 junction, the magnitude and distribution of stresses in the

hardware, and the intradiscal pressure at the IVDs adjacent to the fractured level (i.e. T12-L1 and L1-L2).

In comparing the stiffness of the different constructs, models' predictions indicated that long-segment constructs are stiffer than short-segments ones (Table 3). Also, the inclusion of the pedicle screws at the fracture level had different effects in short- and long-segment constructs. More specifically, in short-segment constructs, the inclusion of the pedicle screws increased the stiffness of the construct by 25%, 13%, 7.5%, and 6.8% in flexion, extension, axial torsion and lateral bending, respectively. This is in agreement with an in vitro study showing that the inclusion of pedicle screws at the fracture level increases 29% the stiffness of the SSPF construct during flexion-extension (175). Also, these findings may explain the results reported in recent clinical studies showing that SSPFI can achieve and maintain kyphosis correction more efficiently than in SSPF (28, 182). On the contrary, in long-segment construct, the addition of the pedicle screw produced minor differences in the values of the stiffness. This is in agreement with a clinical study reporting that LSPF and LSPFI are equivalent in maintaining the kyphosis correction (181). Interestingly, during flexion and extension, LSPF construct was slightly stiffer than LSPFI. A similar behavior was experimentally observed by Baaj and co-workers (183) and justified considering that, in LSPFI, the longitudinal points of fixation increase from 4 to 5 points. The additional point of fixation at L1 may act as a pivot point where the middle segments are forced to bend. In contrast, in LSPF, the L1 can also translate in addition to rotate.

A stress analysis in the hardware components showed that, for all the cases investigated, the largest stress values were found in the posterior rods of the constructs. Also, it was found that inclusion of pedicle screw at the fracture level increased the magnitude of the stress for all the loading conditions tested (Table 4). Larger stress values are a direct consequence of the higher stiffness attained with these constructs. These results are consistent with an experimental biomechanical study showing that SSPFI exhibits larger strains than SSPF during flexion and extension (175). In addition, for both short- and long-segment constructs, the inclusion of the pedicle screw at the fracture level produced a more uniform distribution of the stress along the T12-L1 and L1-L2 segments of the posterior rods (Figures 26 and 27). This is likely due to the fact that, by adding a third point of fixation, the entire construct undergoes three-point bending instead of cantilever bending (174). A three-point bending mechanical load helps distributing the stresses more evenly along the posterior rods, and may extend the lifetime of the short-segment construct (28, 175).

The magnitude of the intradiscal pressure at adjacent segments lends an indication of the stability of the anterior column provided by the construct: the more stable is the construct, the smaller is the relative movement of the fractured vertebra with respect to the adjacent segments and, consequently, the higher is the intradiscal pressure at the adjacent discs [17]. In this analysis, the intradiscal pressure magnitudes and distributions were similar across constructs, and larger than that attained in the intact spine for all the loading conditions with the exception of lateral bending. The only major difference was found at L1-L2, where disc pressure attained in axial torsion with the SSPFI construct

was 15% larger than the corresponding values for SSPF construct (Figure 28 and 29). This finding suggests that, in short-segment constructs, the inclusion of pedicle screws at fracture level would improve the stability of the anterior column.

Some limitations of this study must be noted. The computational models developed in this study did not include spinal muscles, which contribute to the stability and the stiffness of the spine during motion. Accordingly, the models' predicted values of stiffness and ROM might be different from those attained *in-vivo*. However, the objective of this study was to compare the biomechanical performance of short- and long-segment constructs, with and without pedicle screws at fracture level. Since the testing conditions were the same for all the cases investigated, we do not expect relative changes in the biomechanical performance among constructs. Also, all the models were constructed from a CT scan of a healthy subject. Geometric factors (e.g., size and shape of the vertebrae, degree of misalignment of the spine due to fracture, etc.) may affect the biomechanics of the fixed thoracolumbar spine (170). Future studies, including models developed from CT scans of a larger number of subjects, must be conducted in order to broaden the validity of the results hereby presented.

In conclusion, the inclusion of pedicle screws at the fracture level in the short-segment posterior construct increased the stiffness of the thoracolumbar junction and the intradiscal pressure at adjacent IVDs, thus providing greater stability to the spine and more support to the anterior column. Moreover, the additional fixation points at the fractured vertebra helped in distributing stresses more uniformly along the posterior rods,

suggesting that this surgical approach may extend the lifetime of the construct. However, the stiffness of the thoracolumbar junction attained with a SSPFI construct was less than that provided by long-segment ones, making LSPF a biomechanically superior option for the surgical treatment of severe thoracolumbar BF.

Chapter 7 The Biomechanical behavior of The Spine after Performing Minimally Invasive Surgeries for the Treatment of Moderate BF

7.1 Introductory Remark

Conventional spine open surgeries for the treatment of spine traumatic fractures are known by their association with muscle morbidity, ischemia, and visceral herniation (79, 185), especially when an anterior approach is adopted. Hence, over the past decade, spine surgeons have developed new technologies aimed at reducing the morbidity and invasiveness of the surgery (72). In particular, minimally invasive surgeries (MIS) was proposed to obviate the complications of open surgeries and to offer essential benefits, such as less operative pain, reduced blood loss, minimums scarring, and reduced risk of infection (33, 72, 91, 186). Such technology has been used for the treatment of various spine pathologies and yielded admirable outcomes (187-190).

In particular, percutaneous pedicle screws fixation (PPSF) is a minimally invasive approach in which the implants that are utilized in the traditional SSPF are implanted percutaneously (31, 32). A major benefit of PPSF is causing less paraspinal muscle damage than open pedicle screw fixation SSPF, which preserve the natural physiology of the spine (32, 158). However, like SSPF, PPSF still has some long-term limitations: high failure rate of the implants and progressive loss of the sagittal alignment (27, 191). Another novel MIS technique for the treatment of spine fractures is the balloon Kyphoplasty (KP) with Polymethylmethacrylate (PMMA). In this technique, a bone tamp is inserted in the fractured vertebrae and inflated with gas to create a cavity that restore

the height of the vertebral body. The cavity is then filled with PMMA to cement the fractured level (Figure 30). Hence, KP causes an increase in the strength, the load bearing capacity, and the stiffness of the fractured vertebrae (192, 193). With such features, KP had been used effectively in the treatment of compression fractures and reported favorable clinical outcomes (194-196).
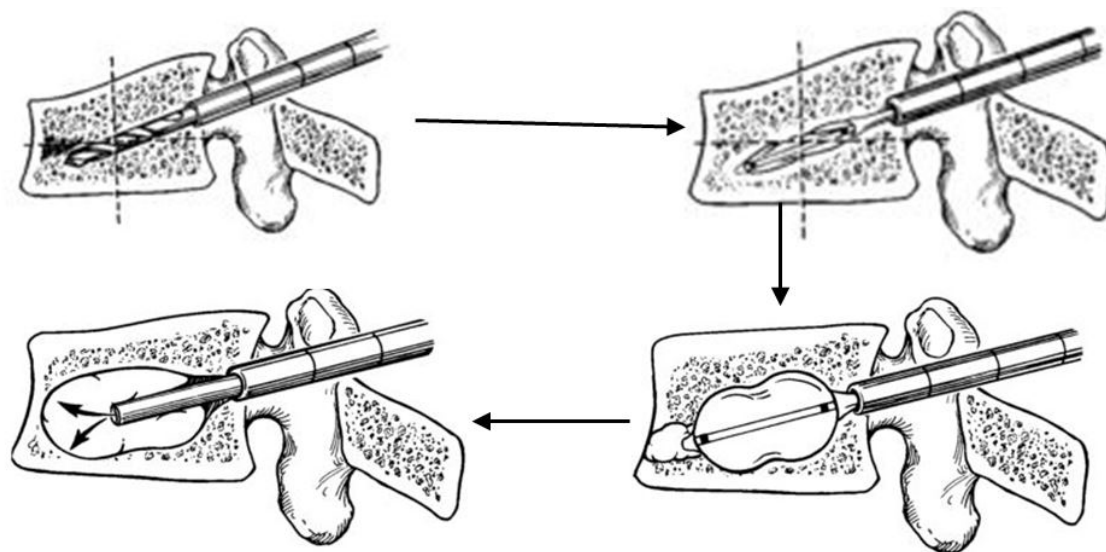
Figure 30: Kyphoplasty procedure steps. Adopted from Garfin et al. (195)

Recently, it had been proposed to apply KP in combination with PPSF as a surgical treatment of Thoracolumbar burst fractures (TBF) to reduce the limitations of stand-alone PPSF (30, 33, 91, 194, 197). By employing such approach, the three spinal columns will be stabilized with the morbidity level associated with only posterior approach (30). While several short-term clinical studies had reported satisfactory outcomes from KP-augmented PPSF in the treatment of TBF, very little is known about the biomechanical changes that associate such approach. Specifically, to what extent KP will change the spinal stiffness when combined with PPSF and what are the implications of such combination on the adjacent intervertebral discs. Moreover, whether their combination

will mitigate the stresses experienced by the implantable hardware remains unclear. It is hypothesized that, by combining KP with PPSF, spinal stiffness will increase and less stresses will be borne by the hardware. Accordingly, the objective of this study is to evaluate and compare the spinal stiffness, hardware stresses, and the intradiscal pressure at the adjacent segments of the thoracolumbar junction after performing KP- augmented PPSF for the treatment of BF.

7.2 Methods

3D FE models from T12 to L2 were constructed following the same general computational approach described in chapter 3. The only exceptions were the addition of the cartilage end plates CEP at each vertebra and assuming osteoporotic material properties at the cortical and cancellous bone of L1 (Table 5). Four models of the thoracolumbar junction T12-L2 that represent the fractured spine and three treatment scenarios were developed. Specifically, to simulate the fracture spine, L1 vertebrae was altered in a way that caused 50% loss of the vertebral body height and 20º kyphotic deformity (Figure 31.a) (10, 198). Such injury is very common in the thoracolumbar junction and was deemed an indication to employ the KP-augmented PPSF in many clinical studies (194, 197, 199). For the treatment of this injury, three surgical procedures were simulated: 1- stand-alone bipedicular KP at L1; 2- stand-alone PPSF with four pedicle screws at T12 and L2; 3- KP-augmented PPSF (KP+PPSF), see Figure (31.b, c, and d). The aim of investigating the three surgical procedures is to quantify the contribution of each approach on the biomechanics of the spine. In all the simulated

procedures, it was assumed that 95% of the vertebral body height was restored and 4º kyphosis angle was attained (31, 91, 199).
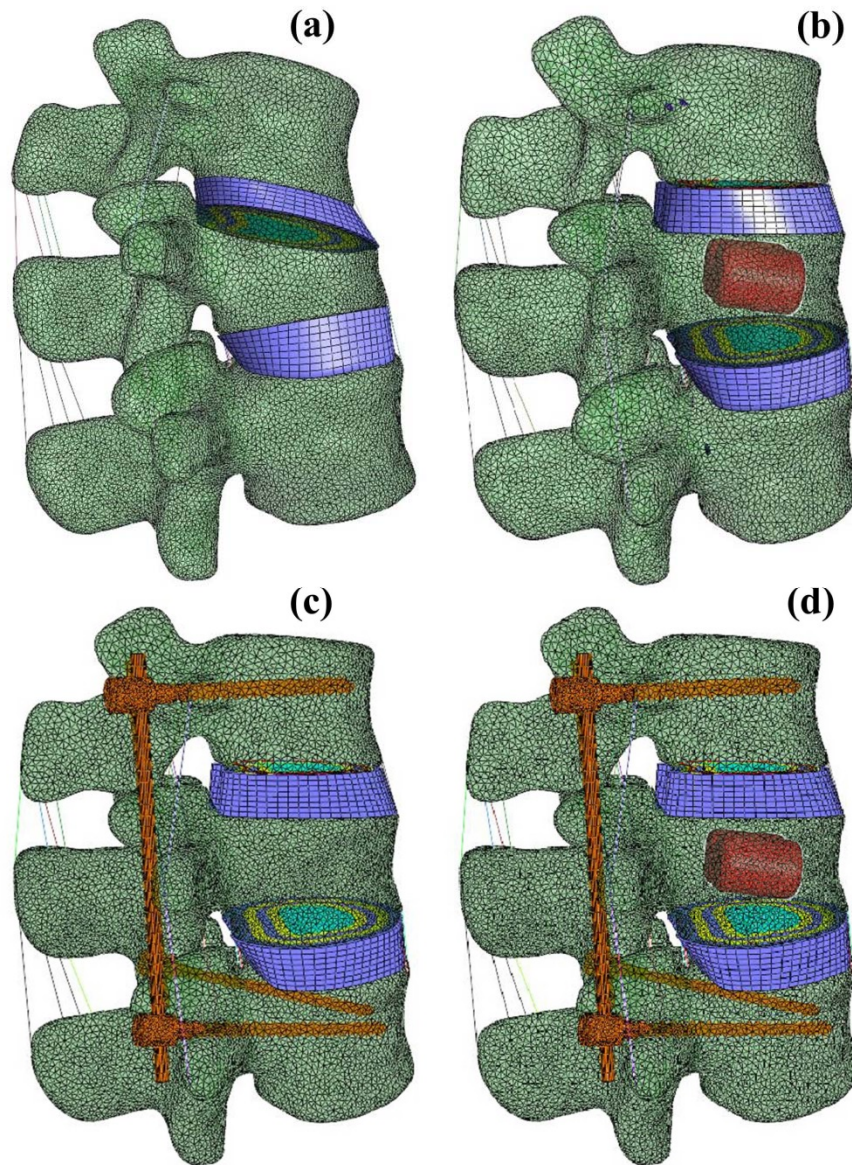
Figure 31: Set up of the investigated procedures: (a) Fracture spine; (b) only Kyphoplasty (KP); (c) Only PPSF; (d) KP+PPSF.

To simulate the bipedecular KP procedure, two bone cement cavities that occupy 13% of the total volume of the vertebral body were modeled symmetrically around the midsagittal plane (192). A layer of 1 mm was modeled at the interface between the cancellous bone and the bone cement zones, which represent a transient mixture between both materials (200). The material properties of the bone cement and the transient layer are listed in Table 5.

Table 5: Material properties used in Kyphoplasty model

Material	Property	Value	Ref.
Osteoporotic Cortical bone	Moduli in MPa	E = 5,000	(201)
	Poisson's ratio	$\nu = 0.2$	
Osteoporotic Cancellous bone	Moduli in MPa	E = 25	
	Poisson's ratio	$\nu = 0.2$	
CEP	Moduli in MPa	E = 466	(202)
	Poisson's ratio	$\nu = 0.166$	
	Hydraulic permeability	0.000059 mm^{4}N^{-1}s^{-1}	
	Volumetric fluid fraction	0.6	
Bone cement	Moduli in MPa	E = 4000	(203)
	Poisson's ratio	$\nu = 0.3$	
Bone cement interface	Moduli in MPa	E = 2012	(200)
	Poisson's ratio	$\nu = 0.3$	

All boundary conditions for the PPSF procedure were similar to those reported for SSPF procedure in chapter 6. Four pure moments of 5 Nm were applied at T12 around the three principal axes: Flexion moment (Flex), extension moment (Ext), lateral bending (LB), and axial torsion (Torsion). L2 was fixed in all directions during all loading conditions. The intact spine was also tested and used as a base line for all the investigated scenarios.

The mechanical performance of each procedure was evaluated by estimating three metrics: (1) range of motion (ROM) of the thoracolumbar junction (T12-L2), (2) Maximum stresses generated in the posterior rods and screws, and (3) Maximum intradiscal pressure at adjacent IVDs (i.e. T12-L1 and L1-L2). Such parameters were chosen to demonstrate the contribution of each procedure in to spinal stiffness, stresses at the posterior rods, and the implications on the adjacent discs. The data of ROM and intradiscal pressure are reported normalized with respect to the intact case, whereas the absolute values will be only reported for the intact case as shown in Table 6.

Table 6: Absolute values of the intact case

Intact Spine	Flex	Ext	LB	Torsion
ROM (degree)	2.87	11.99	8.45	12.95
Intradiscal Pressure at T12-L1 (MPa)	0.37	0.85	0.79	0.26
Intradiscal Pressure at L1-L2 (MPa)	0.19	0.77	1.27	0.51

7.3 Results

With respect to the intact spine, the relative T12-L2 rotation of the fracture spine increased in flexion and torsion reaching up to 115%, while it decreased in extension and LB reaching down to 72% (Figure 32). In contrast, for the KP scenario, the ROM was almost consistent to that of the intact case for all loading conditions, except in LB (111%). Moreover, the PPSF and the KP+PPSF scenarios produced comparable ROM under all loading conditions (Figure 32). It is also observed that, during extension and

lateral bending, the PPSF and the KP+PPSF procedures were the stiffest, whereas, in flexion and torsion, both of them were more flexible (Figure 32).
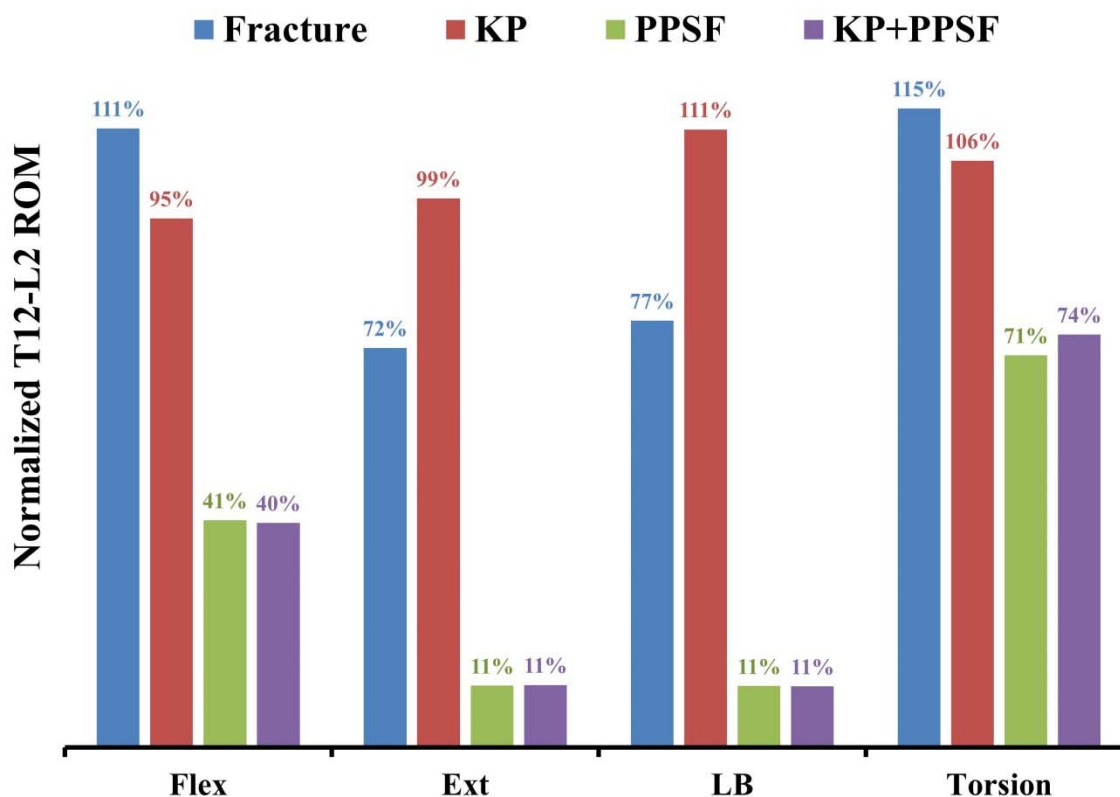
Figure 32: Relative rotation (ROM) between T12 and L2 for all investigated scenarios.

The maximum intradiscal pressure (MIP) at T12-L1 and L1-L2 levels varied considerably according to the adopted scenario and the loading condition. Specifically, at T12-L1, the fracture spine produced higher MIP with respect to the intact case in all loading conditions with the maximum value attained in LB (200%). Conversely, the KP scenario produced similar MIP to that produced from the intact case during flexion and LB, while it produced higher levels during extension and torsion (134% and 137%). Moreover, at T12-L1, the MIP generated in PPSF was comparable to that generated in

KP+PPSF for all loading conditions, with the lowest values attained during extension (35%) (Figure 33.a). On the other hand, at L1-L2 disc, the MIP produced at the fracture spine was less than the intact case, reaching down to 47% during torsion (Figure 33.b). It is also observed that the MIP in the KP scenario had a contradictory behavior: whereas it produced higher pressure during flexion and extension (164% and 162%), it produced less pressure during LB and torsion (62% and 54%), see Figure 33.b. Finally, for PPSF and KP+PPSF procedures, equivalent MIP was generated at L1-L2 during all loading conditions, except in flexion where KP+PPSF produced higher level of pressure than PPSF (144%), see Figure 33.b. Overall, PPSF and KP+PPSF scenarios generated less intradiscal pressure than the intact case at both spinal levels except in flexion.
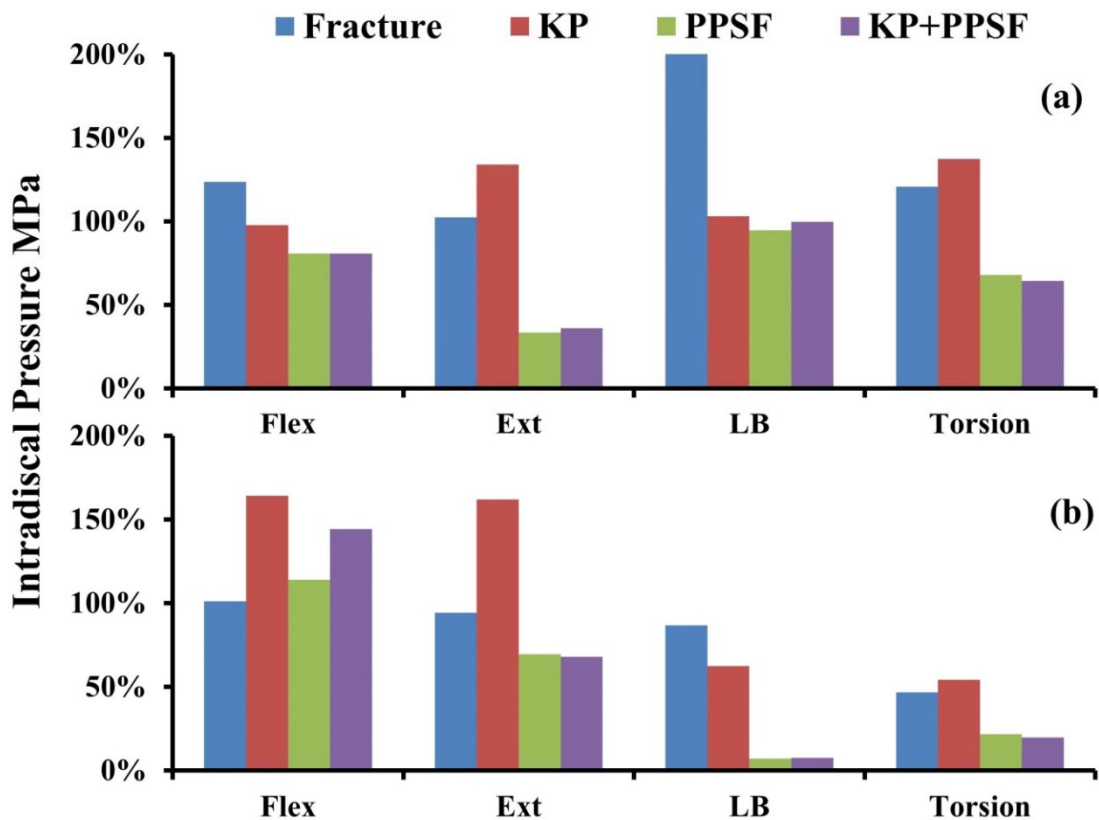
Figure 33: Maximum Intradiscal pressure for all investigated procedures: (a) at T12-L1; (b) at L1-L2.

No major differences were found between the stresses experienced by the hardware in the PPSF and KP+PPSF procedures (Figure 34.a and b). The only exception was at the two posterior rods, where PPSF bore 7% higher stresses than KP+PPSF during torsion (Figure 34.a). It is also apparent that the stress levels at the pedicle screws (Figure 34.b) were higher than that produced in the two posterior rods (Figure 34.a). Moreover, it was observed that the maximum stress levels were attained under torsion loading condition (Figure 34.a and b).
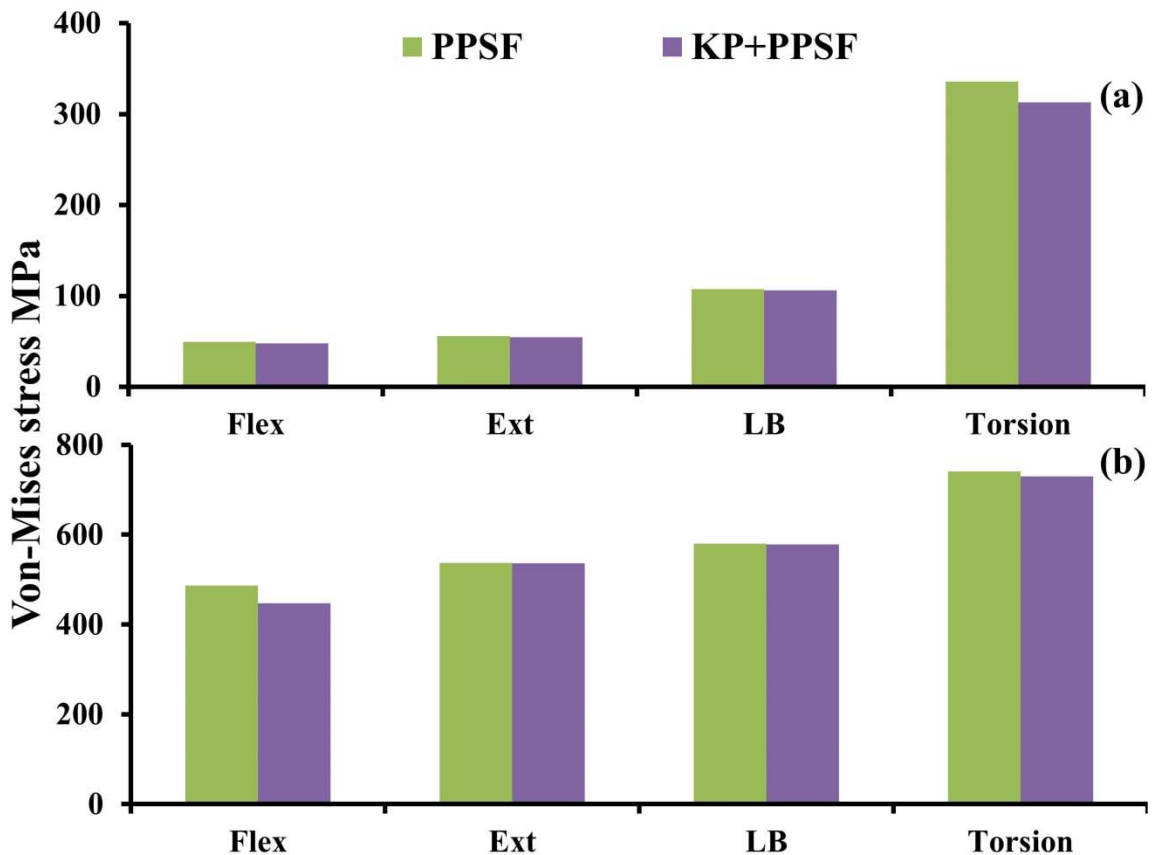
Figure 34: Maximum Von-Mises stress in the PPSF and KP+PPSF hardware: (a) posterior rods; (b) pedicle screws.

7.4 Discussion

The ultimate goals in the treatment of vertebral fractures are restoring neurological function, repairing the damaged segment, and provide stable fixation (72, 204). However, the best procedure to attain these goals for thoracolumbar burst fractures (TBF) is still controversial. With the advent of MIS, new surgical approaches have been introduced (185), such as percutaneous pedicle screw fixation (PPSF); a fixation procedure that allows distraction and solid fixation to the injured level. However, the high failure rate of the implanted hardware in PPSF remains a major concern (32, 205). Another MIS approach is the Kyphoplasty (KP); a technique used in the treatment of vertebral compression fractures by augmenting the injured level with cement (195). Due to the presence of clefts at the posterior wall of the vertebral body, KP was not recommended for TBF (89, 206). Such clefts may allow cement leakage in to the spinal canal, which may cause a neurologic dysfunction. In contrast, other physicians suggested that the balloon inflation in KP may compress the cancellous bone in a way that will cover the clefts and prevent the cement from leakage (186). Hence, some physicians proposed combining PPSF to KP in one approach as an ideal MIS for the treatment of TBF and demonstrated, in short-term clinical studies, the effectiveness of such technique (30, 31, 33, 194, 197, 199). However, the biomechanical alteration of the spine due to combining both procedures in one approach is not well understood. Accordingly, the objective of this study was to evaluate the biomechanical changes induced by performing KP-augmented PPSF for the treatment of TBF.

Following the same general computational approach, four three-dimensional finite element model of a human thoracolumbar spine (T12-L2) was developed. The models represented the fractured spine and three surgical scenarios: stand-alone KP, stand-alone PPSF, and KP-augmented PPSF. Pure moments around the three anatomical axes were applied and three metrics were measured: relative rotational angle between T12 and L1 (ROM), maximum intradiscal pressure (MIP) at T12-L1 and L1-l2 levels, and maximum stresses generated at the posterior hardware.

In comparing the ROM of the investigated approaches, model's predictions indicated that, after the fracture of L1, the rotation of the spine increased in flexion and torsion, while it decreased in extension and lateral bending (Figure 32). This is consistent with the notion that BF occurs from a flexion force, and thus more ROM is expected in flexion than in extension. The normal spine kinematics was completely attained after performing the stand-alone KP that restored 95% of the vertebral body height (Figure 32). This was in agreement with previous clinical studies that proved the effectiveness of using KP in restoring the normal mobility of the spine for incomplete osteoporotic BF (89, 207). However, cement extravasation had been observed in some cases. Another important finding was that both PPSF and KP+PPSF approaches reduced the ROM of the spine in the same fashion for all loading conditions (Figure 32). This could be attributed to the high stiffness provided by the posterior hardware, which predominate the role of KP. This observation was more verified after examining the stresses at the posterior hardware in both approaches. Specifically, as illustrated in Figure 34, minor differences were found in the generated stresses between both approaches, which show the minor contribution of

KP on transferring the load. However, the testing carried out in this study was an immediate postoperative assessment in which all the hardware are still fresh and no long term implications had afflicted them. This finding may support the idea that the advantage of adding KP to PPSF is in the long term maintenance of the hardware and not on the immediate stability of the spine. Moreover, it is clear from Figures 32 and 34 that even after augmenting PPSF with KP, axial torsion are still the most unstable loading mode for the spine.

After the fracture of L1, the MIP increased at T12-L1 level and decreased in L1-L2 level (Figure 33). This result may be explained by the fact that, due to loosing 50% of the vertebral body height, a dramatic change on the alignment and geometry occurred at T12-L1, which may cause a great alteration in the pressure level inside the disc (Figure 33.a). In contrast, there was no consistent trend of the MIP for all surgical approaches in both levels (i.e. T12-L1 and L1-L2). In the KP procedure, the MIP was near the normal levels at T12-L1. In contrast, at L1-L2, pressure levels where higher than the normal levels in some loading conditions, and lower in other loading conditions (Figure 33.b). It has been hypothesized that augmenting the vertebral body with cement during quasi-static compression causes a load shift at the adjacent discs, leading to an increase in the intradiscal pressure (208, 209). However, since the literature lacks any examination of KP by loading conditions similar to the one used in this study, the observed results were not verified. The last finding was the comparable pressure levels generated after performing both PPSF and the KP+PPSF approaches at the two investigated spinal levels, which were always less than the normal levels (Figure 33). These outcomes emphasize

the conclusion that the posterior hardware predominate the role of KP in stabilizing the spine postoperatively and that the major advantage of KP at this stage is in distracting and restoring the height of the vertebral body. Moreover, these result suggest that the transfer of load on the operated level is shifted to the posterior hardware, leading to less levels of the intradiscal pressure

The results of this study might be limited by the indirect validation of the models. Unfortunately, no biomechanical experiments were conducted in the literature to evaluate the examined approaches. Hence, we accounted on our accredited thoracolumbar spine model that had been validated in previous studies (52, 210). Another common limitation is simulating the fragmentation of L1 due to BF as an osteoporotic bone. However, such assumption is accepted in the literature and had been approved in previous studies (200, 209). Finally, it was assumed that the three approaches would be able to restore 95% of the vertebral body height, which might not be the case in reality. This was done in purpose to compare the three approaches after attaining the same level of recovery.

In conclusion, the biomechanical superiority of augmenting PPSF with KP over the stand-alone PPSF was not confirmed in this study. A possible explanation for this might be the focus on investigating the immediate postoperative performance of the spine rather than the long term performance. It is noteworthy that, in actual patients, the loss of the angular correction that was attained after performing the PPSF occurs progressively. In such case, the hardware would have already experienced different loading conditions and more residual stresses have been accumulated, which impair the hardware resistance to

deformation. Therefore, to develop a full picture, a fatigue testing would be required to explore the long-term effect of augmenting PPSF with KP and demonstrate the biomechanical benefits of such approach.

Chapter 8 Dissertation Summary

Low back pain and spinal injuries are the leading ailment that causes activity limitations and work absence, yielding to an enormous economic burden on American individuals and government (211). The degenerative diseases and traumatic injuries that initiate such condition can be managed conservatively; however, in many cases surgical intervention is indispensable. In such cases, by the advent of new surgical spinal implants, the costs of operative management drastically increased, causing a significant burden on the healthcare system in the United States (212). Moreover, adjacent segment disease (ASD), because of the surgical intervention, is another major complication. It is believed that segments adjacent to a fused segment are prone to increased range of motion and intradiscal pressures (67, 162), which may lead to the development of pathological condition at those spinal levels. However, little is known about the relationship between many spinal procedures and the development of ASD. Furthermore, in some cases, revision surgeries are required due to failure on attaining the goals of the initial operation (24, 84). Therefore, there is a clinical need for a tool that can better optimize the surgical treatment by fulfilling the goals of the surgery without jeopardizing the health of the adjacent segments.

Finite element (FE) method has been used as an analytical technique to solve problems in orthopedic applications from decades (92). By the advancement in imaging techniques and the improvements in computational power, 3D models of the spinal tissues were precisely constructed. Accordingly, the main objective of this project is to develop a new

methodology that utilizes the unique capability of FE methods to optimize the surgical techniques performed at the thoracolumbar region without compromising the health of the adjacent segments. The **long-term goal** of this research is to develop a patient-specific computational tool to be used in clinics for optimizing surgical treatment of spine pathologies. Specifically, the CT scans of a normal subject were used to reconstruct the 3D anatomical model of the thoracolumbar spine (T11-S1). Then, the models were employed in a CAD tool to virtually perform specific surgical procedures usually used for a particular pathological condition. Next, the models of the different surgical procedure were discretized (meshed) for a FE analysis. Finally, physiological loading conditions were simulated in each surgical alternative and the optimal surgery was specified.

In this dissertation, two specific-aims addressing a spine degenerative disease and a spinal traumatic injury were studied. Specific-aim#1 focused on analyzing and comparing four decompressive surgeries used for the treatment of lumbar spinal stenosis (LSS); an anatomical reduction of the lumbar spinal canal that causes compression on the spinal cord or nerve roots. Specific-aim#2 focused on analyzing and comparing multiple surgeries that are used for the treatment of thoracolumbar burst fractures (TBF). Due to the different classification and approaches of this kind of fracture, the second specific aim was divided into three sub-aims: sub-aim 2.1, sub-aim 2.2, and sub-aim 2.3. Each sub-aim investigated a set of open or minimally invasive surgical procedures that are usually performed for the same fracture indications. All the virtual surgical procedures were

approved by an orthopedic surgeon and all the simulation/analysis were carried out using the same FE tool (FEBio).

In specific-aim#1, unilateral laminotomy, bilateral laminotomy, facet-sparing laminectomy, and laminectomy with facetectomy surgical procedures were considered. The post-operative changes in the ROM, intradiscal pressure, and peak stresses were measured in each lumbar spine segment. The results suggested that, in the treatment of LSS, laminotomy, whether unilateral or bilateral, represents a superior technique in terms of potential risk reduction for developing either spine instability or mechanically-accelerated disc degeneration in the adjacent segment. Moreover, it is recognized that surgical decision-making must take into account many other factors, among which the severity of the stenosis. While laminotomy has been recommended for cases of moderate or unilateral stenosis, and it might not allow for adequate decompression of severe central or bilateral stenosis [25] in which case laminectomy may represent a better surgical solution despite the increase in instability shown in our study.

In sub-aim2.1, surgical treatment for severe TBF were investigated after performing corpectomy to remove the whole fragments of the vertebral body and place an expandable cage instead. Four different fixation approaches were considered: 2RPC, 1RPC, 2RC, and PC. The results showed that the constructs including pedicle screws (2RPC, 1RPC, 2RC) yielded similar biomechanical performance being the stiffest. Moreover, the same constructs demonstrated comparable stress levels at the adjacent segments, generating 50% higher than that produced from the PC construct. Elevated

mechanical stress is believed to be a cause of disc degeneration. Accordingly, the PC construct, although less reliable in stabilizing the injured segment, represented the most conservative approach for preventing potential development of adjacent disc degeneration.

In sub-aim 2.3, posterior approaches used in the surgical treatment of TBF were analyzed. Specifically, the advantage of adding a pedicle screw at the fracture level for short and long-segment posterior construct (SSPF, SSPFI, LSPF, LSPFI) was investigated. The extracted data confirmed that the inclusion of pedicle screws at the fracture level in the short-segment posterior construct increased the stiffness of the thoracolumbar junction and the intradiscal pressure at adjacent IVDs, thus providing greater stability to the spine and more support to the anterior column. Moreover, the additional fixation points at the fractured vertebra helped in distributing stresses more uniformly along the posterior rods, suggesting that this surgical approach may extend the lifetime of the construct. However, the stiffness of the thoracolumbar junction attained with a SSPFI construct was less than that provided by long-segment ones, making LSPF a biomechanically superior option for the surgical treatment of TBF.

Finally, in sub-aim 2.3, different minimally invasive surgeries were examined for the treatment of TBF. Specifically, the advantage of augmenting percutaneous pedicle screws (PPSF) with balloon Kyphoplasty (KP) was studied. Towards that, the fracture spine junction (T12-L2) together with three potential minimally invasive surgeries was simulated. The results didn't prove any biomechanical superiority of augmenting PPSF

with KP over the stand-alone PPSF. A possible explanation for this might be the focus on investigating the immediate postoperative performance of the spine rather than the long term performance. It is noteworthy that, in actual patients, the loss of the angular correction that was attained after performing the PPSF occurs progressively. In such case, the hardware would have already experienced different loading conditions and more residual stresses have been accumulated, which impair the resistance to deformation. Therefore, to develop a full picture, a fatigue testing would be required to explore the long-term effect of augmenting PPSF with KP and demonstrate the biomechanical benefits of such approach.

Some limitations of this work must be noted. FE method produces approximate solutions, where it converges to the exact solution when the mesh density approximates infinity. However, with the advancement of the computational power and by running convergence tests, the accuracy of the obtained results became very reliable and the errors would not affect the conclusions. Also, in light of high inter-subject variability, the generalization of results of a single model to a population remains a concern. Future studies, including models developed from CT scans of a larger number of subjects, must be conducted in order to broaden the validity of the results hereby presented. Finally, muscles are not included in the models because we were simulating the biomechanical testing on cadavers. The objective of this work was to compare between different surgical procedures, so it is assumed that the contribution of the muscles to all of them is similar which makes our final recommendations reliable. However, it is important to mention that this is not precisely the case *In-vivo*.

Future studies on the current topic are therefore recommended. Specifically, building multiple spine models from CT scans of different patients would help in generalizing the obtained conclusions and make it more accredited. Also, more pathological spine conditions could be tested, especially those produced from traumatic injuries, such as flexion-subluxation and rotational wedge fractures. Moreover, in this project multiple software were utilized to finish the analysis starting from the CT scans until running the simulations. It would be very useful to integrate some software together to ease and expedite the process of generating the models and conducting the analysis. Accordingly, a tool for patient-specific diagnosis and surgical treatment optimization would be very achievable, which will have an enormous impact on the quality and the costs of the provided healthcare.

References

1.   MayFieldClinic. Anatomy of the Human Spine 2016 [Available from: http://www.mayfieldclinic.com/PE-AnatSpine.htm.

2.   Dai L-Y, Jiang S-D, Wang X-Y, Jiang L-S. A review of the management of thoracolumbar burst fractures. Surgical Neurology. 2007;67(3):221-31.

3.   Hitchon PW, Torner JC, Haddad SF, Follett KA. Management options in thoracolumbar burst fractures. Surgical Neurology. 1998;49(6):619-27.

4.   Benz RJ, Garfin SR. Current techniques of decompression of the lumbar spine. Clinical Orthopaedics and Related Research. 2001;384:75-81.

5.   Chad DA. Lumbar spinal stenosis. Neurologic Clinics. 2007;25(2):407-18.

6.   Genevay S, Atlas SJ. Lumbar spinal stenosis. Best Practice & Research Clinical Rheumatology. 2010;24(2):253-65.

7.   Atlas SJ, Keller RB, Wu YA, Deyo RA, Singer DE. Long-term outcomes of surgical and nonsurgical management of lumbar spinal stenosis: 8 to 10 year results from the maine lumbar spine study. Spine. 2005;30(8):936-43.

8.   Englund J. Lumbar spinal stenosis. Current Sports Medicine Reports. 2007;6(1):50-5.

9.   Atlas SJ, Keller RB, Robson D, Deyo RA, Singer DE. Surgical and nonsurgical management of lumbar spinal stenosis: four-year outcomes from the maine lumbar spine study. Spine. 2000;25(5):556-62.

10.   Danisa OA, Shaffrey CI, Jane JA, Whitehill R, Wang G-J, Szabo TA, et al. Surgical approaches for the correction of unstable thoracolumbar burst fractures: a retrospective analysis of treatment outcomes. Journal of Neurosurgery. 1995;83(6):977-83.

11.   Bradford DS, Mcbride GG. Surgical management of thoracolumbar spine fractures with incomplete neurologic deficits. Clinical Orthopaedics and Related Research. 1987;218:201-16.

12.   Battié MC, Lazáry Á, Fairbank J, Eisenstein S, Heywood C, Brayda-Bruno M, et al. Disc degeneration-related clinical phenotypes. European Spine Journal. 2014;23(3):305-14.

13.   Park P, Garton HJ, Gala VC, Hoff JT, McGillicuddy JE. Adjacent segment disease after lumbar or lumbosacral fusion: review of the literature. Spine. 2004;29(17):1938-44.

14.   Huiskes R, Chao E. A survey of finite element analysis in orthopedic biomechanics: the first decade. Journal of Biomechanics. 1983;16(6):385-409.

15.   Maas SA, Ellis BJ, Ateshian GA, Weiss JA. FEBio: finite elements for biomechanics. Journal of Biomechanical Engineering. 2012;134(1):011005.

16.   Goel VK, Gilbertson LG. Spine Update: Applications of the finite element method to thoracolumbar spinal research-past, present, and future. Spine. 1995;20(15):1719-27.

17.   Esses S, Botsford D, Kostuik J. Evaluation of surgical treatment for burst fractures. Spine. 1990;15(7):667-73.

18.   Denis F. The three column spine and its significance in the classification of acute thoracolumbar spinal injuries. Spine. 1983;8(8):817-31.

19.   Magerl F, Aebi M, Gertzbein S, Harms J, Nazarian S. A comprehensive classification of thoracic and lumbar injuries. European Spine Journal. 1994;3(4):184-201.

20.   Been H, Bouma G. Comparison of two types of surgery for thoraco-lumbar burst fractures: combined anterior and posterior stabilisation vs. posterior instrumentation only. Acta Neurochirurgica. 1999;141(4):349-57.

21.   Wood K, Bohn D, Mehbod A. Anterior versus posterior treatment of stable thoracolumbar burst fractures without neurologic deficit: a prospective, randomized study. Journal of Spinal Disorders & Techniques. 2005;18:S15-S23.

22.   Scheer JK, Bakhsheshian J, Fakurnejad S, Oh T, Dahdaleh NS, Smith ZA. Evidence-based medicine of traumatic thoracolumbar burst fractures: A systematic review of operative management across 20 years. Global Spine Journal. 2015;5(1):73.

23.   Scholl BM, Theiss SM, Kirkpatrick JS. Short segment fixation of thoracolumbar burst fractures. Orthopedics. 2006;29(8).

24.   McLain RF. The biomechanics of long versus short fixation for thoracolumbar spine fractures. Spine. 2006;31(11S):S70-S9.

25.   Tezeren G, Kuru I. Posterior fixation of thoracolumbar burst fracture: short-segment pedicle fixation versus long-segment instrumentation. Journal of Spinal Disorders & Techniques. 2005;18(6):485-8.

26.   Waqar M, Van-Popta D, Barone DG, Bhojak M, Pillay R, Sarsam Z. Short versus long-segment posterior fixation in the treatment of thoracolumbar junction fractures: a comparison of outcomes. British Journal of Neurosurgery. 2016:1-4.

27.   Mahar A, Kim C, Wedemeyer M, Mitsunaga L, Odell T, Johnson B, et al. Short-segment fixation of lumbar burst fractures using pedicle fixation at the level of the fracture. Spine. 2007;32(14):1503-7.

28.   Farrokhi MR, Razmkon A, Maghami Z, Nikoo Z. Inclusion of the fracture level in short segment fixation of thoracolumbar fractures. European Spine Journal. 2010;19(10):1651-56.

29.   Guven O, Kocaoglu B, Bezer M, Aydin N, Nalbantoglu U. The use of screw at the fracture level in the treatment of thoracolumbar burst fractures. Journal of Spinal Disorders & Techniques. 2009;22(6):417-21.

30.   Acosta FL, Aryan HE, Taylor WR, Ames CP. Kyphoplasty-augmented short-segment pedicle screw fixation of traumatic lumbar burst fractures: initial clinical experience and literature review. Neurological Focus. 2005;18(3):1-6.

31.   Fuentes S, Blondel B, Metellus P, Gaudart J, Adetchessi T, Dufour H. Percutaneous kyphoplasty and pedicle screw fixation for the management of thoraco-lumbar burst fractures. European Spine Journal. 2010;19(8):1281-7.

32.   Ni W-F, Huang Y-X, Chi Y-L, Xu H-Z, Lin Y, Wang X-Y, et al. Percutaneous pedicle screw fixation for neurologic intact thoracolumbar burst fractures. Clinical Spine Surgery. 2010;23(8):530-7.

33.   Korovessis P, Repantis T, Petsinis G, Iliopoulos P, Hadjipavlou A. Direct reduction of thoracolumbar burst fractures by means of balloon kyphoplasty with calcium phosphate and stabilization with pedicle-screw instrumentation and fusion. Spine. 2008;33(4):E100-E8.

34.   Cramer GD, Darby SA. Clinical anatomy of the spine, spinal cord, and ANS: Elsevier Health Sciences; 2013.

35.   Library HA. Upper Cervical Spine Anatomy 2016 [Available from: http://humananatomylibrary.com/upper-cervical-spine-anatomy/.

36.   Raj PP. Intervertebral disc: anatomy-physiology-pathophysiology-treatment. Pain Practice. 2008;8(1):18-44.

37.   Dreyer SJ, Dreyfuss PH. Low back pain and the zygapophysial (facet) joints. Archives of Physical Medicine and Rehabilitation. 1996;77(3):290-300.

38.   Rodts KBM. Ligaments: Spineuniverse; 2017 [Available from: https://www.spineuniverse.com/anatomy/ligaments.

39.   Resnick D. Degenerative diseases of the vertebral column. Radiology. 1985;156(1):3-14.

40.   Adams MA, Roughley PJ. What is intervertebral disc degeneration, and what causes it? Spine. 2006;31(18):2151-61.

41.   Tokuhashi Y, Matsuzaki H, Uematsu Y, Oda H. Symptoms of thoracolumbar junction disc herniation. Spine. 2001;26(22):E512-E8.

42.   Fujiwara A, Tamai K, An HS, Lim T-H, Yoshida H, Kurihashi A, et al. Orientation and osteoarthritis of the lumbar facet joint. Clinical Orthopaedics and Related Research. 2001;385:88-94.

43.   Kalichman L, Hunter DJ, editors. Lumbar facet joint osteoarthritis: a review. Seminars in Arthritis and Rheumatism; 2007: Elsevier.

44.   Tischer T, Aktas T, Milz S, Putz RV. Detailed pathological changes of human lumbar facet joints L1–L5 in elderly individuals. European Spine Journal. 2006;15(3):308-15.

45.   Fredrickson BE, Baker D, McHolick W, Yuan H, Lubicky J. The natural history of spondylolysis and spondylolisthesis. J Bone Joint Surg Am. 1984;66(5):699-707.

46.   Wiltse LL, Newman P, Macnab I. Classification of spondyloisis and spondylolisthesis. Clinical Orthopaedics and Related Research. 1976;117:23-9.

47.   Szpalski M, Gunzburg R. Lumbar spinal stenosis: clinical features and new trends in surgical treatment. Geriatr Times. 2004;5(4):11.

48.   Long DM, BenDebba M, Torgerson WS, Boyd RJ, Dawson EG, Hardy RW, et al. Persistent back pain and sciatica in the United States: patient characteristics. Journal of Spinal Disorders & Techniques. 1996;9(1):40-58.

49.   Verbiest H. A radicular syndrome from developmental narrowing of the lumbar vertebral canal. Bone & Joint Journal. 1954;36(2):230-7.

50.   Thome C, Zevgaridis D, Leheta O, Bazner H, Pockler-Schoniger C, Wohrle J, et al. Outcome after less-invasive decompression of lumbar spinal stenosis: a randomized comparison of unilateral laminotomy, bilateral laminotomy, and laminectomy. Journal of Neurosurgery: Spine. 2005;3(2):129-41.

51.   Lee MJ, Bransford RJ, Bellabarba C, Chapman JR, Cohen AM, Harrington RM, et al. The effect of bilateral laminotomy versus laminectomy on the motion and stiffness of the human lumbar spine: a biomechanical comparison. Spine. 2010;35(19):1789-93.

52.   Travascio F, Asfour S, Gjolaj J, Latta L, Elmasry S. Implications of decompressive surgical procedures for lumbar spine stenosis on the biomechanics of the adjacent segment: A finite element analysis. J Spine. 2015;4(220):2.

53.   Natelson SE. The injudicious laminectomy. Spine. 1986;11(9):966-9.

54.   Johnsson K-E, Redlund-Johnell I, Uden A, Willner S. Preoperative and postoperative instability in lumbar spinal stenosis. Spine. 1989;14(6):591-3.

55.   Aryanpur J, Ducker T. Multilevel lumbar laminotomies: an alternative to laminectomy in the treatment of lumbar stenosis. Neurosurgery. 1990;26(3):429-33.

56.   Tsai RY, Yang R, Bray RD. Microscopic laminotomies for degenerative lumbar spinal stenosis. Journal of Spinal Disorders. 1998;11(5):389-94.

57.   Fu Y-S, Zeng B-F, Xu J-G. Long-term outcomes of two different decompressive techniques for lumbar spinal stenosis. Spine. 2008;33(5):514-8.

58.   Hansraj KK, O'Leary PF, Cammisa Jr FP, Hall JC, Fras CI, Cohen MS, et al. Decompression, fusion, and instrumentation surgery for complex lumbar spinal stenosis. Clinical Orthopaedics and Related Research. 2001;384:18-25.

59.   Dorward IG, Lenke LG, Bridwell KH, O'Leary PT, Stoker GE, Pahys JM, et al. Transforaminal versus anterior lumbar interbody fusion in long deformity constructs: a matched cohort analysis. Spine. 2013;38(12):E755-E62.

60.   Faundez AA, Schwender JD, Safriel Y, Gilbert TJ, Mehbod AA, Denis F, et al. Clinical and radiological outcome of anterior–posterior fusion versus transforaminal lumbar interbody fusion for symptomatic disc degeneration: a retrospective comparative study of 133 patients. European Spine Journal. 2009;18(2):203-11.

61.   Hsieh PC, Koski TR, O'Shaughnessy BA, Sugrue P, Salehi S, Ondra S, et al. Anterior lumbar interbody fusion in comparison with transforaminal lumbar interbody fusion: implications for the restoration of foraminal height, local disc angle, lumbar lordosis, and sagittal balance. Journal of Neurosurgery. 2007; 7(4):379-86.

62.   Winder MJ, Gambhir S. Comparison of ALIF vs. XLIF for L4/5 interbody fusion: pros, cons, and literature review. Journal of Spine Surgery. 2015;2(1):2-8.

63.   McAfee PC, Shucosky E, Chotikul L, Salari B, Chen L, Jerrems D. Multilevel extreme lateral interbody fusion (XLIF) and osteotomies for 3-dimensional severe deformity: 25 consecutive cases. The International Journal of Spine Surgery. 2013;7(1):e8-e19.

64.   Brau SA, Delamarter RB, Schiffman ML, Williams LA, Watkins RG. Vascular injury during anterior lumbar surgery. The Spine Journal. 2004;4(4):409-12.

65.   Okuda S, Miyauchi A, Oda T, Haku T, Yamamoto T, Iwasaki M. Surgical complications of posterior lumbar interbody fusion with total facetectomy in 251 patients. Journal of Neurosurgery: Spine. 2006;4(4):304-9.

66.   Cardoso MJ, Dmitriev AE, Helgeson M, Lehman RA, Kuklo TR, Rosner MK. Does superior-segment facet violation or laminectomy destabilize the adjacent level in lumbar transpedicular fixation?: an in vitro human cadaveric assessment. Spine. 2008;33(26):2868-73.

67.   Mannion AF, Leivseth G, Brox J-I, Fritzell P, Hägg O, Fairbank JC. ISSLS Prize Winner: Long-term follow-up suggests spinal fusion is associated with increased adjacent segment disc degeneration but without influence on clinical outcome: results of a combined follow-up from 4 randomized controlled trials. Spine. 2014;39(17):1373-83.

68.   Morishita Y, Ohta H, Naito M, Matsumoto Y, Huang G, Tatsumi M, et al. Kinematic evaluation of the adjacent segments after lumbar instrumented surgery: a comparison between rigid fusion and dynamic non-fusion stabilization. European Spine Journal. 2011;20(9):1480-5.

69.   Auerbach JD, Wills BP, McIntosh TC, Balderston RA. Evaluation of spinal kinematics following lumbar total disc replacement and circumferential fusion using in vivo fluoroscopy. Spine. 2007;32(5):527-36.

70.   Rao RD, Wang M, Singhal P, McGrady LM, Rao S. Intradiscal pressure and kinematic behavior of lumbar spine after bilateral laminotomy and laminectomy. The Spine Journal. 2002;2(5):320-6.

71.   Grazer K, Holbrock T, Kelsey J. The frequency of occurrence, impact, and cost of musculoskeletal conditions in the United States. Proceedings of the American Academy of Orthopaedic Surgeons Chicago, IL: American Academy of Orthopaedic Surgeons. 1984.

72.   Wood KB, Li W, Lebl DS, Ploumis A. Management of thoracolumbar spine fractures. The Spine Journal. 2014;14(1):145-64.

73.   Denis F. Spinal instability as defined by the three-column spine concept in acute spinal trauma. Clinical Orthopaedics and Related Research. 1984;189:65-76.

74.   Wood KB, Khanna G, Vaccaro AR, Arnold PM, Harris MB, Mehbod AA. Assessment of two thoracolumbar fracture classification systems as used by multiple surgeons. J Bone Joint Surg Am. 2005;87(7):1423-9.

75.   Patel AA, Vaccaro AR, Albert TJ, Hilibrand AS, Harrop JS, Anderson DG, et al. The adoption of a new classification system: time-dependent variation in interobserver reliability of the thoracolumbar injury severity score classification system. Spine. 2007;32(3):E105-E10.

76.   Vaccaro AR, Lehman Jr RA, Hurlbert RJ, Anderson PA, Harris M, Hedlund R, et al. A new classification of thoracolumbar injuries: the importance of injury morphology, the integrity of the posterior ligamentous complex, and neurologic status. Spine. 2005;30(20):2325-33.

77.   Vaccaro AR, Lee JY, Schweitzer KM, Lim MR, Baron EM, Öner F, et al. Assessment of injury to the posterior ligamentous complex in thoracolumbar spine trauma. The Spine Journal. 2006;6(5):524-8.

78.   Jacobs RR, Casey MP. Surgical management of thoracolumbar spinal injuries general principles and controversial considerations. Clinical Orthopaedics and Related Research. 1984;189:22-35.

79.   Pneumaticos SG, Triantafyllopoulos GK, Giannoudis PV. Advances made in the treatment of thoracolumbar fractures: current trends and future directions. Injury. 2013;44(6):703-12.

80.   Hsu JM, Joseph T, Ellis AM. Thoracolumbar fracture in blunt trauma patients: guidelines for diagnosis and imaging. Injury. 2003;34(6):426-33.

81.   Radcliff KE, Kepler CK, Delasotta LA, Rihn JA, Harrop JS, Hilibrand AS, et al. Current management review of thoracolumbar cord syndromes. The Spine Journal. 2011;11(9):884-92.

82.   Öner FC, Wood KB, Smith JS, Shaffrey CI. Therapeutic decision making in thoracolumbar spine trauma. Spine. 2010;35(21S):S235-S44.

83.   Gurr KR, McAfee PC, Shih C. Biomechanical analysis of anterior and posterior instrumentation systems after corpectomy. A calf-spine model. The Journal of Bone & Joint Surgery. 1988;70(8):1182-91.

84.   McLain RF, Sparling E, Benson DR. Early failure of short-segment pedicle instrumentation for thoracolumbar fractures. A preliminary report. The Journal of Bone & Joint Surgery. 1993;75(2):162-7.

85.   Zahra B, Jodoin A, Maurais G, Parent S, Mac-Thiong J-M. Treatment of thoracolumbar burst fractures by means of anterior fusion and cage. Journal of Spinal Disorders & Techniques. 2012;25(1):30-7.

86.   Lin B, Chen Z, Guo Z, Liu H, Yi Z. Anterior approach versus posterior approach with subtotal corpectomy, decompression, and reconstruction of spine in the treatment of thoracolumbar burst fractures: A prospective randomized controlled study. Journal of Spinal Disorders & Techniques. 2011.

87.   Bishop FS, Samuelson MM, Finn MA, Bachus KN, Brodke DS, Schmidt MH. The biomechanical contribution of varying posterior constructs following anterior thoracolumbar corpectomy and reconstruction: Laboratory investigation. Journal of Neurosurgery: Spine. 2010;13(2):234-9.

88.   Rampersaud YR, Annand N, Dekutoski MB. Use of minimally invasive surgical techniques in the management of thoracolumbar trauma: current concepts. Spine. 2006;31(11S):S96-S102.

89.   Maestretti G, Cremer C, Otten P, Jakob RP. Prospective study of standalone balloon kyphoplasty with calcium phosphate cement augmentation in traumatic fractures. European Spine Journal. 2007;16(5):601-10.

90.   Assaker R. Minimal access spinal technologies: state-of-the-art, indications, and techniques. Joint Bone Spine. 2004;71(6):459-69.

91.   Korovessis P, Hadjipavlou A, Repantis T. Minimal invasive short posterior instrumentation plus balloon kyphoplasty with calcium phosphate for burst and severe compression lumbar fractures. Spine. 2008;33(6):658-67.

92.   Kallemeyn NA, Shivanna KH, DeVries NA, Kode S, Gandhi AA, Fredericks DC, et al. Advancements in spine FE mesh development: Toward patient-specific models. Patient-Specific Modeling in Tomorrow's Medicine: Springer; 2011. p. 75-101.

93.   Belytschko T, Kulak R, Schultz A, Galante J. Finite element stress analysis of an intervertebral disc. Journal of Biomechanics. 1974;7(3):277-85.

94.   Yoganandan N, Myklebust J, Ray G, Sances Jr A. Mathematical and finite element analysis of spine injuries. Critical Reviews in Biomedical Engineering. 1986;15(1):29-93.

95.   Yoganandan N, Kumaresan S, Voo L, Pintar FA. Finite element applications in human cervical spine modeling. Spine. 1996;21(15):1824-34.

96.   Natarajan RN, Williams JR, Andersson GB. Recent advances in analytical modeling of lumbar disc degeneration. Spine. 2004;29(23):2733-41.

97.   Campbell J, Petrella A. Automated finite element modeling of the lumbar spine: Using a statistical shape model to generate a virtual population of models. Journal of Biomechanics. 2016.

98.   Neal ML, Kerckhoffs R. Current progress in patient-specific modeling. Briefings in Bioinformatics. 2009:bbp049.

99.   Gilbertson LG, Goel VK, Kong WZ, Clausen JD. Finite element methods in spine biomechanics research. Critical Reviews™ in Biomedical Engineering. 1995;23(5-6).

100.   Stuff N.   [Available from: https://nccastaff.bournemouth.ac.uk/xyang/Research/FEM/EDT.htm.

101.   Lai P-L, Chen L-H, Niu C-C, Fu T-S, Chen W-J. Relation between laminectomy and development of adjacent segment instability after lumbar fusion with pedicle fixation. Spine. 2004;29(22):2527-32.

102.   Medicine UNLo. The Visible Human Project®: US National Library of Medicine; 2014 Available from: https://www.nlm.nih.gov/research/visible/visible_human.html.

103.   Ateshian GA, Maas S, Weiss JA. Solute transport across a contact interface in deformable porous media. Journal of Biomechanics. 2012;45(6):1023-7.

104.   Pintar FA, Yoganandan N, Myers T, Elhagediab A, Sances A. Biomechanical properties of human lumbar spine ligaments. Journal of Biomechanics. 1992;25(11):1351-6.

105.   Bowen RM. Incompressible porous media models by use of the theory of mixtures. International Journal of Engineering Science. 1980;18(9):1129-48.

106.   Mow VC, Kuei S, Lai WM, Armstrong CG. Biphasic creep and stress relaxation of articular cartilage in compression: theory and experiments. Journal of Biomechanical Engineering. 1980;102(1):73-84.

107.   Shirazi-Adl A, Ahmed AM, Shrivastava SC. Mechanical response of a lumbar motion segment in axial torque alone and combined with compression. Spine. 1986;11(9):914-27.

108.   Zander T, Rohlmann A, Calisse J, Bergmann G. Estimation of muscle forces in the lumbar spine during upper-body inclination. Clinical Biomechanics. 2001;16:S73-S80.

109.   Schmidt H, Heuer F, Simon U, Kettler A, Rohlmann A, Claes L, et al. Application of a new calibration method for a three-dimensional finite element model of a human lumbar annulus fibrosus. Clinical Biomechanics. 2006;21(4):337-44.

110.   Natarajan RN, Andersson GB. The influence of lumbar disc height and cross-sectional area on the mechanical response of the disc to physiologic loading. Spine. 1999;24(18):1873.

111.   Antoniou J, Steffen T, Nelson F, Winterbottom N, Hollander AP, Poole RA, et al. The human lumbar intervertebral disc: evidence for changes in the biosynthesis and denaturation of the extracellular matrix with growth, maturation, ageing, and degeneration. Journal of Clinical Investigation. 1996;98(4):996.

112.   Iatridis JC, Setton LA, Foster RJ, Rawlins BA, Weidenbaum M, Mow VC. Degeneration affects the anisotropic and nonlinear behaviors of human anulus fibrosus in compression. Journal of Biomechanics. 1998;31(6):535-44.

113.   Périé D, Korda D, Iatridis JC. Confined compression experiments on bovine nucleus pulposus and annulus fibrosus: sensitivity of the experiment in the determination of compressive modulus and hydraulic permeability. Journal of Biomechanics. 2005;38(11):2164-71.

114.   Schmidt H, Galbusera F, Rohlmann A, Zander T, Wilke H-J. Effect of multilevel lumbar disc arthroplasty on spine kinematics and facet joint loads in flexion and extension: a finite element analysis. European Spine Journal. 2012;21(5):663-74.

115.   Cowin SC. Bone mechanics handbook. Press C, editor2001.

116.	Musculoskeletal Research Laboratories UoU. FEBio user's manual V 2.4. 2015.

117.	Rohlmann A, Neller S, Claes L, Bergmann G, Wilke H-J. Influence of a follower load on intradiscal pressure and intersegmental rotation of the lumbar spine. Spine. 2001;26(24):E557-E61.

118.	Panjabi MM. Hybrid multidirectional test method to evaluate spinal adjacent-level effects. Clinical Biomechanics. 2007;22(3):257-65.

119.	Sasaki K. Magnetic resonance imaging findings of the lumbar root pathway in patients over 50 years old. European Spine Journal. 1995;4(2):71-6.

120.	Aota Y, Kumano K, Hirabayashi S. Postfusion instability at the adjacent segments after rigid pedicle screw fixation for degenerative lumbar spinal disorders. Journal of Spinal Disorders & Techniques. 1995;8(6):464-73.

121.	Throckmorton TW, Hilibrand AS, Mencio GA, Hodge A, Spengler DM. The impact of adjacent level disc degeneration on health status outcomes following lumbar fusion. Spine. 2003;28(22):2546-50.

122.	Rahm MD, Hall BB. Adjacent-segment degeneration after lumbar fusion with instrumentation: a retrospective study. Journal of Spinal Disorders. 1996;9(5):392-400.

123.	Ekman P, Möller H, Shalabi A, Yu YX, Hedlund R. A prospective randomised study on the long-term effect of lumbar fusion on adjacent disc degeneration. European Spine Journal. 2009;18(8):1175-86.

124.	Thomé C, Zevgaridis D, Leheta O, Bäzner H, Pöckler-Schöniger C, Wöhrle J, et al. Outcome after less-invasive decompression of lumbar spinal stenosis: a randomized comparison of unilateral laminotomy, bilateral laminotomy, and laminectomy. Journal of Neurosurgery: Spine. 2005;3(2):129-41.

125.	Abumi K, Panjabi MM, Kramer KM, Duranceau J, Oxland T, Crisco JJ. Biomechanical evaluation of lumbar spinal stability after graded facetectomies. Spine. 1990;15(11):1142-7.

126.	Zander T, Rohlmann A, Klöckner C, Bergmann G. Influence of graded facetectomy and laminectomy on spinal biomechanics. European Spine Journal. 2003;12(4):427-34.

127.	Bresnahan L, Ogden AT, Natarajan RN, Fessler RG. A biomechanical evaluation of graded posterior element removal for treatment of lumbar stenosis: comparison of a minimally invasive approach with two standard laminectomy techniques. Spine. 2009;34(1):17-23.

128.	Lee KK, Teo EC, Qiu TX, Yang K. Effect of facetectomy on lumbar spinal stability under sagittal plane loadings. Spine. 2004;29(15):1624-31.

129. Natarajan R, Andersson G, Patwardhan A, Andriacchi T. Study on effect of graded facetectomy on change in lumbar motion segment torsional flexibility using three-dimensional continuum contact representation for facet joints. Journal of Biomechanical Engineering. 1999;121(2):215-21.

130. Shirazi-Adl A, Parnianpour M. Load-bearing and stress analysis of the human spine under a novel wrapping compression loading. Clinical Biomechanics. 2000;15(10):718-25.

131. Arbit E, Pannullo S. Lumbar stenosis: a clinical review. Clinical Orthopaedics and Related Research. 2001;384:137-43.

132. Yong-Hing K, Kirkaldy-Willis WH. The pathophysiology of degenerative disease of the lumbar spine. The Orhopedic Clinics of North America. 1983;14(3):491-504.

133. Stokes AF, Iatridis JC. Mechanical conditions that accelerate intervertebral disc degeneration: overload versus immobilization. Spine. 2004;29(23):2724-32.

134. Iatridis JC, MacLean JJ, Roughley PJ, Alini M. Effects of mechancial loading on intervertebral disc metabolism in vivo. Journal of Bone and Joint Surgery. 2006;88(2):41-6.

135. Lee MJ, Bransford RJ, Bellabarba C, Chapman JR, Choen AM, Harington RM, et al. The effect of bilateral laminotomy versus laminectomy on the motion and stiffness of the human lumbar spine: a biomechanical comparison. Spine. 2010;35(19):1789-93.

136. Tai CL, Hsieh PH, Chen WP, Chen LH, Chen WJ, Lai PL. Biomechanical comparison of lumbar spine instability between laminectomy and bilateral laminotomy for spinal stenosis syndrome – an experimental study in porcine model. BMC Musculoskeletal Disorders. 2008;9(1):84.

137. Abumi K, Panjabi MM, Kramer KM, Duranceau J, Oxland TR, Crisco JJ. Biomechanical evaluation of lumbar spinal stability after graded facetectomies. Spine. 1990;15(11):1142-7.

138. Elgafy H, Goel VK, Terai T, Kiapour A, Ebraheim N. Midline sparing bilateral laminotomy prevents disc collapse as compared to traditional laminectomy – A biomechanical finite element analysis. The Spine Journal. 2009;9(10):134S-5S.

139. Zander T, Rohlmann A, Klockner C, Bergmann G. Influence of graded facetectomy and laminectomy on spinal biomechanics. European Spine Journal. 2003;12(4):427-34.

140. Sairyo K, Goel VK, Masuda A, Biyani A, Ebraheim N. Biomechanical rationale of endoscopic decompression for lumbar spondylolysis as an effective minimally invasive procedure-a study based on the finite element analysis. Minimally Invasive Neurosurgery. 2005;48(2):119-22.

141. Rao RD, Wang M, Shinghai P, McGrady LM, Rao S. Intradiscal pressure and kinematic behavior of lumbar spine after bilateral laminotomy and laminectomy. The Spine Journal. 2002;2(5):320-6.

142. Bresnahan L, Ogden AT, Natarajan RN, Fessler RG. A biomechanical evaluation of graded posterior element removal for treatment of lumbar stenosis. Spine. 2009;34(1):17-23.

143. Postacchini F, Cinotti G, Perugia D, Gumina S. The surgical treatment of central lumbar stenosis. Multiple laminotomy compared with total laminectomy. Bone & Joint Surgery, British Volume. 1993;75(3):386-92.

144. Goel VK, Fromknecht SJ, Nishiyama K, Weinstein JN, Liu YK. The role of lumbar spinal elements in flexion. Spine. 1985;10(6):516-23.

145. Holm S, Nachemson A. Variations in the nurtition of the canine intervertebral disc induced by motion. Spine. 1983;8(8):866-74.

146. Hutton WC, Toribatake Y, Elmer WA, Ganey TM, Tomita K, Whitesides TE. The effect of compressive force applied to the intervertebral disc in vivo: a study of proteoglycans and collagen. Spine. 1998;23(23):2524-37.

147. Natarajan RN, Andersson GBJ, Patwardhan AG, Andriacchi TP. Study on effect of graded facetectomy on change in lumbar motion segment torsional flexibility using three-dimensional continuum contact representation for facet joints. Journal of Biomechanical Engineering. 1999;121(2):215-21.

148. Lee KK, Teo EC, Qiu TX, Eng M, Yang KH. Effect of facetectomy on lumbar spinal stability under sagittal plane loadings. Spine. 2004;29(15):1624-31.

149. Lee KK, Teo EC. Effects of laminectomy and facetectomy on the stability of the lumbar motion segment. Medical Engineering & Physics. 2004;26(3):183-92.

150. Shirazi-Adl SA, Shrivastava SC, Ahmed AM. Stress analysis of the lumbar disc-body unit in compression A three-dimensional nonlinear finite element study. Spine. 1984;9(2):120-34.

151. White AA, Panjabi MM. Clinical biomechanics of the spine. Philadelphia, PA: Lippincott; 1990.

152. Yoganandan N, Maiman DJ, Pintar FA, Ray G, Myklebust JB, Sances A, et al. Microtrauma in the lumbar spine: a cause of low back pain. Neurosurgery. 1988;23(2):162-68.

153. Shono Y, McAfee PC, Cunningham BW. Experimental study of thoracolumbar burst fractures: A radiographic and biomechanical analysis of anterior and posterior instrumentation systems. Spine. 1994;19(15):1711-22.

154. Kramer DL, Rodgers W, Mansfield FL. Transpedicular instrumentation and short-segment fusion of thoracolumbar fractures: a prospective study using a single instrumentation system. Journal of Orthopaedic Trauma. 1995;9(6):499-506.

155. Stovall Jr D, Goodrich A, MacDonald A, Blom P. Pedicle screw instrumentation for unstable thoracolumbar fractures. Journal of the Southern Orthopaedic Association. 1995;5(3):165-73.

156. Sasani M, Özer AF. Single-stage posterior corpectomy and expandable cage placement for treatment of thoracic or lumbar burst fractures. Spine. 2009;34(1):E33-E40.

157. Papanastassiou ID, Gerochristou M, Aghayev K, Vrionis FD. Defining the indications, types and biomaterials of corpectomy cages in the thoracolumbar spine. Expert Review of Medical Devices. 2013;10(2):269-79.

158. Kim S-M, Lim TJ, Paterno J, Park J, Kim DH. Biomechanical comparison: stability of lateral-approach anterior lumbar interbody fusion and lateral fixation compared with anterior-approach anterior lumbar interbody fusion and posterior fixation in the lower lumbar spine. Journal of Neurosurgery: Spine. 2005;2(1):62-8.

159. Eleraky M, Papanastassiou I, Tran ND, Dakwar E, Vrionis FD. Comparison of polymethylmethacrylate versus expandable cage in anterior vertebral column reconstruction after posterior extracavitary corpectomy in lumbar and thoraco-lumbar metastatic spine tumors. European Spine Journal. 2011;20(8):1363-70.

160. Hamill CL, Lenke LG, Bridwell KH, Chapman MP, Blanke K, Baldus C. The use of pedicle screw fixation to improve correction in the lumbar spine of patients with idiopathic scoliosis: Is it warranted? Spine. 1996;21(10):1241-9.

161. Lee MJ, Dettori JR, Standaert CJ, Brodt ED, Chapman JR. The natural history of degeneration of the lumbar and cervical spines: a systematic review. Spine. 2012;37:S18-S30.

162. Hilibrand AS, Robbins M. Adjacent segment degeneration and adjacent segment disease: the consequences of spinal fusion? The Spine Journal. 2004;4(6):S190-S4.

163. Kim Y. Finite element analysis of anterior lumbar interbody fusion: threaded cylindrical cage and pedicle screw fixation. Spine. 2007;32(23):2558-68.

164. Polikeit A, Ferguson SJ, Nolte LP, Orr TE. Factors influencing stresses in the lumbar spine after the insertion of intervertebral cages: finite element analysis. European Spine Journal. 2003;12(4):413-20.

165. Park WM, Park Y-S, Kim K, Kim YH. Biomechanical comparison of instrumentation techniques in treatment of thoracolumbar burst fractures: a finite element analysis. Journal of Orthopaedic Science. 2009;14(4):443-9.

166.   Gjolaj JP, Hirsch BP, Latta L, Eismont FJ. Biomechanical evaluation of lateral-access anterior instrumentation for thoracolumbar instability. The Spine Journal. 2016;16(10):S256.

167.   Panjabi MM. Biomechanical evaluation of spinal fixation devices: I. A conceptual framework. Spine. 1988;13(10):1129-34.

168.   Goto K, Tajima N, Chosa E, Totoribe K, Kubo S, Kuroki H, et al. Effects of lumbar spinal fusion on the other lumbar intervertebral levels (three-dimensional finite element analysis). Journal of Orthopaedic Science. 2003;8(4):577-84.

169.   Stokes IA, Iatridis JC. Mechanical conditions that accelerate intervertebral disc degeneration: overload versus immobilization. Spine. 2004;29(23):2724-32.

170.   Panjabi MM, Goel V, Oxland T, Takata K, Duranceau J, Krag M, et al. Human lumbar vertebrae: quantitative three-dimensional anatomy. Spine. 1992;17(3):299-306.

171.   Wilke H-J, Wolf S, Claes LE, Arand M, Wiesend A. Stability increase of the lumbar spine with different muscle groups: A biomechanical in vitro study. Spine. 1995;20(2):192-7.

172.   Dai LY, Jiang SD, Wang XY, Jiang LS. A review of the management of thoracolumbar burst fractures. Surgical Neurology. 2007;67(3):221-32.

173.   Hitchon PW, Torner J, Eichholz KM, Beeler SN. Comparison of anterolateral and posterior approaches in the management of thoracolumbar burst fractures. Journal of Neurosurgery: Spine. 2006;5(2):117-25.

174.   McLain RF. The biomechanics of long versus short fixation for thoracolumbar spine fractures. Spine. 2006;31(115):S70-9.

175.   Norton RP, Milne EL, Kaimrajh DN, Eismont FJ, Latta LL, Williams SK. Biomechanical analysis of four-versus six-screw constructs for short-segment pedicle screw and rod instrumentation of unstable thoracolumbar fractures. The Spine Journal. 2014;14(8):1734-39.

176.   McLain RF, Sparling E, Benson DR. Early failure of short-segment pedicle instrumentation for thoracolumbar fractures. A preliminary report. The Journal of Bone & Joint Surgery. 1993;75(2):162-67.

177.   Chiba M, McLain RF, Yerby SA, Moseley TA, Smith TS, Benson DR. Short-segment pedicle instrumentation: biomechanical analysis of supplemental hook fixation. Spine. 1996;21(3):288-94.

178.   Wahba GM, Bhatia N, Bui CN, Lee KH, Lee TQ. Biomechanical evaluation of short-segment posterior instrumentation with and without crosslinks in a human cadaveric unstable thoracolumbar burst fracture model. Spine. 2010;35(3):278-85.

179.	Alanay A, Acaroglu E, Yazici M, Oznur A, Surat A. Short-segment pedicle instrumentation of thoracolumbar burst fractures: does transpedicular intracorporeal grafting prevent early failure? Spine. 2001;26(2):213-17.

180.	Mahar A, Kim C, Wedemeyer M, Mitsunaga L, Odell T, Johnson B, et al. Short-segment fixation of lumbar burst fractures using pedicle fixation at the level of the fracture. Spine. 2007;32(14):1503-07.

181.	Guven O, Kocaoglu B, Bezer M, Aydin N, Nalbantoglu U. The use of screw at the fracture level in the treatment of thoracolumbar burst fractures. Journal of Spinal Disorders & Techniques. 2009;22(6):417-21.

182.	Dobran M, Nasi D, Brunozzi D, di Somma L, Gladi M, Iacoangeli M, et al. Treatment of unstable thoracolumbar junction fractures: short-segment pedicle fixation with inclusion of the fracture level versus long-segment instrumentation. Acta Neurochirurgica. 2016;158(10):1883-89.

183.	Baaj AA, Reyes PM, Yaqoobi AS, Uribe JS, Vale FL, Theodore N, et al. Biomechanical advantage of the index-level pedicle screw in unstable thoracolumbar junction fractures: Laboratory investigation. Journal of Neurosurgery: Spine. 2011;14(2):192-97.

184.	Pellisé F, Barastegui D, Hernandez-Fernandez A, Barrera-Ochoa S, Bagó J, Issa-Benítez D, et al. Viability and long-term survival of short-segment posterior fixation in thoracolumbar burst fractures. The Spine Journal. 2015;15(8):1796-803.

185.	Oppenheimer JH, DeCastro I, McDonnell DE. Minimally invasive spine technology and minimally invasive spine surgery: a historical review. Neurosurgical Focus. 2009;27(3):E9.

186.	Zhang L, Zou J, Gan M, Shi J, Li J, Yang H. Treatment of thoracolumbar burst fractures: short-segment pedicle instrumentation versus kyphoplasty. Acta Orthop Belg. 2013;79(6):718-25.

187.	Adamson TE. Microendoscopic posterior cervical laminoforaminotomy for unilateral radiculopathy: results of a new technique in 100 cases. Journal of Neurosurgery: Spine. 2001;95(1):51-7.

188.	Allen TL, Tatli Y, Lutz GE. Fluoroscopic percutaneous lumbar zygapophyseal joint cyst rupture: a clinical outcome study. The Spine Journal. 2009;9(5):387-95.

189.	Anand N, Baron EM, Thaiyananthan G, Khalsa K, Goldstein TB. Minimally invasive multilevel percutaneous correction and fusion for adult lumbar degenerative scoliosis: a technique and feasibility study. Clinical Spine Surgery. 2008;21(7):459-67.

190.	German JW, Adamo MA, Hoppenot RG, Blossom JH, Nagle HA. Perioperative results following lumbar discectomy: comparison of minimally invasive discectomy and standard microdiscectomy. Journal of Neurosurgery. 2008;25(2):E20.

191. Norton RP, Milne EL, Kaimrajh DN, Eismont FJ, Latta LL, Williams SK. Biomechanical analysis of four-versus six-screw constructs for short-segment pedicle screw and rod instrumentation of unstable thoracolumbar fractures. The Spine Journal. 2014;14(8):1734-9.

192. Belkoff SM, Mathis JM, Jasper LE, Deramond H. The biomechanics of vertebroplasty: the effect of cement volume on mechanical behavior. Spine. 2001;26(14):1537-41.

193. Dean J, Ison K, Gishen P. The strengthening effect of percutaneous vertebroplasty. Clinical Radiology. 2000;55(6):471-6.

194. Blondel B, Fuentes S, Metellus P, Adetchessi T, Pech-Gourg G, Dufour H. Severe thoracolumbar osteoporotic burst fractures: treatment combining open kyphoplasty and short-segment fixation. Orthopaedics & Traumatology: Surgery & Research. 2009;95(5):359-64.

195. Garfin SR, Yuan HA, Reiley MA. New technologies in spine: kyphoplasty and vertebroplasty for the treatment of painful osteoporotic compression fractures. Spine. 2001;26(14):1511-5.

196. Wardlaw D, Cummings SR, Van Meirhaeghe J, Bastian L, Tillman JB, Ranstam J, et al. Efficacy and safety of balloon kyphoplasty compared with non-surgical care for vertebral compression fracture (FREE): a randomised controlled trial. The Lancet. 2009;373(9668):1016-24.

197. Afzal S, Akbar S, Dhar SA. Short segment pedicle screw instrumentation and augmentation vertebroplasty in lumbar burst fractures: an experience. European Spine Journal. 2008;17(3):336-41.

198. Alanay A, Acaroglu E, Yazici M, Oznur A, Surat A. Short-segment pedicle instrumentation of thoracolumbar burst fractures: does transpedicular intracorporeal grafting prevent early failure? Spine. 2001;26(2):213-7.

199. Bironneau A, Bouquet C, Millet-Barbe B, Leclercq N, Pries P, Gayet L-E. Percutaneous internal fixation combined with kyphoplasty for neurologically intact thoracolumbar fractures: a prospective cohort study of 24 patients with one year of follow-up. Orthopaedics & Traumatology: Surgery & Research. 2011;97(4):389-95.

200. Villarraga ML, Bellezza AJ, Harrigan TP, Cripton PA, Kurtz SM, Edidin AA. The biomechanical effects of kyphoplasty on treated and adjacent nontreated vertebral bodies. Journal of Spinal Disorders & Techniques. 2005;18(1):84-91.

201. Silva MJ, Keaveny TM, Hayes WC. Load sharing between the shell and centrum in the lumbar vertebral body. Spine. 1997;22(2):140-50.

202.   Zhu Q, Jackson AR, Gu WY. Cell viability in intervertebral disc under various nutritional and dynamic loading conditions: 3d finite element analysis. Journal of Biomechanics. 2012;45(16):2769-77.

203.   Lewis G. Properties of acrylic bone cement: state of the art review. Journal of Biomedical Materials Research Part A. 1997;38(2):155-82.

204.   Lee YS, Sung JK. Long-term follow-up results of short-segment posterior screw fixation for thoracolumbar burst fractures. J Korean Neurosurg Soc. 2005;37:416-21.

205.   Blondel B, Fuentes S, Pech-Gourg G, Adetchessi T, Tropiano P, Dufour H. Percutaneous management of thoracolumbar burst fractures: evolution of techniques and strategy. Orthopaedics & Traumatology: Surgery & Research. 2011;97(5):527-32.

206.   Boszczyk B, Bierschneider M, Potulski M, Robert B, Vastmans J, Jaksche H. Extended kyphoplasty indications for stabilization of osteoporotic vertebral compression fractures. Der Unfallchirurg. 2002;105(10):952-7.

207.   Krüger A, Zettl R, Ziring E, Mann D, Schnabel M, Ruchholtz S. Kyphoplasty for the treatment of incomplete osteoporotic burst fractures. European Spine Journal. 2010;19(6):893-900.

208.   Baroud G, Nemes J, Heini P, Steffen T. Load shift of the intervertebral disc after a vertebroplasty: a finite-element study. European Spine Journal. 2003;12(4):421-6.

209.   Dabirrahmani D, Becker S, Hogg M, Appleyard R, Baroud G, Gillies M. Mechanical variables affecting balloon kyphoplasty outcome–a finite element study. Computer Methods in Biomechanics and Biomedical Engineering. 2012;15(3):211-20.

210.   Elmasry S, Asfour S, Travascio F. Implications of spine fixation on the adjacent lumbar levels for surgical treatment of thoracolumbar burst fractures: a finite element analysis. Journal of Spine Care. 2016;1(1):1-5.

211.   Hoy D, March L, Brooks P, Blyth F, Woolf A, Bain C, et al. The global burden of low back pain: estimates from the Global Burden of Disease 2010 study. Annals of the Rheumatic Diseases. 2014;73:968-74.

212.   Deyo RA, Gray DT, Kreuter W, Mirza S, Martin BI. United States trends in lumbar fusion surgery for degenerative conditions. Spine. 2005;30(12):1441-5.